# Eruptive History of Late Miocene to Recent Caldera Volcanoes and Related Volcaniclastic Sedimentation in an Intra-arc Basin, Aizu Volcanic Field, Northeast Japan

Yamamoto, Takahiro

神戸大学博士論文

# Eruptive History of Late Miocene to Recent Caldera Volcanoes and Related Volcaniclastic Sedimentation in an Intra-arc Basin, Aizu Volcanic Field, Northeast Japan

東北日本，会津地域の後期中新世－完新世カルデラ火山群の噴火史と
弧内堆積盆における火砕物堆積作用

平成5年　7月

July, 1993

山元　孝広

Takahiro Yamamoto

# CONTENTS

## Abstract

Within the Aizu volcanic field in the southern Northeast Honshu arc, late Miocene to Recent six large calderas, >10 km in diameter, form a prominent cluster concentrated in a 60 by 30 km area, with several medium to small calderas and stratovolcanoes. These volcanoes are built on a WNW-ESE trending topographic high terrain, that is coincident with regional positive Bouguer gravity anomalies, and have shed extensive pyroclastic flow sheets interstratified with various epiclastic debris in intra-arc basins. The large calderas are characterized by voluminous intracaldera pyroclastic flow deposits (>100 km$^3$), ring-like patterns of postcaldera igneous activity, and resurgent uplift within the calderas; these features are similar to well-known "Valles type" calderas. On the other hand, the medium to small calderas have been interpreted as diatremelike subsurface structures, based on the borehole data. The geochronological data indicates that the large-caldera formations have occurred at six times since 8 Ma, at every 1 to $2 \times 10^6$ years intervals; this cycle is more than ten times as long as those of well-known other Cenozoic caldera volcanoes accompanied with extensional grabens, such as the San Juan volcanic field and the Taupo volcanic zone. Furthermore, the results of a sedimentary facies analysis for extracaldera volcaniclastic aprons in the intra-arc basin suggest that a preceding increase of the felsic volcanism occurred at about 10 Ma, represented by a high rate of volcaniclastic sediments supply. This caldera-forming volcanism had caused progradation of volcaniclastic aprons toward the back-arc side, controlled by sea-level changes, until about 3 Ma. Although appearances of alluvial fans and flexural subsidence within the basin indicate the beginning of reverse-faulting at about 3 Ma, there is no change of an eruption style in the caldera-forming volcanism corresponding to this tectonic event. On the other words, the different calderas in size and internal structures were formed under a same compressional stress field during this period. Paleogeographic reconstruction shows that the Aizu volcanic field has been topographically high during the caldera-forming volcanism due to magmatic uplift, but this field lacks an extensional deformation caused by inflation of high-level batholithic magma bodies. The observed long-tern cycle of large-caldera formations

seems to be directly caused by a slow rate of magma accumulation in the crust beneath the Aizu volcanic field.

# 1. INTRODUCTION

The Northeast Honshu (or Northeast Japan) arc, related to the subduction of the Pacific plate, is the type example of mature volcanic arc systems having complex geologic histories. Whereas the recent active elements of this volcanic arc are many andesitic composite volcanoes, these young volcanoes are built on late Miocene- Pleistocene caldera volcanoes that produced regionally extensive ignimbrite sheets in intra-arc basins with volumes in excess of 1000 km$^3$. These caldera volcanoes are not uniformly distributed along the arc, but make clustered volcanic fields at every 40 to 80 km intervals, such as the Hakkoda (Muraoka et al., 1991), Sengan (Suto, 1987), Kurikoma (Ito et al., 1989), and Aizu volcanic field (Yamamoto, 1992a). These calderas would provide rare examples from an island arc region under a compressional stress field, although Cenozoic clustered calderas have been commonly reported from continental regions such as the western United States (Lipman, 1984) and the central Andes (de Silva, 1989).

This paper focuses an eruptive history of late Miocene- Recent clustered calderas in the Aizu district (Fig. 1). Their eruptive products formed either voluminous intracaldera formations filling individual depressions and related extracaldera volcaniclastic aprons interstratified with various epiclastic debris. The geochronological outline of caldera-forming events in this volcanic fields has been defined by Yamamoto (1992a), but little has been done on depositional evolution of their volcaniclastic aprons or volcanism-tectonics relationships. Detailed documentation of these volcaniclastic sequences is crucial to understanding the volcanological evolution of this field, as they were strongly influenced by synvolcanic and syntectonic sedimentations, similar to other volcano-adjacent formations (Smith, 1987; Turbeville et al., 1989; Kano, 1991; Orton, 1991). These relationships are well displayed in the late Miocene- middle Pleistocene intra-arc basin fills, Shiotsubo, Fujitoge, Izumi, Nanaorezaka, and Todera Formations, which are exposed on the western side of the Aizu Basin. These formations are ideal for study because of their fine exposure and close spatial, temporal, and lithologic association with the caldera volcanoes. The extracaldera volcaniclastic deposits, therefore, provide valuable insight into the history of late Miocene- Recent caldera-
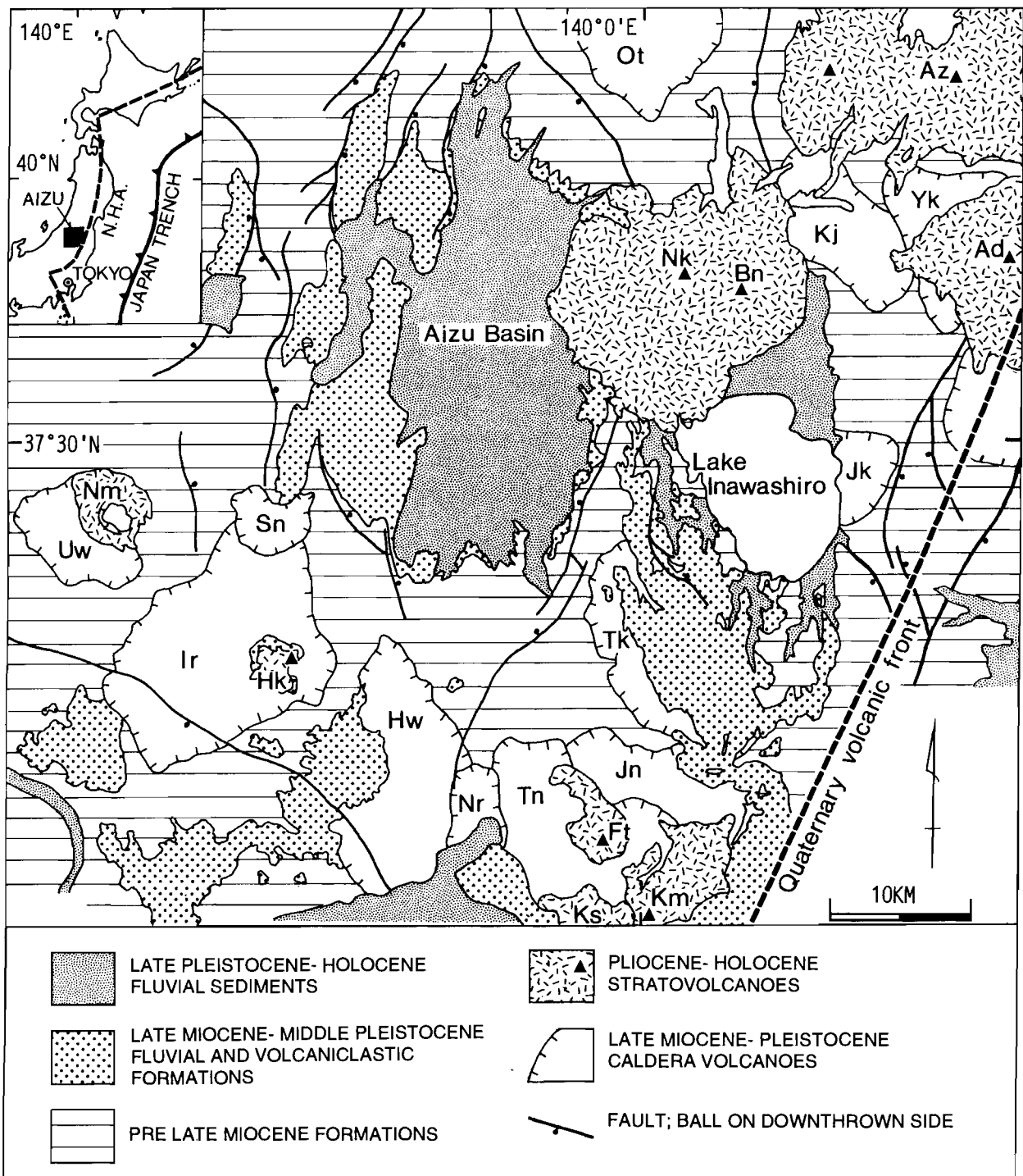
Fig. 1. Location map of late Miocene to Recent volcanoes and associated
volcaniclastic aprons in the Aizu district. Az= Azuma volcano; Ad=
Adatara volcano; Yk= Yokomuki caldera; Kj= Kijigoya caldera; Bn=
Bandai volcano; Nk= Nekoma volcano; Ot= Otoge caldera; Jk= Joko
caldera; Tk= Takagawa caldera; Jn= Jonoirisawa caldera; Ft=
Futamatayama volcano; Km= Kamafusayama pyroclastic flow deposit;
Ks= Kasshi volcano; Tn= Tonohetsuri caldera; Nr= Narioka caldera; Hw=
Hiwada caldera; Hk= Hakaseyama volcano; Ir= Iriyamazawa caldera; Nm=
Numazawa caldera volcano; Uw= Uwaigusa caldera. N.H.A. is the
Northeast Honshu arc.

forming volcanism in this field.

## 2. GEOLOGICAL SETTING

The Aizu district is located on the southern part of the Northeast Honshu arc behind the volcanic front marked by Quaternary andesitic stratovolcanoes, such as Adatara and Kasshi volcanoes (Fig. 1). Late Miocene- Recent volcanoes in this district are separated into two prominent clusters by the intra-arc basin. The south of the basin is the Aizu volcanic field and the northeast of the basin is the Inawashiro one. These clustered calderas and stratovolcanoes are built on WNW-ESE trending high terrains, which are normal to the volcanic front and roughly coincident with regional positive Bouguer gravity anomalies (Fig. 2; GSJ, 1993). Furthermore, they overlie unconformably upon early- middle Miocene marine formations; the timing of ignimbrite flare-up coincides well with late Miocene uplift of the submerged arc (Ito et al., 1989). This caldera-forming volcanism is quite different from the 20- 15 Ma felsic volcanism forming parallel dike swarms, that was related to back-arc extension of the Japan Sea (Amano and Sato, 1989; Yamamoto and Yoshioka, 1992).

The present intra-arc Aizu Basin, measuring 30 by 12 km, is filled by late Pleistocene- Holocene fluvial sediments which interbed with various volcaniclastic debris shed from recent volcanoes, and their western and eastern margins are cut by active reverse faults. A large negative Bouguer gravity anomaly (about 50 mgal) concentrated on this basin (Fig. 2; GSJ, 1993) is interpreted to reflect downwarping basement morphology. This basin overlaps the late Miocene- middle Pleistocene fluvial basin and have migrated eastward due to faulting. Also, the present main drainage within the basin is represented by braided river systems controlled by the active faults. The 1611 strong Aizu earthquake was caused by the recent activity of reverse-faulting on the western side of the Aizu Basin and resulted in subsidence of the basin (Sangawa, 1987).
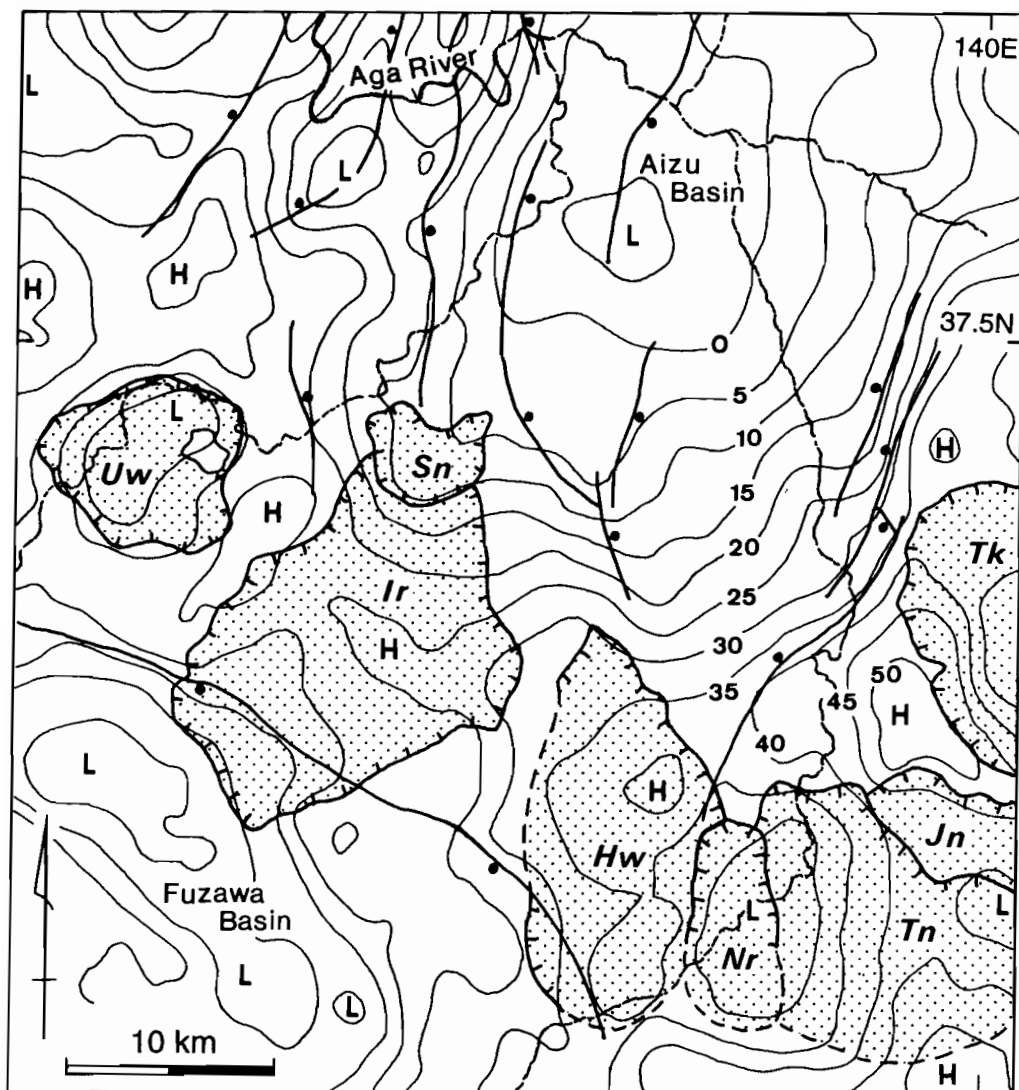
Fig. 2. Map showing distribution of caldera volcanoes and Bouguer gravity anomalies in the Aizu volcanic field. H= area of higher gravity; L= area of lower gravity; Tk= Takagawa caldera; Jn= Jonoirisawa caldera; Tn= Tonohetsuri caldera; Nr= Narioka caldera; Hw= Hiwada caldera; Ir= Iriyamazawa caldera; Uw= Uwaigusa caldera. Contour interval, 5 mgal; gravity data from GSJ (1993).

# 3. CALDERA VOLCANOES IN THE AIZU VOLCANIC FIELD

The late Miocene- Recent nine caldera volcanoes and three basalt-andesitic stratovolcanoes align on the high terrain south of the Aizu Basin and form a prominent volcanic cluster, about 60 by 30 km across (Fig. 1). Little geologic work for pre-Quaternary caldera volcanoes in the field was done prior to Yamamoto (1991; 1992a) and this paper. Kitamura et al. (1968), Suzuki et al. (1972), and Masuda et al. (1974) mapped the quadrangles on the southern side of the basin, but they did not identify caldera volcanoes. Although, Komuro (1984) recognized that voluminous felsic tuffs erupted after individual depressions in this field, he misunderstood the eruptive ages and stratigraphic relationships of intracaldera formations.

The Jonoirisawa, Iriyamazawa, Takagawa, Uwaigusa, Hiwada, Tonohetsuri, Narioka, and Sunagohara Formations are filling their individual caldera-depressions. They show the upper caldera-fill sequences which accumulated during and after collapse, but no caldera floor is exposed in this field. The caldera-forming unit consists of densely welded, thick pyroclastic flow deposit and intercalated thin debris avalanche deposits comprising lithic fragments of basement rocks. These deposits show similar lithofacies reported from other eroded calderas by Lambert (1974), Lipman (1976; 1984), and Fridrich et al. (1991); the interbedded lithic debris has been interpreted as products of large-scale slope failures from a caldera wall during collapse. On the other hand, the post-caldera unit is made up of various caldera-lake sediments and post-collapse volcanic products; they rest on the caldera-forming unit without significant erosion.

All presently available geochronological data for this field are compiled on Tables 1 and 2, while the locations are shown on Fig. 3 (new results of dating are described in an appendix). The data obtained in my studies (Yamamoto, 1992a; 1992b; this paper) are in good agreement with stratigraphic observations, as well as with data of other previous workers. These results are regarded as geologically meaningful and as the best available information for correlation between the intracaldera and extracaldera pyroclastic flow deposits (Figs. 4 and 5). In general, intracaldera pyroclastic flow deposits differ from their cogenetic extracaldera equivalents in thickness, degree of welding, devitrification, abundance and size of lithic

8

Table 1.  Available radiogenic ages from extracaldera formations in the Aizu district.

| Unit/Sample [Site] | | Age±error (Ma) | Method [Material] | Reference |
|---|---|---|---|---|
| **Todera Formation** | | | | |
| Td2 PFD: GSJ R57405 | [1] | 0.29±0.06 | Ft [Zr] | Yamamoto (1992b) |
| **Nanaorezaka Formation** | | | | |
| Nn2 PFD: GSJ R60147 | [2] | 1.2 ±0.1 | Ft [Zr] | This paper |
| Nn1 PFD: GSJ R56951 | [3] | 1.3 ±0.3 | K-Ar [wr] | Yamamoto (1992a) |
| Ot-1 | [4] | 1.1 ±0.4 | K-Ar [wr] | Yamaguchi (1986) |
| Ot-2 | [5] | 1.2 ±0.2 | K-Ar [wr] | ditto |
| **Izumi Formation** | | | | |
| Iz1 PFD: GSJ R56952 | [6] | 2.94±0.15 | K-Ar [gm] | Yamamoto (1992a) |
| 15 | [7] | 2.66±0.19 | K-Ar [Hb] | HCRG (1990) |
| **Fujitoge Formation** | | | | |
| Fj5 PFD: GSJ R56956 | [8] | 4.3 ±0.5 | Ft [Zr] | Yamamoto (1992a) |
| Fj4 PFD: GSJ R56953 | [9] | 4.1 ±0.3 | Ft [Zr] | ditto |
| Fj3 PFD: GSJ R56954 | [10] | 6.5 ±0.6 | Ft [Zr] | ditto |
| Fj1 PFD: GSJ R56955 | [11] | 8.9 ±0.8 | Ft [Zr] | ditto |
| **Komadotoge Formation** | | | | |
| Kd1 PFD: KD-3 [12] | Av | 7.12±0.09 | K-Ar [Bt] | Yamaguchi (1991) |

PFD: pyroclastic flow deposit;  Ft: fission track age;  Bt: biotite;  Hb: hornblende;  Zr: zircon;  wr: whole rock;  gm: groundmass;  HCRG: Hakaseyama Collaborative Research Group.

Table 2. Available radiogenic ages from intracaldera formations and stratovolcanoes the Aizu district.

| Unit/Sample [Site] | Age±error | Method [Material] | Reference |
|---|---|---|---|
| **Numazawa  volcano** | (Ka) | | |
| Nm2 PFD: Gak-6751 [13] | 4.98±0.10 | $C^{14}$ | MITI (1978) |
| Gak-6754 [14] | 5.06±0.12 | $C^{14}$ | ditto |
| **Futamatayama  volcano** | (Ma) | | |
| Lava:  U-203 [15] | 0.11±0.04 | Ft [Zr] | NEDO (1990) |
| **Sunagohara  Formation** | | | |
| Postcaldera PFD:  No.8 [16] | 0.22±0.05 | Ft [Zr] | NEDO (1985) |
| Postcaldera lava: No.10[17] | 0.21±0.03 | K-Ar [wr] | ditto , |
| No.7 [18] | 0.31±0.16 | Ft [Zr] | ditto |
| No.6 [19] | 0.59±0.27 | Ft [Zr] | ditto |
| No.5 [20] | 0.5 ±0.1 | K-Ar [wr] | ditto |
| **Kamafusayama  pyroclastic  flow  deposit** | | | |
| PFD: U-204  [21] | 0.38±0.05 | K-Ar [wr] | NEDO (1990) |
| U-2  [22] | 0.59±0.06 | K-Ar [wr] | ditto |
| **Tonohetsuri  Formation** | | | |
| Postcaldera lava: U-12[23] | 0.94±0.05 | K-Ar [wr] | NEDO (1990) |
| Tn1 PFD: U-206  [24] | 1.28±0.13 | K-Ar [wr] | ditto |
| GSJ R60146 [25] | 1.4 ±0.2 | Ft [Zr] | This paper |
| U-209  [26] | 1.76±0.33 | K-Ar [wr] | NEDO (1990) |
| **Hakaseyama  volcano** | | | |
| Lava: SK841110 [27] | Av 2.69±0.12 | K-Ar [wr] | Kobayashi & Inomata (1986) |
| No.11  [28] | 2.78±0.15 | K-Ar [wr] | NEDO (1985) |
| **Hiwada  Formation** | | | |
| Hw1 PFD: GSJ R57402 [29] | 2.64±0.20 | K-Ar [gm] | Yamamoto (1992a) |
| **Uwaigusa  Formation** | | | |
| Postcaldera lava: | | | |
| GSJ R60145 [30] | 3.22±0.16 | K-Ar [gm] | This paper |
| TML-1  [31] | 3.4 ±0.1 | K-Ar [gm] | Sugawara (1991) |
| Uw1 PFD: GSJ R60144 [32] | 4.2 ±0.2 | Ft [Zr] | This paper |

### Takagawa Formation
Tk1 PFD: GSJ R56957 [33]   6.3  ±0.4   Ft [Zr]      Yamamoto (1992a)

### Iriyamazawa Formation
Ir1 PFD: GSJ R57404 [34]   7.1  ±1.0   Ft [Zr]      Yamamoto (1992a)

### Jonoirisawa Formation
Postcaldera pyroclastics
: U-210 [35]         8.19±0.29  K-Ar  [wr]  NEDO (1990)

---

PFD: pyroclastic flow deposit;   Ft: fission track age;   Zr: zircon;   wr: whole rock;   gm: groundmass.
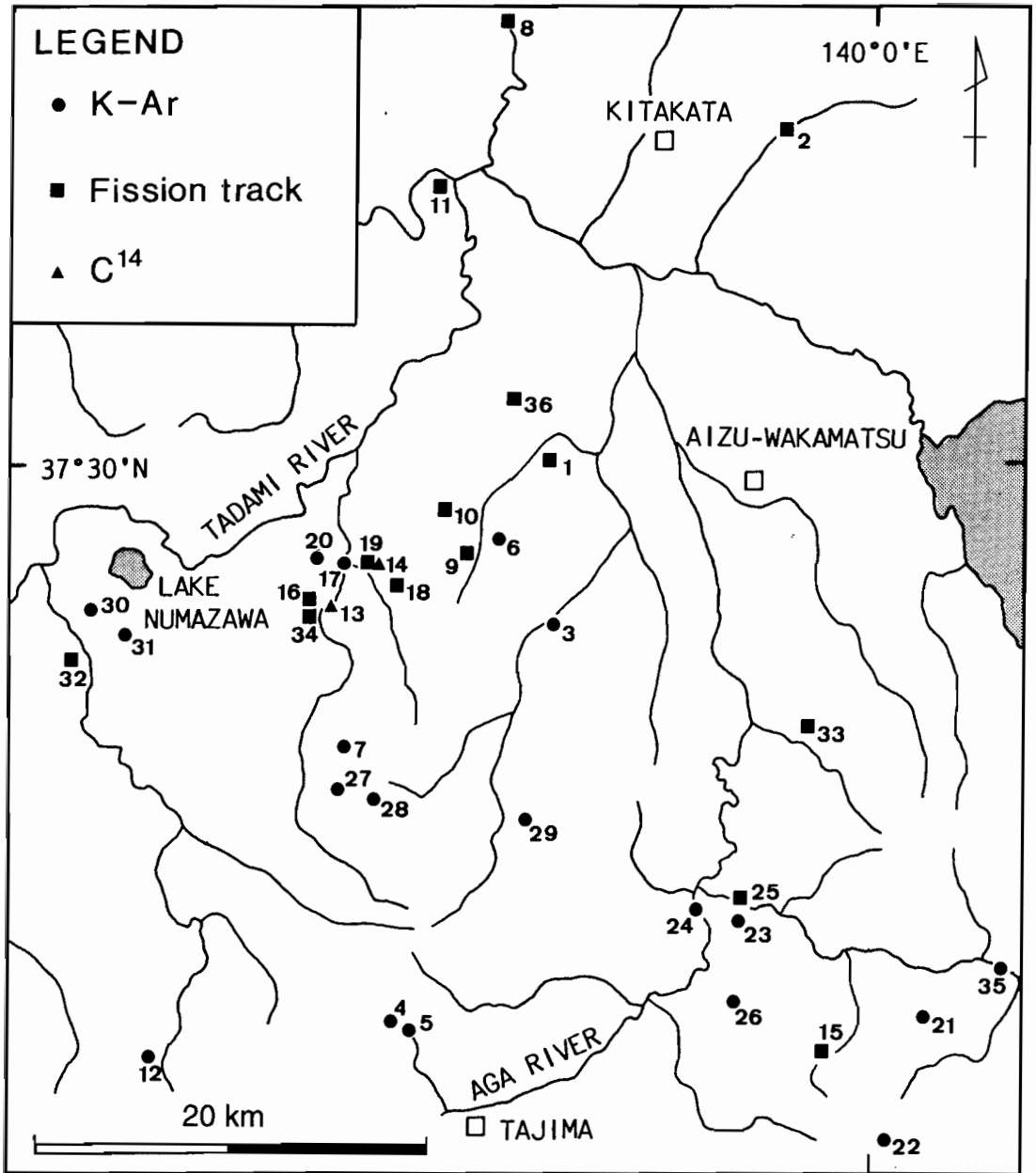
Fig. 3. Locations of all currently available radiogenic ages for late Miocene to Recent volcanic rocks in the Aizu volcanic field. Numbers of the sites refer to data presented on Tables 1, 2, A1, and A2.
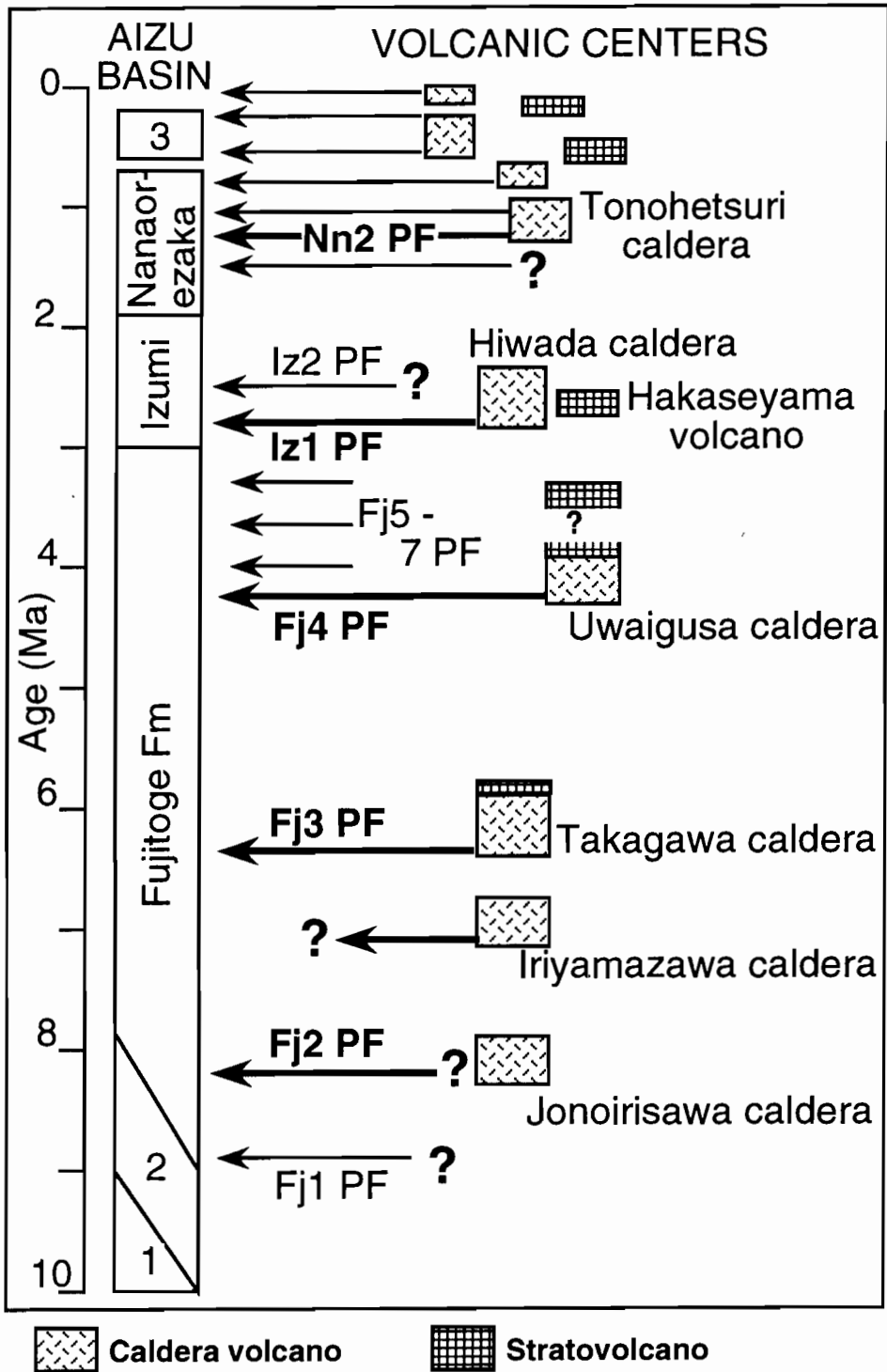
Fig. 4. Schematic representation of the stratigraphy of the late Miocene to Recent volcanic centers and extracaldera formations in the Aizu volcanic field. Arrows indicate pyroclastic flows (PF); thick arrows indicate large-volume (>100 km$^3$) ones. 1= Yuzuritoge Formation; 2= Shiotsubo Formation; 3= Todera Formation.
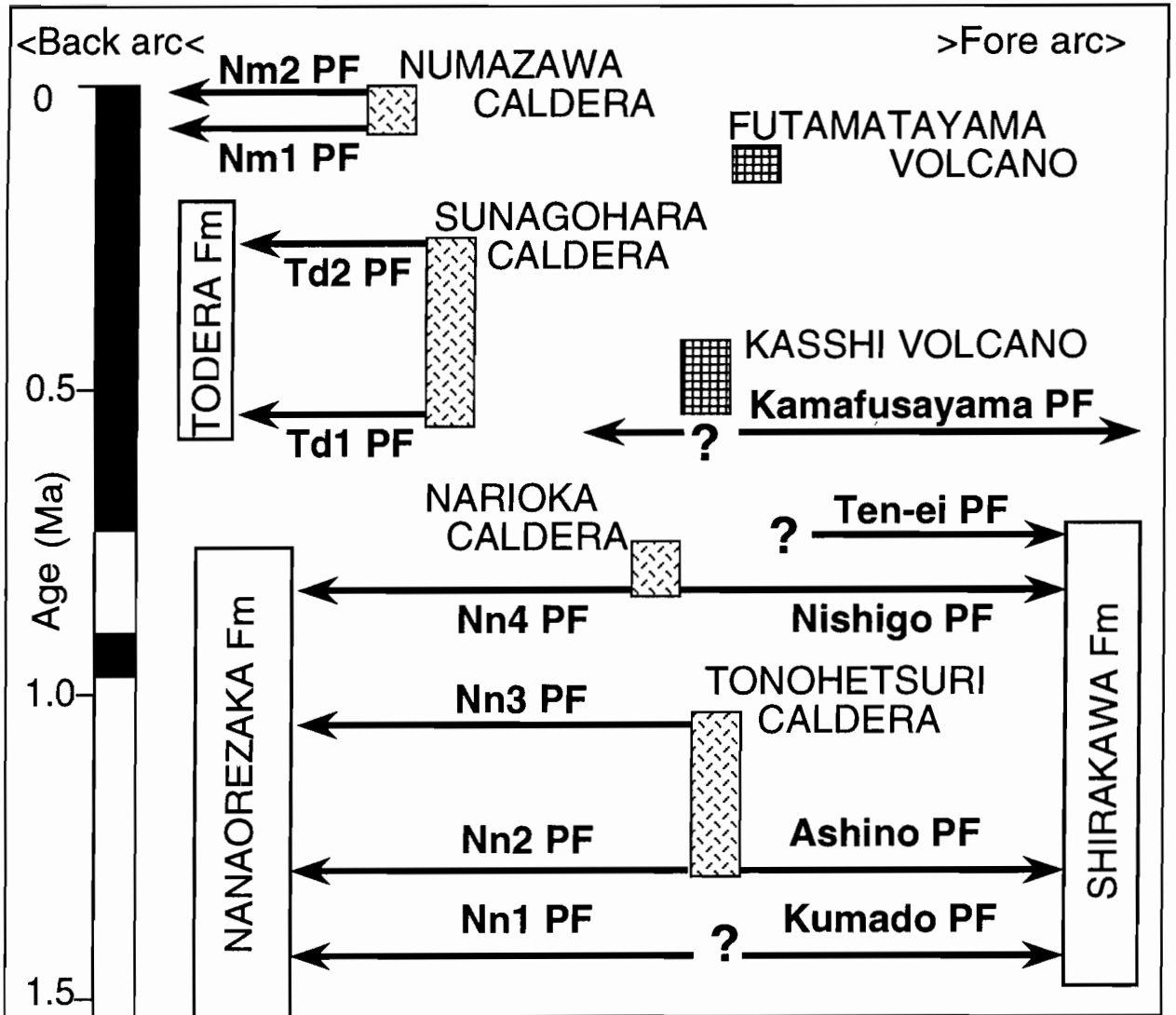
Fig. 5. Schematic representation of the stratigraphy of the Quaternary volcanic centers and extracaldera formations in the Aizu volcanic field. Arrows indicate pyroclastic flows (PF). Symbols are same as Fig. 4.
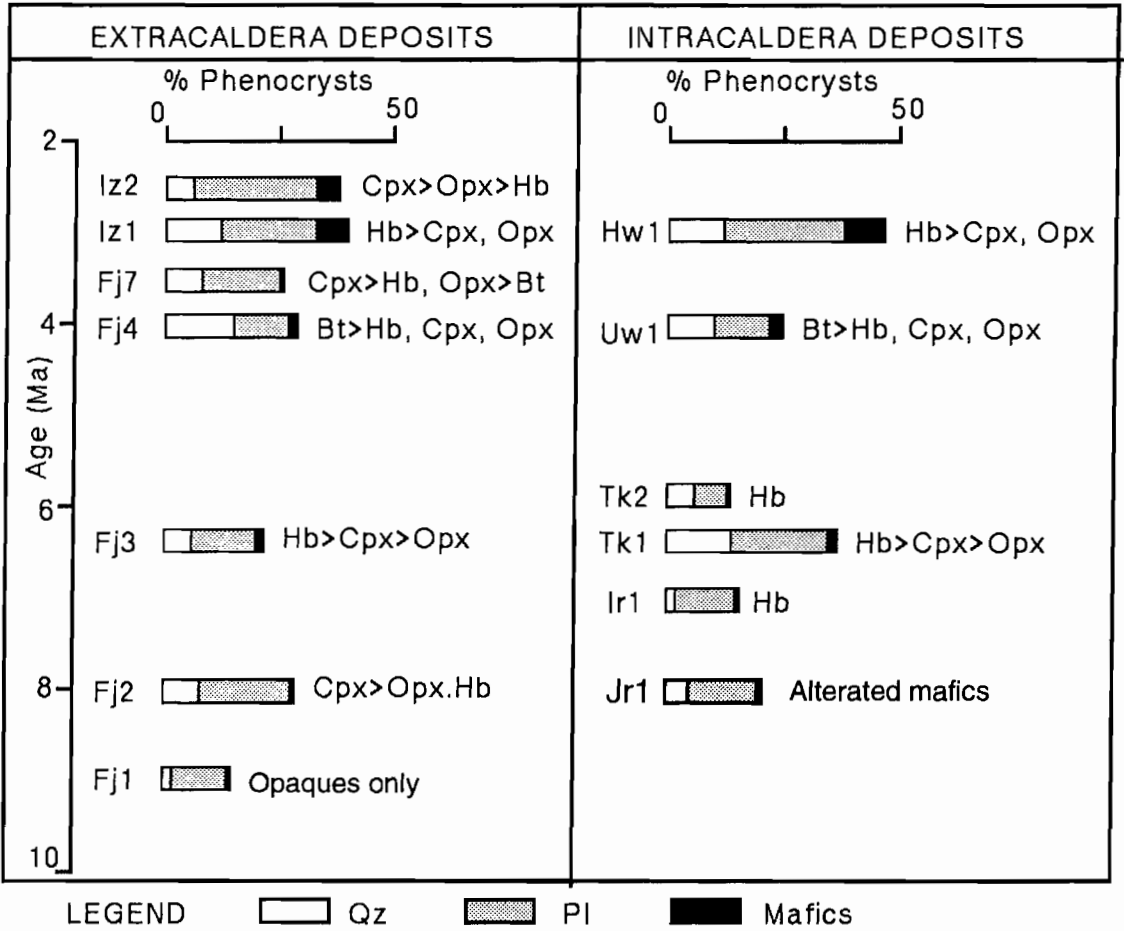
Fig. 6. Modal compositions (normalized 100% lithic free) of the late Miocene to Pliocene extracaldera and intracaldera pyroclastic flow deposits with geochronological positions in the Aizu volcanic field.
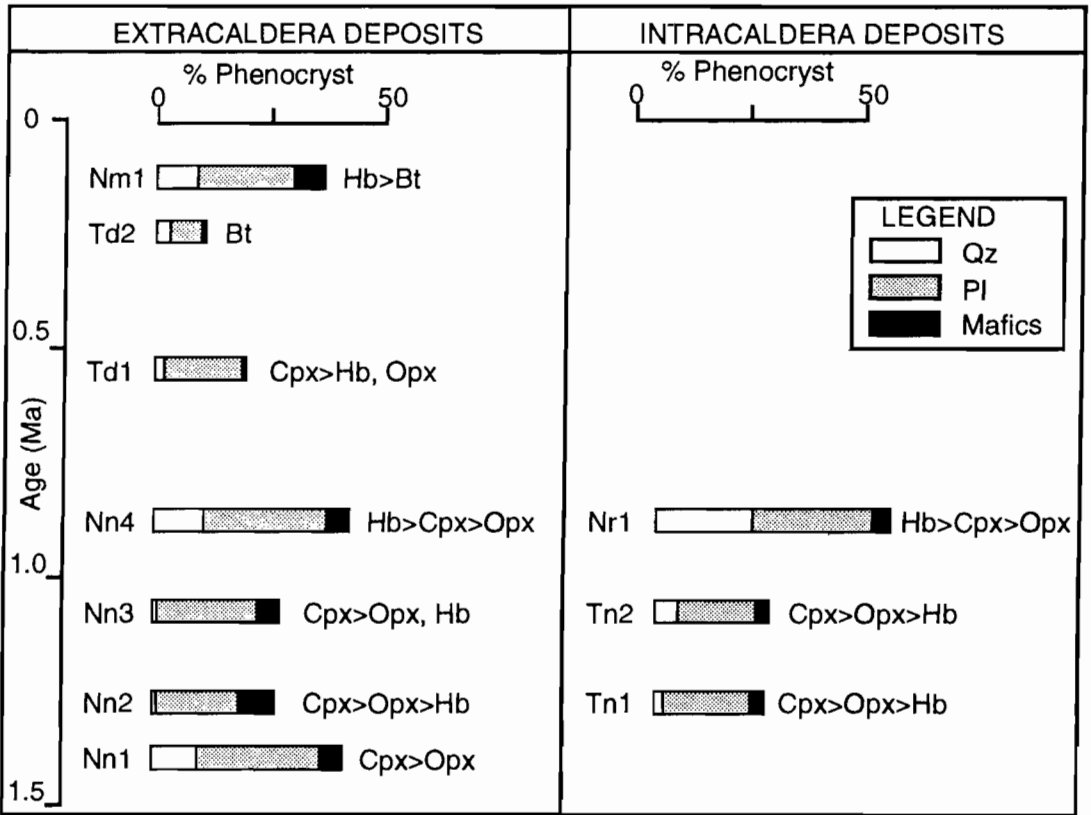
Fig. 7. Modal compositions (normalized 100% lithic free) of the Quaternary extracaldera and intracaldera pyroclastic flow deposits with geochronological positions in the Aizu volcanic field.

fragments, associated breccia lenses, and alterations. However, the correlation between intracaldera and extracaldera pyroclastic flow deposits in this field is not so difficult. Because, both of them have identical phenocryst-assemblages, although intracaldera pyroclastic flow deposits commonly contains larger phenocrysts, especially of quartz, than extracaldera equivalents (Figs. 6 and 7). Most extracaldera pyroclastic flow deposits have no obvious phenocryst-compositional zonation, except for the Fj4 pyroclastic flow deposit.


## Jonoirisawa caldera volcano


The Jonoirisawa Formation (after Masuda et al., 1974) is filling the oldest and least preserved caldera, which was destroyed by the Tonohetsuri caldera collapse and buried by Pleistocene pyroclastic flow deposits. The remnant part of this caldera is a 10 by 5 km across (Fig. 1). The caldera-forming Jn1 pyroclastic flow deposit is pyroxene (?) dacitic welded lapilli tuff and more than 500 m in thickness; its appearance of varies in degree of welding and abundance of lithic fragments. Furthermore, this deposit is wholly affected by hydrothermal alteration; their glassy matrix is intensely recrystallized and most phenocrysts are replaced by chlorite, calcite, sericite, epidote, and other alteration minerals. The fission track age of 5.52±1.40 Ma for zircon was reported from the altered Jn1 pyroclastic flow deposit, however the whole rock K-Ar age for the postcaldera pyroclastic rocks was determined as 8.19±0.29 Ma (NEDO, 1990). This age for the Jn1 deposit is unavailable, because this formation is apparently covered by the Takagawa Formation. the Post-caldera plutonic rocks, which are fine-grained biotite-hornblende tonalite, intruded in the central part of this caldera. The Tenei mordenite mine is developed in postcaldera vitric tuff within the caldera.


## Iriyamazawa caldera volcano


The Iriyamazawa Formation (after Kitamura et al., 1968; Yamamoto, 1992a) is horizontally filling a quadrangular large caldera measuring 20 by 15 km (Fig. 1). This formation is overlain by the Fj4 and Iz1 pyroclastic flow deposits, Hakaseyama volcano, and

the Sunagohara Formation (Yamamoto, 1992a). The caldera-forming Ir1 pyroclastic flow deposit was formed at about 7.1 Ma (Table 2), but no extracaldera pyroclastic flow deposit is found within the Fujitoge Formation (Fig. 4). This caldera is characterized by the basal thick intracaldera pyroclastic flow deposit and an U-shaped alignment of post-caldera lava domes (Yamamoto, 1992a). No typical resurgent uplift was developed in this caldera (Fig. 8-B).

*Caldera-forming unit*

This unit is composed of the voluminous Ir1 pyroclastic flow deposit and intercalated minor debris avalanche deposits. They were produced by a major ignimbrite eruption and contemporaneous caldera collapse. The thickness of these deposits is about 1000 m in the 44EAN-1 borehole (MITI, 1970; Fig. 8-B); they are about 150 km$^3$ volume of magma. The Ir1 pyroclastic flow deposit is hornblende-quartz dacitic weakly- to non-welded pumice lapilli tuff. This deposit heterogeneously contains accidental blocks, more than 10 m in maximum diameter. The debris avalanche deposits occur as horizontal lenses which consist of lithic breccia of fossiliferous sandstone, siltstone and rhyolitic volcaniclastic rocks derived from early- middle Miocene formations. They are locally interlayered with the marginal part of the Ir1 pyroclastic flow deposit.

*Post-caldera unit*

This unit consists of caldera-lake sediments and intrusive-extrusive lava domes. The post-caldera sediments are about 200 m thick and made up of 10-cm to 4-m-thick normally-, reverse-to-normally-, or non-graded pebbly sandstone and conglomerate, parallel laminated siltstone and fine-grained sandstone, and massive vitric tuff. They represent various sediment gravity flows washed from the caldera wall and minor eruptions of fine-grained pyroclastics. The lava domes are 0.5- 4 km in diameter and made up of orthopyroxene-clinopyroxene-hornblende-quartz dacite, hornblende-biotite-quartz dacite, and orthopyroxene-clinopyroxene andesite. They form a prominent U-shape alignment, 12 km in diameter, opening northwestward.
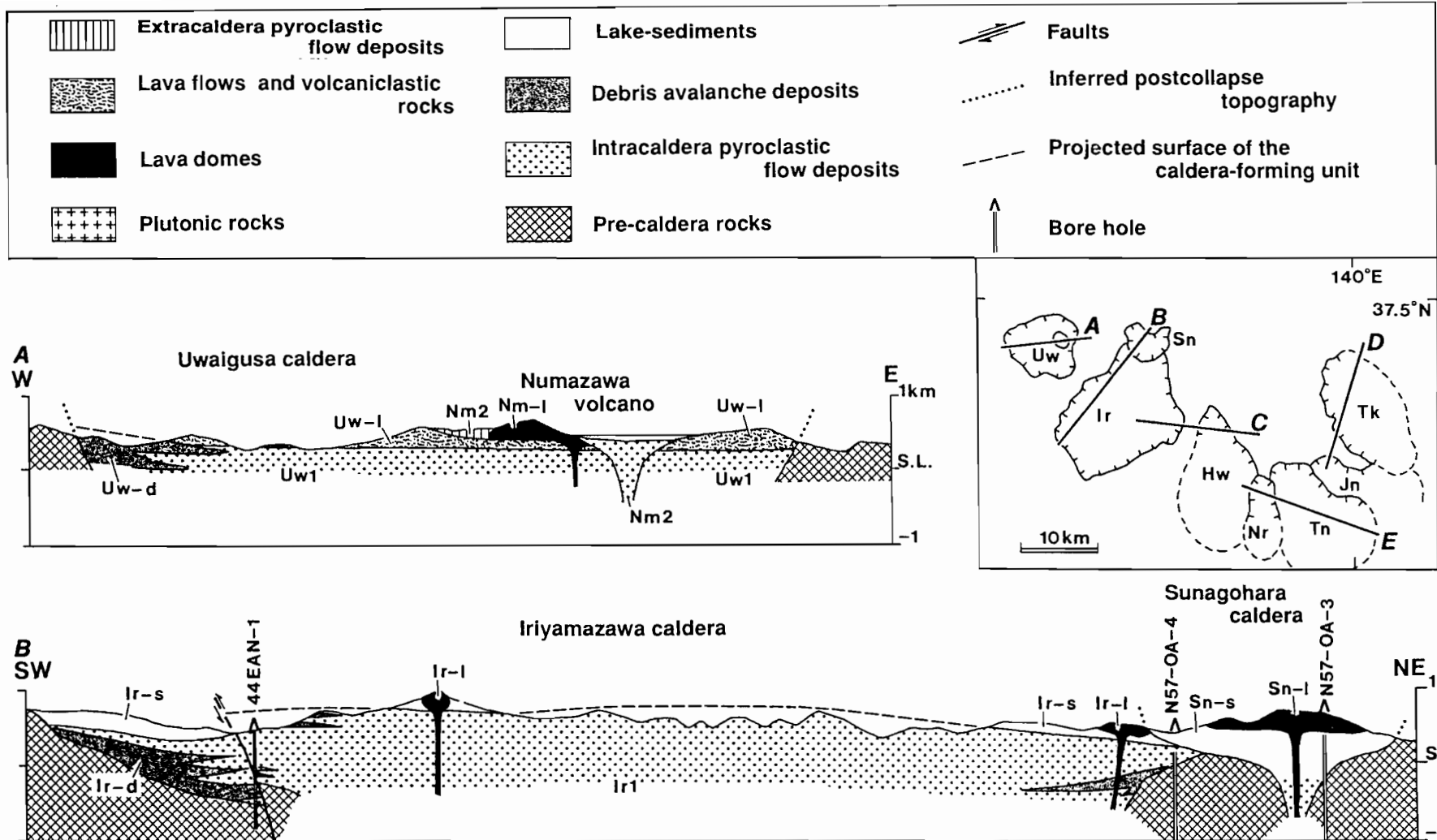
Fig. 8. Geological cross sections through eight caldera volcanoes in the Aizu volcanic field. Ft= Futamatayama volcano; Hk= Hakaseyama volcano; Hw= Hiwada Formation; Ir= Iriyamazawa Formation; Jn= Jonoirisawa Formation; Km= Kamafusayama pyroclastic flow deposit; Nm= Numazawa volcano; Nn= Nanaorezaka Formation; Nr= Narioka Formation; Sn= Sunagohara Formation; Tk= Takagawa Formation; Tn= Tonohetsuri Formation; Uw= Uwaigusa Formation; l= lava flows or lava domes; s= lake-sediments; p= plutonic rocks; d= debris avalanche deposits. Borehole data from MITI (1970) and NEDO (1985). No vertical exaggeration.
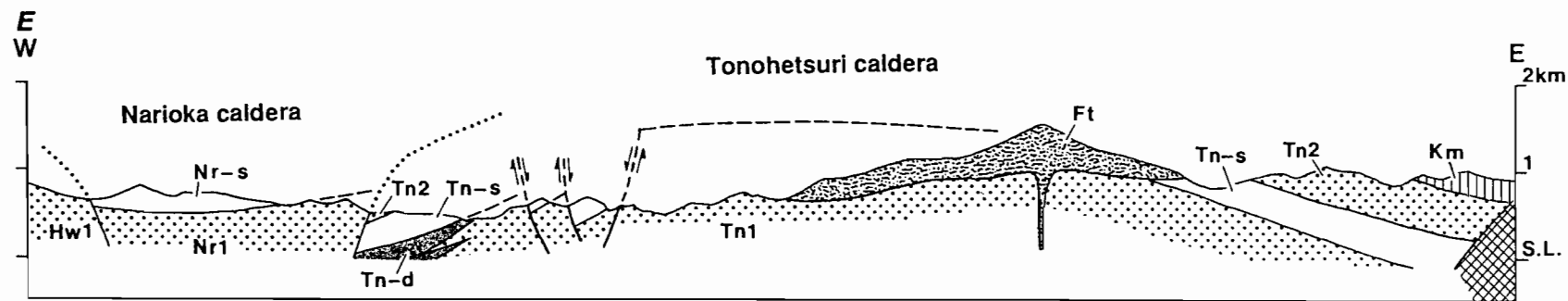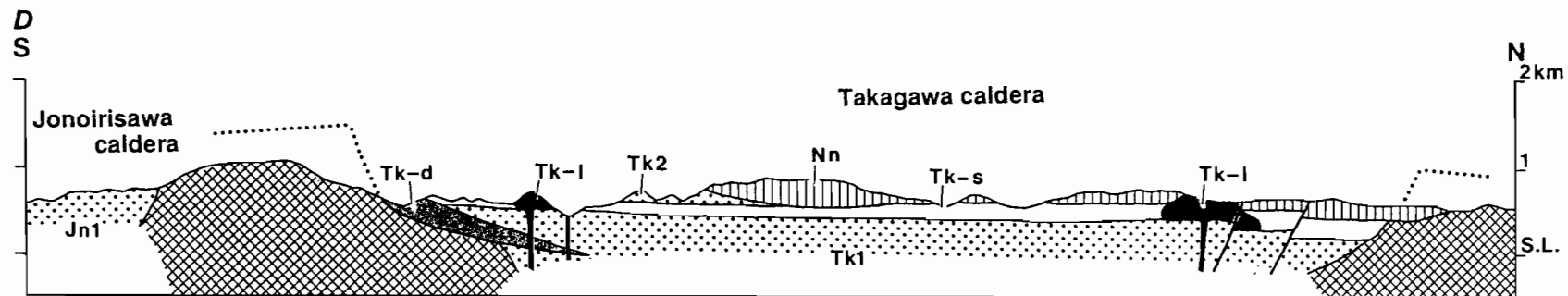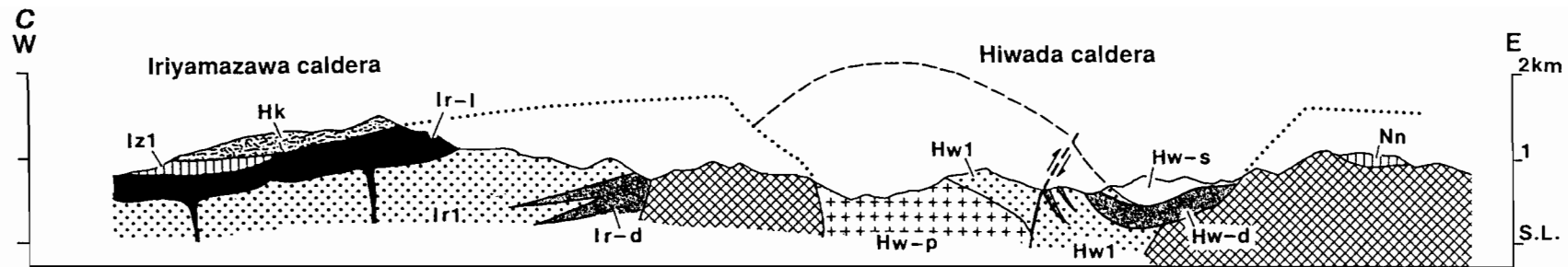
Fig. 8 (Continued)

## Takagawa caldera volcano

The Takagawa Formation (after Suzuki et al., 1972; Yamamoto, 1991) is horizontally filling an elliptical large caldera, 15 by 10 km across (Fig. 1). This formation is half overlain by the Nn1 pyroclastic flow deposit. The caldera-forming eruption occurred at about 6.3- 6.5 Ma and formed the intracaldera Tk1 and the extracaldera Fj3 pyroclastic flow deposits (Fig. 4). The post-caldera volcanism of this caldera is characterized by a discontinuous ring of lava domes and dikes (Yamamoto, 1991). No resurgent uplift was developed in this caldera (Fig. 8-D).

*Caldera-forming unit*

This unit consists of the Tk1 pyroclastic flow deposit and debris avalanche deposits; they are interbedded and form a single cooling unit. The exposed part of these deposits is now about 200 m thick, and the further voluminous part is presumably buried within the depression, because of its 30 mgal negative Bouguer gravity anomaly (Fig. 2; GSJ, 1993). The exposed Tk1 pyroclastic flow deposit is densely-welded, orthopyroxene-clinopyroxene-hornblende-quartz dacitic lapilli tuff and its appearance is homogeneous. The debris avalanche deposits are tabular sheets thinning out toward the caldera center, and consisting of ill-sorted lithic breccia of Mesozoic granodiorite and sedimentary rocks and early Miocene volcanic rocks. These breccia sheets characteristically contain abundant less-disturbed masses of debris, which preserves original stratigraphic structures of basement formations after pulverization; it is suggested that the breccia initially descended as a -avalanche from the caldera wall and moved without major turbulence (Yamamoto, 1991). Based on their distribution and kinds of the collapsed debris, a 1000-m-high topographic wall was presumably formed by the caldera-forming eruption (Yamamoto, 1991).

*Post-caldera unit*

This unit consists of caldera-lake sediments, the Tk2 pyroclastic flow deposit, andesite lava flows and resedimented volcaniclastic rocks, in ascending order, with intrusive lava

domes deforming the lake sediments (Yamamoto, 1991). The caldera-lake sediments are 100 to 250 m thick and composed mainly of 10-cm to 3-m-thick normally-, reverse-to-normally-, or non-graded pebbly sandstone and conglomerate, and parallel laminated siltstone and fine-grained sandstone with abundant plant fossils. These sedimentary rocks represent high-density turbidite or debris flow deposits and suspension-fallout deposits; they are presumably generated by minor slumps or rock-falls from the caldera wall after collapse. The Tk2 pyroclastic flow deposit is non-welded, hornblende-quartz dacite pumice lapilli tuff; the thickness is about 200 m and the magma volume is about 25 $km^3$. This deposit poorly contains lithic fragments except for the basal part which encloses large blocks of underlying sedimentary rocks. Its extracaldera equivalent is not found in the contemporaneous Fujitoge Formation. The uppermost deposits of this formation are less than 100 m thick and composed of orthopyroxene-clinopyroxene andesitic auto-brecciated lava flows and matrix-supported tuff breccia which represent debris flow deposits. This uppermost unit seems to represent a small stratovolcano within or near this caldera in the final stage, but it is uncertain that these products erupted using a vent system related to the caldera volcano. The intrusive lava domes are 0.5-1.5 km in diameter and made up of orthopyroxene-clinopyroxene andesite, orthopyroxene-clinopyroxene-quartz dacite, and hornblende-quartz dacite; they form a discontinuous ring of post-caldera volcanic centers.

## Uwaigusa caldera volcano

The Uwaigusa Formation (after Kitamura et al., 1968) is horizontally filling a quadrangular large caldera, 10 km in diameter (Fig. 1). This Formation underlies Numazawa volcano. The caldera-forming eruption occurred at about 4.1- 4.2 Ma and formed the intracaldera Uw1 and the extracaldera Fj4 pyroclastic flow deposits (Fig. 4). After the caldera depression, an andesitic composite volcano was formed within the caldera lake.

### *Caldera-forming unit*

This units consist of the Uw1 pyroclastic flow deposit and intercalated debris avalanche

deposits. The exposed part of these deposits is now about 200 m thick, and the further

voluminous part is presumably buried within the depression, because of its 25-30 mgal

negative Bouguer gravity anomaly (Fig. 2; GSJ, 1993). The exposed Uw1 pyroclastic flow

deposit is weakly- to non-welded, orthopyroxene- clinopyroxene-hornblende-bearing biotite-

quartz rhyolitic lapilli tuff. The cogenetic extracaldera Fj4 pyroclastic flow deposit, however,

is zoned from a hornblende-orthopyroxene-clinopyroxene-quartz dacitic base to a biotite-quartz

rhyolitic top. Some of feeder vents of the pyroclastic flow have been found along the western

margin of the caldera depression; the Uw1 pyroclastic material intrude into basement rocks as

clastic dikes, 10 cm to 2 m in thickness. These dikes occasionally contains carbonized woods

which are fall-back from the surface. The debris avalanche deposits are more than 200 m thick

sheets interbedded with the western part of the Uw1 pyroclastic flow deposit (Fig. 8-A), and

made up of ill-sorted lithic breccia of middle Miocene volcanic and sedimentary rocks. The

breccia contains abundant less-disturbed masses of debris, which preserves original

stratigraphic structures of basement formations after pulverization (Fig. 9-A); it results from

large-scale slope failures of the caldera wall during depression.


*Post-caldera unit*

This unit consists of abundant andesite lava flows and intercalated minor sedimentary

and volcaniclastic rocks. The lava is orthopyroxene-clinopyroxene andesitic and hornblende-

orthopyroxene-clinopyroxene-quartz andesitic. Most lava flows in lower and middle levels are

wholly auto-brecciated; they are made up of monolithic breccia in which polyhedral fragments

loosely fit together as in a three-dimensional jigsaw puzzle. The upper-level lava flows are

composed mainly of thick massive lava, whose K-Ar ages have been determined as 3.2- 3.4

Ma (Table 2). It is incredible that the volcanic activity had continued in 1 million years since

the caldera-forming eruption, but a quiescent interval has not been found in this unit such as a

major unconformity. The caldera-lake deposits interlayered with the lava flows consist of lithic

and pumiceous debris flow deposits, scoria lapillistone, and parallel-laminated vitric tuff and

siltstone. These deposits and lava are partly affected by hydrothermal alteration and

mineralization. No typical alignment of extrusive and intrusive centers are observed in this
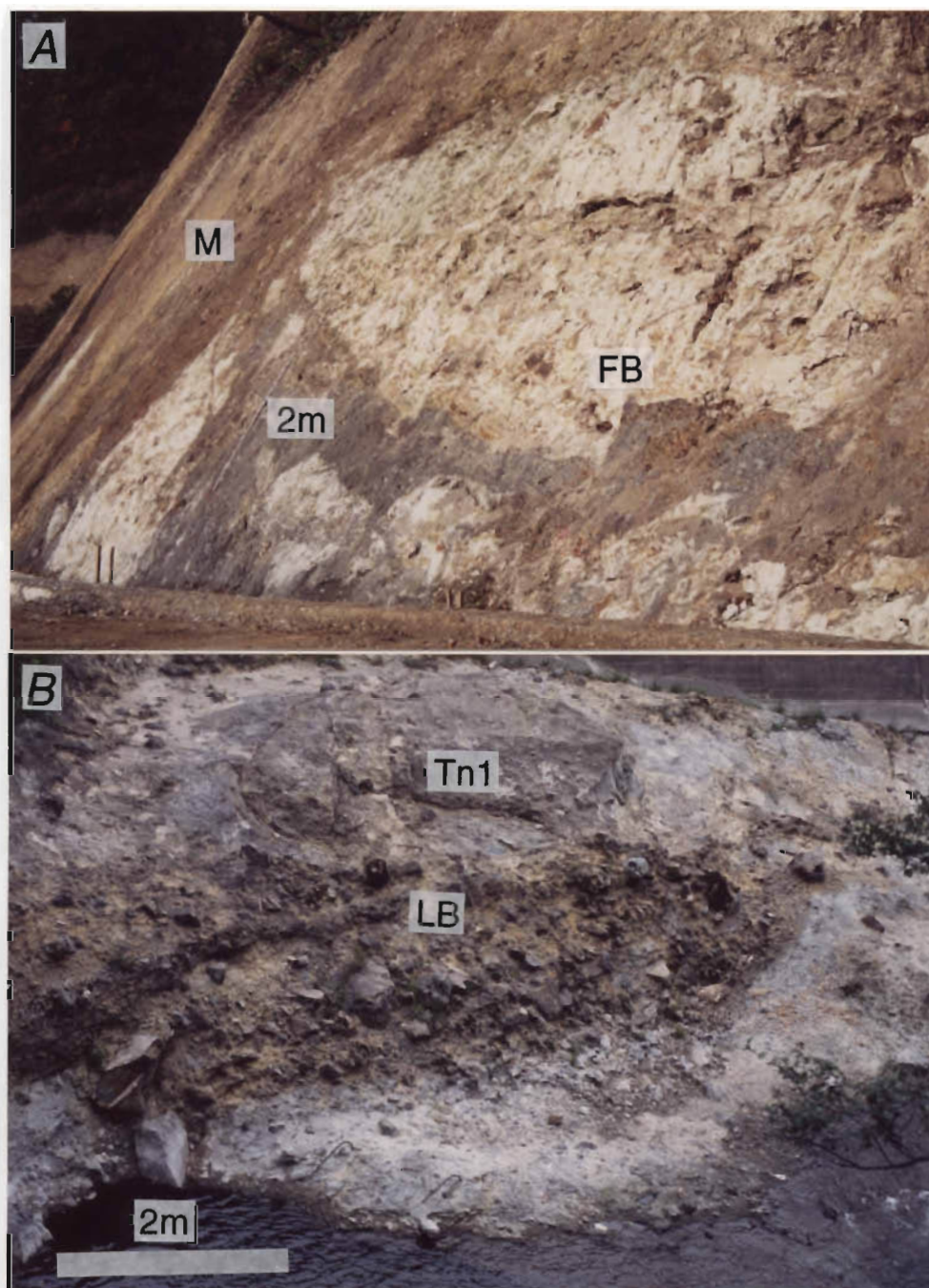
Fig. 9. Outcrop photographs of debris avalanche deposits in the intracaldera formations. (a) A faulted block (FB) of early Miocene alternating siltstone and vitric tuff within chaotic-sorted polylithic matrix (M) in the Uwaigusa Formation (Honna, Kanayama Town). (b) A lithic breccia lens (LB) intercalated with the Tn1 pyroclastic flow deposit (Tn1) in the Tonohetsuri Formation. The breccia is composed only of angular tonalite fragments, derived from the late Miocene Jonoirisawa Formation (Ashinohara, Shimogo Town).

caldera.

## Hiwada caldera volcano

The Hiwada Formation (after Yamamoto, 1992a) is filling an elliptical large caldera measuring 18 by 10 km (Fig. 1). This formation is partly overlain by the Nn1 pyroclastic flow deposit and the Narioka Formation. The caldera-forming eruption occurred at about 2.7 -2.9 Ma and formed the intracaldera Hw1 and the extracaldera Iz1 pyroclastic flow deposits (Fig. 4). This caldera is characterized by a prominent post-caldera resurgence and an intrusion of plutonic rocks. The resurgence took the form of a horst-like uplift bounded on its both sides by steep faults trending northward (Yamamoto, 1992a). No ring-dike system was developed in this caldera.

*Caldera-forming unit*

This unit consists of the voluminous Hw1 pyroclastic flow deposit and intercalated minor debris avalanche deposits. It is more than 1000 m thick in the uplifted core; the estimated magma volume is more than 110 $km^3$. The Hw1 pyroclastic flow deposits is densely- to weakly-welded, orthopyroxene-clinopyroxene-hornblende-quartz dacitic lapilli tuff. Especially, the lower part of this deposits is homogeneous, massive densely welded tuff with a minor amount of accidental materials. However, included lithic fragments and interlayered thin lenses of breccia, which consists of ill-sorted debris from early Miocene siltstone and volcanic rocks, are abundant in the upper part of the deposits. The breccia contains less-disturbed monolithic masses as same as those of the Takagawa caldera; it results from debris avalanches from the caldera wall. Hydrothermal alteration intensely affected these deposits surrounding post-caldera plutonic rocks.

*Post-caldera unit*

The postcaldera sedimentary rocks are only present along the northeastern and southwestern margins of the caldera, and are cut by faults and folded on the both sides of the

resurgent horst-like block (Fig. 8-C).  These rocks are 350 m in total thickness and composed mainly of 10-cm to 2-m-thick normally-, reverse-to-normally-, or non-graded pebbly sandstone and conglomerate, and parallel laminated siltstone and fine-grained sandstone with abundant plant fossils.  The coarse lake-sedimentary rocks contain abundant lithic fragments of basement rocks surrounding the caldera or rounded pumice of orthopyroxene-clinopyroxene-hornblende dacite; they are presumably washed from the caldera wall.  No evidence suggests that the debris was derived from the uplifted core consisting intracaldera welded tuff and plutonic rocks.

Gently tumescent-roofed tonalitic plutons are partly exposed within the uplifted core and accompanied with proceeding granodiorite porphyry dikes; they intruded into the caldera-forming unit.  The exposed part of plutons, representing the marginal facies, are less than 250 m in thickness and consist of fine-grained porphyritic biotite-hornblende tonalite.  A coarse-grained, voluminous interior of the intrusion presumably exists beneath the surface, because the vertical displacement of the resurgent block is estimated to be more than 1000 m (Fig. 8-C). Most intrusive rocks were subjected to hydrothermal alteration.


## Hakaseyama  volcano


The Hakaseyama Formation (after HCRG, 1990), 5 km northwest of the Hiwada caldera, is a dissected small stratovolcano made up of basalt and basaltic andesite thin lava flows and pyroclastics (Figs. 1 and 8-C).  This formation is 250 m in maximum thickness, and overlies the Iriyamazawa Formation and  the Fj4 and Iz1 pyroclastic flow deposits.  All rocks are porphyritic and contain phenocrysts of plagioclase, augite, hypersthene, and olivine.  The K-Ar ages of lava were reported at about 2.7 Ma (NEDO, 1985; Kobayashi and Inomata, 1986; Table 2).  This volcano was contemporaneous with Hiwada caldera volcano.


## Tonohetsuri  caldera  volcano


The Tonohetsuri Formation is filling an elliptical large caldera measuring 18 by 12 km,

and overlain by the Narioka Formation, Kasshi volcano, and Futamatayama volcano (Fig. 1). This revised formation contains the previous Tonohetsuri Formation, the Nagurasawa Formation, and the eastern part of the Yunokami Formation (Masuda et al., 1974; NEDO, 1990). The caldera-forming eruption occurred at about 1.4- 1.2 Ma and formed the intracaldera Tn1 and the extracaldera Nn2 (Ashino) pyroclastic flow deposits (Fig. 5); the magma volume of the Nn2 deposits is >30 km$^3$. Also, the post-caldera Tn2 eruption occurred at about 1.2- 0.9 Ma and fed the extracaldera Nn3 pyroclastic flow deposit (Fig. 5). This caldera is characterized by the thick intracaldera pyroclastic flow deposit and a resurgent dome (Fig. 8-E).

*Caldera-forming unit*

This unit is composed of the voluminous Tn1 pyroclastic flow deposit and intercalated minor debris avalanche deposits. They were produced by a major ignimbrite eruption and contemporaneous caldera collapse. The estimated thickness of these deposits is more than 1000 m in the resurgent dome; they are presumably more than 100 km$^3$ volume of magma. The Tn1 pyroclastic flow deposit is hornblende-orthopyroxene-clinopyroxene-quartz dacitic densely- to non-welded pumice lapilli tuff. Included lithic fragments and interlayered thin lenses of breccia are abundant in the upper and marginal part of the deposits (Fig. 9-B). The breccia is ill-sorted and made up of angular fragments of Mesozoic sedimentary rocks and Miocene volcanic, plutonic, and sedimentary rocks surrounding the caldera. Furthermore, it contains less-disturbed monolithic masses of debris; the breccia lenses represent debris avalanches caused by large-scale slope failures of the caldera wall.

*Post-caldera unit*

This unit consists of caldera-lake sediments, extrusive lava domes, and the Tn2 pyroclastic flow deposit. The post-caldera sedimentary rocks are about 300 m thick and represented by various sediment gravity flows washed from the caldera wall and from the post-caldera lava domes, as well as interbedded pyroclastic deposits and parallel-laminated siltstone. The gravity flow deposits are represented by 10-cm to 6-m-thick normally, reverse-to-

Fig. 10. Photographs of post-caldera lake sediments in the Tonohetsuri
Formation. (a) Matrix supported, nongraded or normally-graded debris
flow deposits, containing abundant pre-caldera rock debris. They are
interpreted to be generated by minor slumps from the caldera wall
after collapse (Shiroiwa, Shimogo Town). (b) Normally-graded
volcaniclastic turbidites, consisting wholly of comminuted glassy
dacite. They represent sublacustrine fan deposits at the foot of a post-
caldera lava dome (Tonohetsuri, Shimogo Town).

normally, or non-graded pebbly sandstone and conglomerate, made up of various debris from basement formation and cogenetic extracaldera pyroclastic deposits or of polyhedral dacite fragments from the extrusive lava domes (Fig. 10). The lava domes erupted on the northeastern flank of the resurgent dome; the K-Ar age of one of them was reported at 0.94± 0.05 Ma (Table 2). They are 1- 2.5 km in diameter and composed of hornblende-orthopyroxene-clinopyroxene-quartz dacite. The Tn2 pyroclastic flow deposit is 500 m thick and composed of non-welded, hornblende-orthopyroxene-clinopyroxene-quartz dacitic lapilli tuff; its estimated magma volume is about 35 $km^3$. This deposit conformably overlie the lake-sediments, and contains deformed rip-up clasts of laminated siltstone at the base. On the other hand, this deposit is covered by massive poorly-sorted pebbly pumiceous sandstone and horizontal discontinuous bedded sandstone and pumice conglomerate with a erosional base; they represent resedimented lahars from pyroclastic debris. No vent of this pyroclastic flow is found within the caldera.

The post-caldera resurgence produced an gentle-sided uplifted dome whose apical part was broken and tilted by normal faults with small displacements (Fig. 8-E). This dome is symmetrically positioned within the this elliptical caldera and characterized by radially outward dips of all deposits filling the caldera. The vertical displacement in the center of the dome is estimated to be about 1500 m. Major resurgence occurred after the Tn2 eruption, because the thickness of the lake-sediments interlayered between the Tn1 and Tn2 tuffs is almost constant in the dome. However, it is uncertain that minor deformation within the caldera did not occur after the Tn1 eruption and immediately before the Tn2 eruption.

## Narioka caldera volcano

The Narioka Formation is horizontally filling an elliptical medium caldera, 8? by 4 km across. This formation is located on the western side of the Tonohetsuri caldera and overlain by the volcaniclastic fan deposits of Kasshi volcano and the Kamafusayama pyroclastic flow deposit (Fig. 1). This revised formation contains the previous Narioka Formation and the western part of the Yunokami Formation (Masuda et al., 1974). This caldera is characterized

by absence of post-caldera volcanism and resurgence.

*Caldera-forming unit*

This unit consists of the Nr1 pyroclastic flow deposit. The exposed part of this deposit is now about 250 m in thickness (7 $km^3$ in volume), and the further voluminous part is presumably buried within the depression (Fig. 8-E), because of its 25- 30 mgal negative Bouguer gravity anomaly (Fig. 2; NEDO, 1990; GSJ, 1993). The Nr1 pyroclastic flow deposit is densely- to weakly-welded, orthopyroxene- clinopyroxene-hornblende-quartz dacitic lapilli tuff. This deposit heterogeneously incloses external large blocks of the Tn2 pyroclastic flow deposits, laminated siltstone and sandstone, granodiorite, etc., some blocks are more than 60 m in diameter. Pyroclastics surrounding such blocks are only weakly-welded.

The caldera-forming eruption presumably occurred at about 0.9- 0.7 Ma and shed the extracaldera Nn4 (Nishigo) pyroclastic flow deposit (Fig. 5). A previous paleomagnetic study for the extracaldera formations (Manabe, 1980) has revealed that the eruption of the Nn4 pyroclastic flow occurred in the end of the Matsuyama epoch younger than the Jaramillo event, 0.73- 0.90 Ma, although the K-Ar ages of 1.4- 1.6 Ma have been reported for this deposit by Suzuki et al. (1976) at the Sirakawa district. Also, these K-Ar ages are evidently older than the various ages for the underlying Nn2 pyroclastic flow deposit (Suzuki et al., 1976; this study). Similarly, the K-Ar ages of 1.4- 1.5 Ma have been reported for the Nr1 pyroclastic flow deposit by NEDO (1990), but these ages are older than the ages for the underlying intracaldera Tn1 pyroclastic flow deposit (NEDO, 1990; this study). Thus, both geochronologically unavailable results suggest that the Nn4 and Nr1 pyroclastic flow deposits contain excess argon. Their stratigraphic relations and comparable phenocryst populations (Fig. 7) point out that the Nr1 and Nn4 pyroclastic flow deposits are cogenetic. The magma volume of the Nn4 deposit is about 40 $km^3$.

*Post-caldera unit*

This unit consists of caldera-lake sediments, 300 m in maximum thickness. These sediments are made up of 10-cm- to 3.5-m-thick normally-, reverse-to-normally-, or non-

graded pebbly sandstone and conglomerate, and parallel laminated siltstone and fine-grained sandstone. Coarse lake-deposits contains various fragments of basement rocks and cogenetic extracaldera pyroclastic materials; they represent sediments gravity flows washed from the caldera wall. No product of post-caldera volcanism, including lava, intrusions, and resurgence, is found within the caldera.

## Sunagohara caldera volcano

The Sunagohara Formation (after Komuro, 1978; NEDO, 1985) is horizontally filling a polyhedral medium caldera, 6 by 4 km across (Fig. 1). This is covered by the Nm1 and Nm2 pyroclastic products of Numazawa volcano. The Oku-Aizu geothermal system is developed within this caldera and various explorations have been carried out by the New Energy Development Organization and the Okuaizu Geothermal Co., Ltd. Based on the abundant borehole data, they have revealed that a broad funnel-shaped floor exists beneath the caldera-lake sediments, 600 m in maximum thickness, and the vertical displacement of pre-caldera basements is small (NEDO, 1985; Fig. 8-B). According to Mizugaki (1992), there is a narrow central conduit filled by caldera-forming, lithic-rick pyroclastic deposits in the deepest part of this caldera, similar to late Pleistocene Nigorikawa caldera in northern Japan (Ando, 1981).

*Caldera-forming unit*

No caldera-forming pyroclastic deposit is exposed within the caldera. Yamamoto (1992b) has concluded that the extracaldera Td1 pyroclastic flow was formed by this caldera-forming eruption at 0.7- 0.5 Ma (Fig. 5), based on the age data of the Sunagohara Formation (Table 2; NEDO, 1985) and an interpretation of sedimentary facies in the extracaldera Todera Formation. The fission track age of the Td1 deposit was newly determined as 0.96±0.18 Ma (Table A1), although Manabe's (1980) paleomagnetic data indicate the Td1 eruption occurred at the Brunhes epoch. This older age for the Td1 deposit might be caused by contaminations of accidental zircons, in fact, the Td1 deposit is filling incised valleys within volcaniclastic rocks of the Nanaorezaka Formation (Yamamoto, 1992b). The Td1 pyroclastic flow deposit is non-

welded hornblende-orthopyroxene-clinopyroxene-quartz dacite lapilli tuff. Although the large part of this deposit was vanished by fluvial erosion, the magma volume of the Td1 deposit may be several 10 $km^3$.

*Post-caldera unit*

The exposed part of this formation is about 300 m thick and consists of caldera-lake sediments, lava domes, and the Sn2 post-caldera pyroclastic flow deposit. The caldera-lake sediments are made up matrix-supported massive lithic breccia, non-graded thick pumiceous pebbly sandstone, massive vitric tuff, and parallel- or ripple-laminated siltstone and pumiceous sandstone. The lava domes are 0.5- 2.5 km in diameter and composed of biotite-hornblende perlitic rhyolite; one dome intruded into the lake-sediments, but the other shed a volcaniclastic debris intercalated with the sediments. The Sn2 pyroclastic flow deposits is non-welded biotite rhyolitic lapilli tuff containing accessory fragments of biotite-hornblende rhyolite; this deposits overlie the lake-deposits and 100 m in thickness. The Sn2 deposit is an intracaldera equivalents of the Td2 pyroclastic flow deposits in the Aizu Basin (Yamamoto, 1992b), but its vent location has not been found within the caldera. The post-caldera Td2 eruption occurred at about 0.22- 0.29 Ma. The magma volume of the Td2 deposit is estimated to be less than 10 $km^3$. The post-caldera pyroclastic eruption presumably occurred independently of the extrusion of a lava dome, because there is no cogenetic lava dome of the Sn2 pyroclastics.

## Kasshi and Futamatayama volcanoes

These two volcanos are Quaternary composite volcanoes built on the Tonohetsuri caldera (Fig. 1); they form the northern part of Nasu volcanic group. Kasshi volcano is a highly dissected stratovolcano, and its main edifice is made up of alternated layers of lava flows and pyroclastic rocks of pyroxene andesite. The Kamafusayama pyroclastic deposits, which are orthopyroxene-clinopyroxene dacitic pyroclastic flow and air-fall deposits, crop out at the eastern and western foots of the volcano and underlie the andesitic fan deposits. The K-Ar ages of both of them were reported as 0.6- 0.4 Ma (NEDO, 1990; Ban and Fujimaki,

32

1992), however it is uncertain that the Kamafusayama pyroclastics erupted using a vent system of Kasshi volcano. The Kamafusayama pyroclastic deposits represent more than five episodes of pyroclastic eruption, and their total magma volume was estimated to be about 10 km$^3$ (Yoshida and Takahashi, 1991). Futamatayama volcano consists of thick lava flows and pyroclastic rocks of olivine-quartz-bearing pyroxene andesite. This volcano was formed at about 0.1 Ma (NEDO, 1990; Ban and Fujimaki, 1992).

## Numazawa caldera volcano

Numazawa volcano (after Takahashi and Sugawara, 1985) is located on the western end of the caldera cluster and overlies the Uwaigusa caldera volcano (Figs. 1 and 8-A). Its products are composed of the Nm1 (Mizunuma) pyroclastic flow deposit, the central lava domes, and the Nm2 (Numazawako) pyroclastic flow deposit, in ascending order. At the center of the volcano, there exists a small caldera lake, 2 km in diameter, Lake Numazawa, formed by the Nm2 eruption. The Nm1 eruption produced densely- to weakly-welded pyroclastic flow and air-fall deposits of biotite-hornblende-quartz dacite. The Nm1 fall-out deposits are interposed between the Td2 pyroclastics of Sunagohara caldera volcano at about 0.22-0.29 Ma (Yamamoto, 1992b) and the Hp2 pyroclastics of Bandai volcano (Chuman and Yoshida, 1982), which is stratigraphically just above the widespread On-Pm1 tephra at about 80 ka (Machida and Arai, 1992, p.132-133). The five lava domes surround the caldera lake and are cut by its collapsed wall; they are composed of orthopyroxene-clinopyroxene-hornblende-quartz dacite and hornblende-biotite-quartz dacite. No cogenetic pyroclastic deposit of individual lava domes is found around the volcano. The Nm2 eruption occurred at about 5 ka (Table 1), and produced pyroclastic flow, surge, and air-fall deposits of hornblende-orthopyroxene-quartz dacite. The pyroclastic flow and surge deposits are non-welded and form a terrace along the river; the total magma volume of both of them is estimated to be about 2 km$^3$.

# 4. EXTRACALDERA FORMATIONS IN THE AIZU BASIN: OVERVIEWS

Late Miocene- middle Pleistocene extracaldera formations, the Shiotsubo, Fujitoge, Izumi, Nanaorezaka, and Todera Formations in ascending order (Suzuki, 1951; Suzuki et al., 1972; 1977), are mainly exposed on the western side of the present Aizu Basin (Fig. 11). The Shiotsubo Formation consists of coarsening-upward shallow marine deposits, but other formations are made up of fluvial sediments and intercalated many pyroclastic flow deposits (Yamamoto, 1992b; Yamamoto and Yoshioka, 1992). These formations are about 1000 m in total thickness and rest conformably upon middle- late Miocene offshore shelf deposits in the central part of the extracaldera basin, but they are more thin and rest unconformably upon underlying formations in the marginal part.

The extensive pyroclastic flow deposits within these formations are mainly shed from the caldera volcanoes in the Aizu volcanic field, based on the geochronological, petrographical, and lithological correlations (Figs. 4 and 5). However, source volcanoes of the extracaldera Fj1, Fj2, Fj5, Fj6, Fj7, Iz2, and Nn1 pyroclastic flow deposits are unknown. The distribution and lithic-clast size of the Nn1 (Kumado) pyroclastic flow deposit have suggested that its source is presumed to be located around Futamatayama or Kasshi volcanoes, namely beneath Tonohetsuri caldera formed after the Nn1 eruption (Yoshida and Takahashi, 1991). Furthermore, the Fj5, Fj6, and Fj7 pyroclastic flow deposits are minor units filling paleo-channels in the northern part of the extracaldera basin, and they are presumed to be shed westward from caldera volcanoes around Bandai and Azuma volcanoes (Fig. 1). No comparable information is obtained between the extracaldera Fj2 and intracaldera Jn1 pyroclastic flow deposits, although two deposits appear to be in a same stratigraphic position (Fig. 4).

LEGEND

- ALLUVIUM
- TODERA FM.
- NANAOREZAKA FM.
- IZUMI FM.
- FUJITOGE FM.
- SHIOTSUBO FM.
- EARLY-MIDDLE MIOCEME FM.
- MESOZOIC ROCKS
- FAULT
- ROUTE OF SECTION
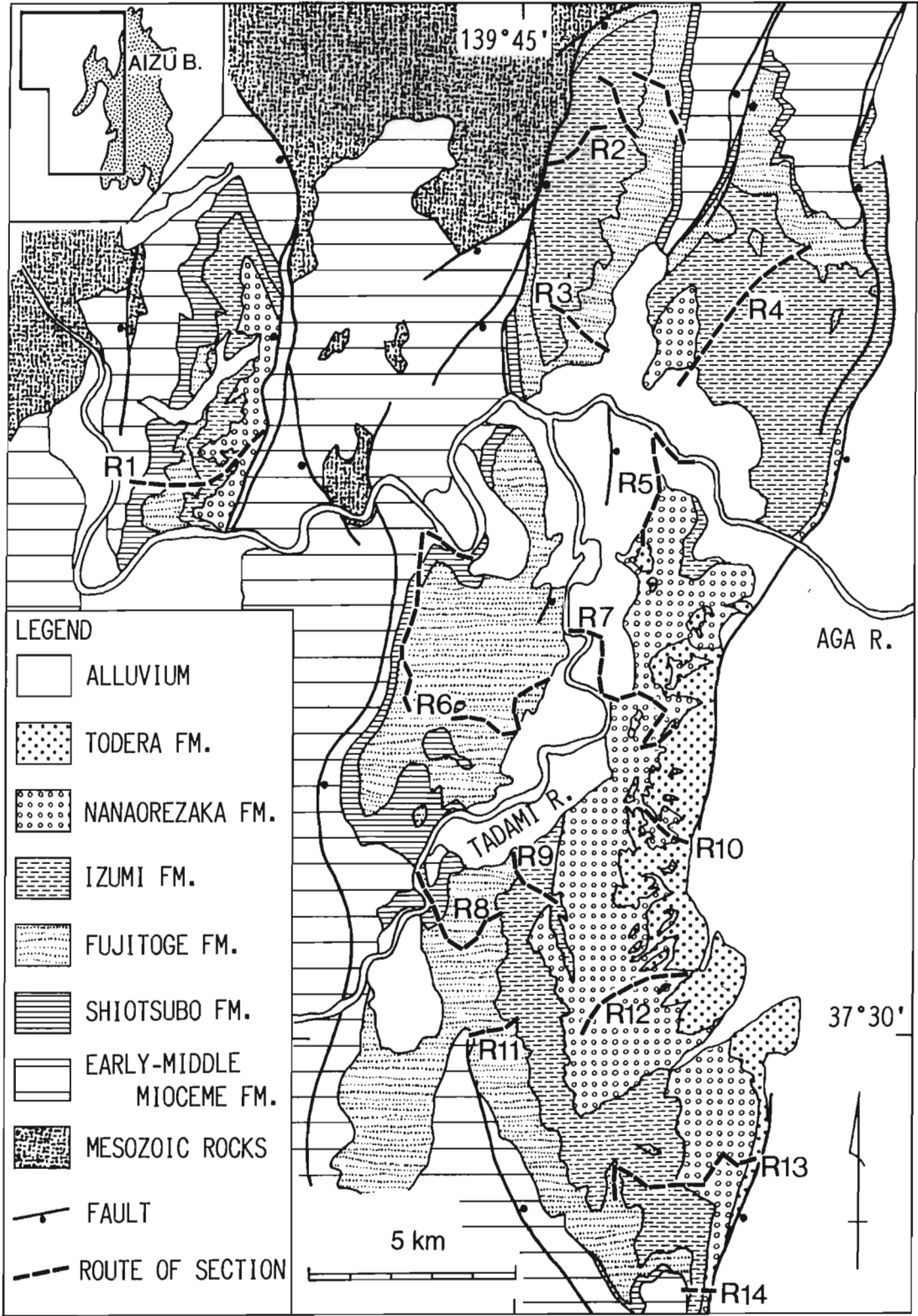
AIZU B.

139°45'

AGA R.

TADAMI R.

37°30'

5 km

Fig. 11. Geologic map of the extracaldera formations on the west of the Aizu Basin. R1- 14 are the numbers for measured sections.

35

# 5. FACIES ASSOCIATION OF EXTRACALDERA FORMATIONS

The extracaldera formations consist of nine sedimentary facies associations. There are: (1) primary pyroclastics, (2) lahars, (3) gravelly fluvial-channels, (4) sandy fluvial-channels, (5) floodplains, (6) tidal flats, (7) delta fronts, (8) pro-delta slopes, and (9) pro-delta turbidites. Assignation of facies associations and respective depositional environments are inferred from lithologies, lithologic sequences, sedimentary structures, and the adjacent associations. Boundaries between facies associations, particularly the subaerial ones, are often gradational.

"Lahar" in the broad sense is a mass flowage of water-mobilized rock debris from a volcano (Crandell, 1971; Fisher and Schmincke, 1984, p.298). Lahars are events that can display a complex history of changes in flow type. Both debris flow and hyperconcentrated flood flow can occur in a single lahar at different times and places (Pierson and Scott, 1985; Lowe et al., 1986; Best, 1992). Debris flows are high-sediment-concentrated flows with plastic properties that deposit sediment by mass emplacement, when shear stress decreases below the yield strength of the debris (Middleton and Hampton, 1976). Hyper-concentrated flood flows contain intermediate sediment-concentrations between debris flow and stream flow, and cause rapid grain-by-grain deposition from both suspension and traction (Smith, 1986).

## Lithofacies codes

A lithofacies code system was introduced by Miall (1977, 1978) and Rust (1978) to standardize descriptive classification of lithologies and sedimentary structures, that is applicable to most fluvial deposits, and has received wide usage. Table 3 lists Miall's (1978) facies codes appropriate for this study, and those used by Mathisen and Vondra (1983), Smith (1987), and Orton (1991) for some non-marine and shallow-marine volcaniclastic sediments.

## Facies association 1: primary pyroclastic deposits

Many pyroclastic flow deposits are interbedded with fluvial sediments in the

Table 3.  Facies nomenclature for the extracaldera formations in the Aizu district.

| Code | Lithofacies | Interpretation |
|------|-------------|----------------|
| Gms[a] | Matrix supported, nongraded, massive gravel. Thin inversely graded base.  Poorly sorted ashy matrix and pumice lapilli.  No gas-escape pipe. | Debris flow |
| Gmb[b] | Clast supported, relatively well sorted, massive or crudely bedded gravel.  Imbricated on b-axis. | Traction deposits; longitudinal bars, channel lags |
| Gma[b] | Clast supported, normally or reverse-to-normally graded gravel with abundant sandy matrix.  Gravel clast oriented with both a- and b-axis transverse to flow direction.  Poorly imbricated. | Rapid deposition both from suspension and by traction; high-density turbidite, hyper-concentrated flood flow |
| Gt[a] | Trough crossbedded gravel | Channel fill |
| Gp[a] | Planar crossbedded gravel | Straight-crested transverse bar |
| Sm[c] | Massive, medium-to-very coarse grained sand with poorly sorted ashy matrix and pumice lapilli.  Random distribution of clast. | Debris flow; analogous to Gms |
| Smg[b] | Massive or normally graded, moderate to poorly sorted fine-to-very coarse grained sand, may be pebbly | Rapid deposition from suspension; turbidite, overbank flood flow |
| Smb | Massive, bioturbated, moderately to poorly sorted, fine-to-very coarse grained sand with pebble cluster.  Marine mollusca and concretions. | Inner-shelf deposits |
| Shb[b] | Horizontal but discontinuous bedded, moderately to poorly sorted, fine-to-very coarse grained sand.  Gradational contacts between fine and coarse beds, 0.5 to 10 cm thick.  Individual beds are rarely normally graded. | Possibly produced by low-amplitude, long-wave length dunes; hyper-concentrated flood flow |
| Ss[a,d] | Low-angle trough crossbedded or scour-fill bedded, well to poorly sorted, pebbly or fine-to-very coarse grained sand.  Gravel lags and rounded pumice. | Scour and fill by shallow, high-discharge flow |
| St[a] | Trough crossbedded, moderately to well sorted, pebbly or medium-to-very coarse grained sand | Sinuous-crested dune |
| Sp[a] | Planar crossbedded, moderately to well sorted, pebbly or medium-to-very coarse grained sand | Straight-crested bars (sandwaves, transverse bars) and linguoid bars |

| | | |
|---|---|---|
| Shl[b] | Horizontal laminated, fine-to-coarse grained sand | Formed in shallow upper flow regime |
| Sr[a] | Ripple-laminated, very fine-to-medium grained sand | Waning flow, overbank flow |
| Fl[a] | Finely laminated very fine sand, silt and mud. Small ripples and convolute bedding. | Waning flow, overbank flow |
| Fm[a] | Massive silt and mud | Suspension sedimentation in quiet-water |
| Fr[a] | Silt and mud. Root casts and rootlets. Usually oxidized, organic rich tops. | Paleosols |
| C[a] | Lignite. Silt and mud films. | Swamp |

[a] Miall (1978),  [b] Smith (1987),  [c] Orton (1991),  [d] Palmer & Neal (1991)

Table 4.  Facies associations

| Facies Association | Dominant Facie | Minor Facies | Interpretation |
|---|---|---|---|
| FA1 | | | Primary  pyroclastics |
| FA2 | *Shb, Ss* | *Gms, Gma, Sm, Fr* | Lahar |
| FA3 | *Gmb* | *Shl, St, Sp, Fl, Fm* | Gravelly  fluvial-channels |
| FA4 | *St, Gt* | *Sr, Shl, Fl, Fm* | Sandy  fluvial-channels |
| FA5 | *Fm* | *Shl, St, Smg, Sr, Fl* | Floodplain |
| FA6 | *Fr, Fl* | *St, Sp* | Tidal  flat |
| FA7 | *St, Sp, Gt, Gp* | *Gms, Sm, Shl, Fl* | Delta  front |
| FA8 | *Smb* | *Gma, Shl, Sr* | Pro-delta  slope |
| FA9 | *Smg, Shl* | *Sr, Fl, Fm* | Pro-delta  turbidites |

extracaldera basin. They are massive sheets, 2 - 200 m thick, composed of pumice lapilli and lithic fragments supported in a matrix of vitric ash and shattered crystals. All sheets contain abundant gas-escape pipes, and some sheets are welded. The Nn3 and Nn4 pyroclastic flow deposits are accompanied with basal layered deposits (layer 1), 10 to 50 cm thick, consisting of well-sorted ash layers and clast-supported lithic pebble beds (Figs. 12 and 13). The Fj4 pyroclastic flow deposit overlies 8- to 15-m-thick pyroclastic surge deposits containing abundant accretionary lapilli. However, most massive pyroclastic sheets directly cover fluvial sediments with a sharp inversely-graded base. Rip-up clasts from underlying beds are locally found near the base of the sheets. Overlying ash-cloud deposits (layer 3) are hardly found above the massive sheets, that are overlaid by sandy lahar or fluvial-channel deposits with an erosional contact (Fig. 13).

**Facies association 2: lahar deposits**

*Description*

This facies association (Table 4; Fig. 14) consists of horizontal discontinuous bedded sandstone (*Shb*), low-angle trough or scour-fill crossbedded sandstone (*Ss*), massive poorly sorted sandstone (*Sm*), and poorly sorted conglomerate (*Gma* and *Gms*). Sequences are 1 to 20 m thick and commonly represented by facies *Shb* and *Ss* alternation or facies *Sm* alone. Sandstone is moderate to poorly sorted, fine- to very coarse-grained, and is composed almost exclusively of dacitic or rhyolitic detritus; quartz, plagioclase and mafic crystals, glass shards, and rounded pumice. Facies *Gms* is made up of sandy matrix and pumice lapilli with thin inversely graded base. Facies *Gma* consists of tight-packing lithic pebbles and grads upward into facies *Shb*. These sandy and pebbly deposits contain logs and plant debris. Massive siltstone containing lignite (*Fm* and *C*) or pedogenically oxidized siltstone (*Fr*) often cap these sequences.

In a proximal environment, pumiceous pebbly coarse-grained sandstone sheets over pyroclastic flow deposits with broad erosional contacts (Fig. 12). Facies *Shb*, *Sm*, and *Gms* are prominent and relatively thick above the Fj4, Iz1, and Nn1- 4 pyroclastic flow deposits.
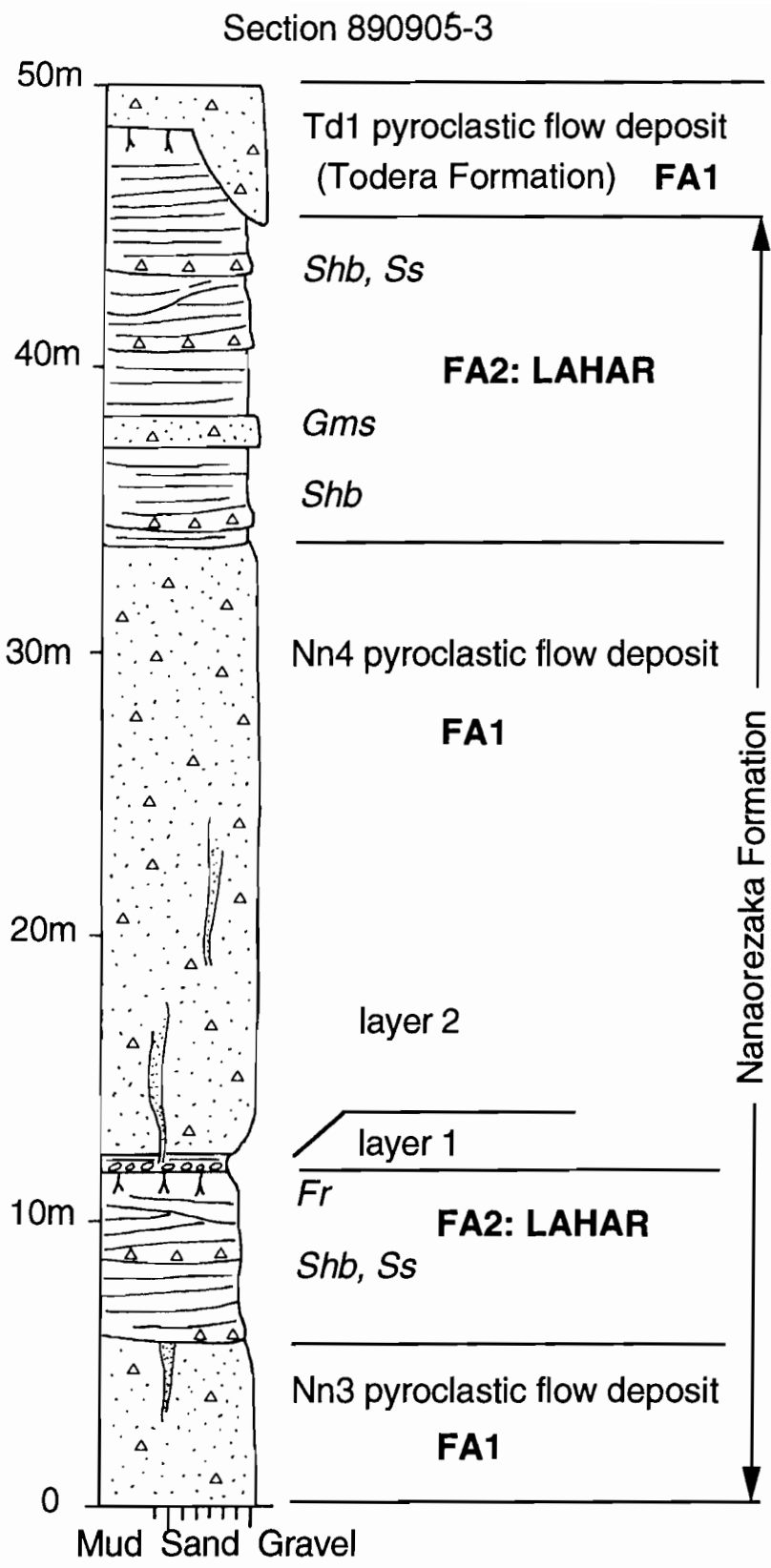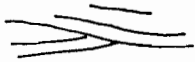
Section 890905-3

50m — Td1 pyroclastic flow deposit
(Todera Formation)  **FA1**

*Shb, Ss*

**FA2: LAHAR**

40m — *Gms*

*Shb*

30m — Nn4 pyroclastic flow deposit

**FA1**

layer 2

20m —

layer 1

*Fr*

10m — **FA2: LAHAR**

*Shb, Ss*

Nn3 pyroclastic flow deposit
**FA1**

0 —

Mud  Sand  Gravel

Nanaorezaka Formation
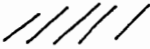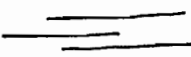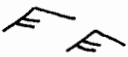
Fig. 12.  Typical section of alternating primary pyroclastics (facies association 1) and proximal lahar deposits (facies association 2) in the Nanaorezaka Formation, the upper part of R12 (Fig. 11).  Facies abbreviated as in Table 3.

41

| | SCOUR-FILL CROSSBEDDING |
| | TROUGH CROSSBEDDING |
| ///// | PLANAR CROSS BEDDING |
| | HORIZONTAL STRATIFICATION |
| | RIPPLE CROSS-STRATIFICATION |
| λ  λ | ROOT TRACES |
| | LIGNITE |
| U  U | BURROWS |
| | MOLLUSCA |
| △ △ ◁ | PUMICE |
| ◎ ◎ ◉ | ACCRETIONARY LAPILLI |
| | GAS-ESCAPE PIPE |

| CLAY | VERY FINE | FINE | MEDIUM | COARSE | VERY COARSE | |
| Mud | SILT | | Sand | | PEBBLE | Gravel |
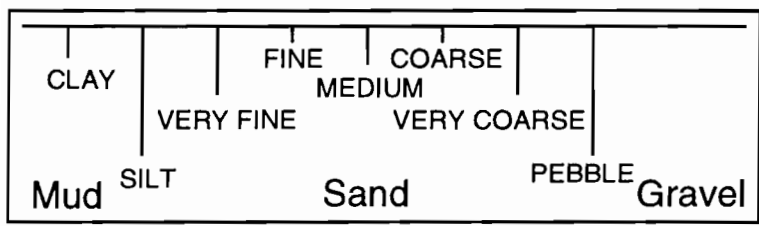
Fig. 12 (Continued)
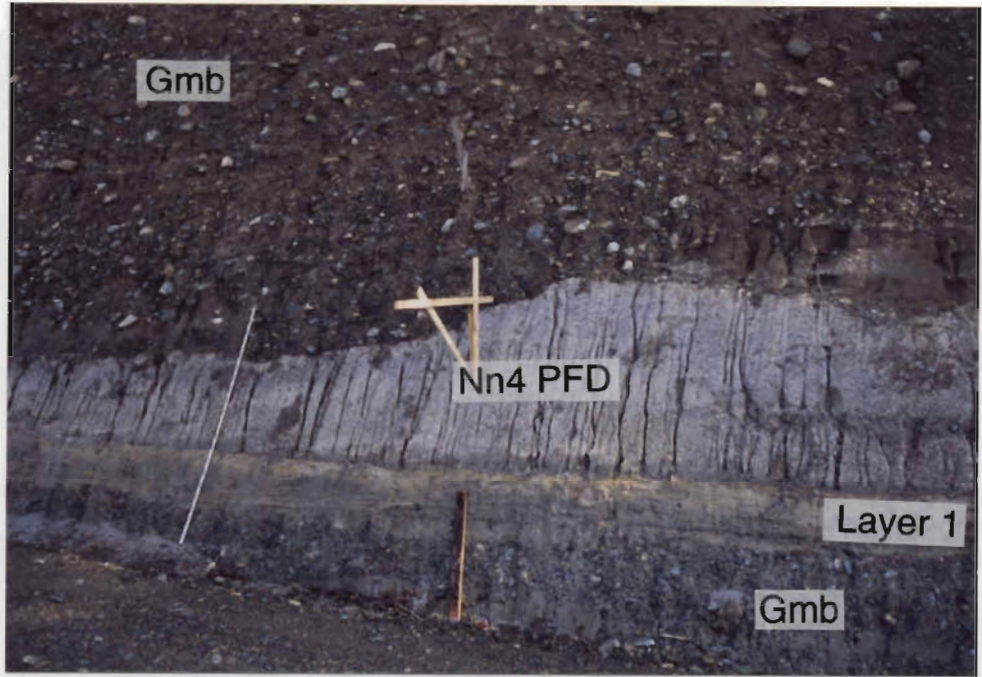
Fig. 13.  Outcrop photograph of the highly eroded Nn4 pyroclastic flow deposit, the Nanaorezaka Formation (Sakashita, Aizubange town; the upper part of R7; Fig. 11).  Massive, clast-supported gravel (*Gmb*) is filling the erosional channel.  The layer 1 is ground surge deposits made up of parallel- or low-angle-cross-laminated ash.  The scale is 2 m.
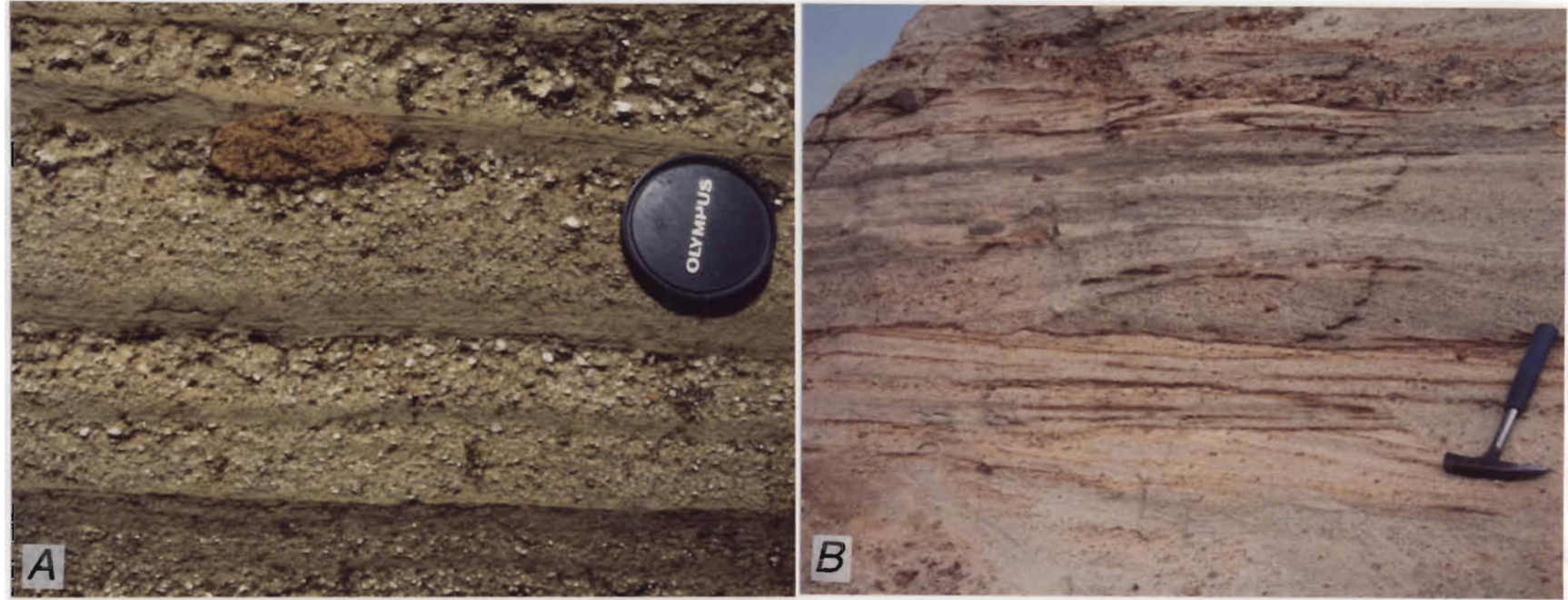
Fig. 14. Examples of lahar deposits (facies association 2). (a) Horizontal bedding (*Shb*) in hyperconcentrated flood flow deposits, the Nanaorezaka Formation (Iritazawa, Niitsuru Village, the upper part of R12; Fig. 11). Abundant rounded pumice is concentrated at the upper part of individual coarse-grained pebbly sandstone. (b) Scour-fill crossbedding (*Ss*) in sheet-flood deposits, the Todera Formation (Sakasegawa, Niituru Village, 3 km north of R13; Fig. 11).

**Section 901020-2**

| | | |
|---|---|---|
| St | **FA4: SANDY FLUVIAL-CHANNELS** | |
| Sr, Fl | **FA6: TIDAL PLAIN** | |
| Shb | | |
| Fr | **FA2: LAHAR** | |
| Shb | | |
| Ss | | |
| Fl | **FA5: FLOOD PLAIN** | |
| Smg | | |
| Shb | | |
| Fm | **FA2: LAHAR** | |
| Shb, Ss | | |
| | pyroclastic fall deposits **FA1** | |
| Smg | | |
| Fm | **FA5: FLOOD PLAIN** | |
| Smg | | |
| Fm | | |
| Shl | | |
| Shb | **FA2** | |
| | Fj1 pyroclastic flow deposit **FA1** | |
| Fm | **FA5** | |
| Shl | **FA7: DELTA FRONT** | |
| Sp | (Shiotsubo Formation) | |

Fujitoge Formation

40m / 30m / 20m / 10m / 0

Mud Sand Gravel

Fig. 15. Measured section of the lowermost part of the Fujitoge Formation, representing sandy lahar-dominated fluvial deposits in a distal environment, 3 km south of R3 (Fig. 11). These deposits overlie delta front deposits (facies association 7) aggradationally and interpose tidal plain deposits (facies association 6).

On the other hand, in a distal or medial environment, for example in the lowermost part of the Fujitoge Formation (Fig. 15), this facies association is composed of unchannelized fine- to medium-grained sandstone sheets (*Ss* and *Shb*), that are interbedded with floodplain, tidal flat, and sandy fluvial-channel deposits. These sheets are sometimes accompanied with pyroclastic fall deposits, containing abundant pumice lapilli or felsic accretionary lapilli, at the bases of sequences.

*Interpretation*

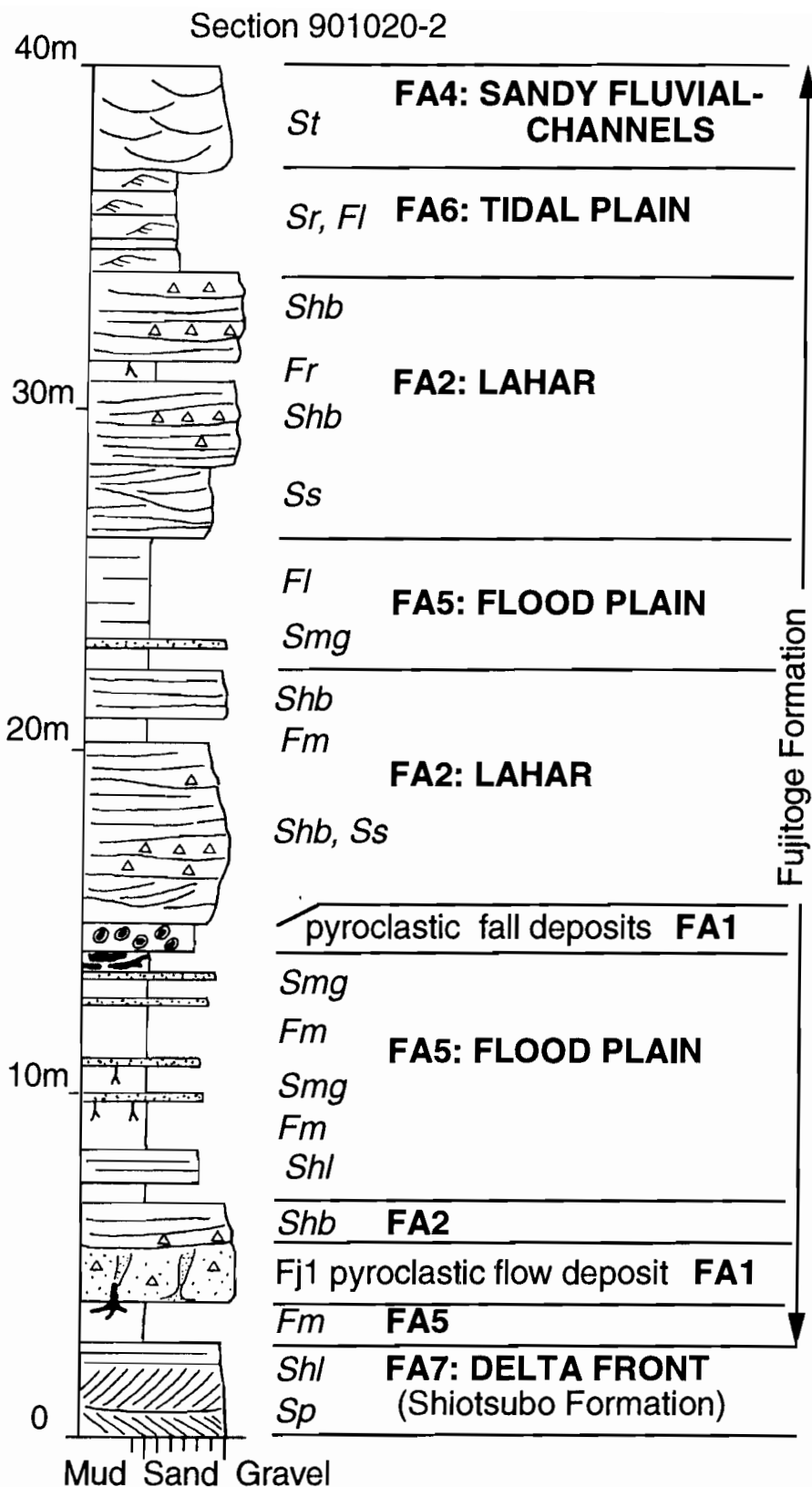The nearly monolithological character and abundant pumice in these facies suggest deposition in response to pyroclastic eruptions that choked streams with dacitic or rhyolitic detritus. Facies *Sm* and *Gms* represent debris flows (Middleton and Hampton, 1976; Palmer and Neall, 1991); poor sorting, nongraded beds and lack of stratification imply a high yield strength and plastic behavior. Facies *Shb* is interpreted to be hyperconcentrated flood flows (Person and Scott, 1985; Smith, 1986) based on their stratification, which is discontinuous and thicker than upper-regime parallel lamination. Also, thin-bedded nature, dominance of upper-regime structure, low relief of scours, and low amplitude of crossbeds indicate that facies *Ss* resulted from shallow, high-discharged flood flows (Gloppen and Steel, 1981; Smith, 1987). Some hyperconcentrated flood flow deposits were presumed to be produced by primary lahars, not by dilution-transformation processes of debris flows (Pierson and Scott, 1985), because facies *Shb* directly overlie primary pyroclastic deposits. The occurrence of facies *Ss* rather increases in a distal environment as coarse-grained facies *Shb* diminish, suggesting the dilution of hyperconcentrated flood flows.

**Facies association 3: gravelly fluvial-channel deposits**

*Description*

Massive or crudely stratified, 50 cm to 3 m thick, clast-supported conglomerate (*Gmb*) with lenses and/or thin beds of stratified, medium to coarse-grained sandstone (*Shl*, *St*, and *Sp*) form a gravelly facies association (Table 4; Fig. 16). The conglomerate consists of well-
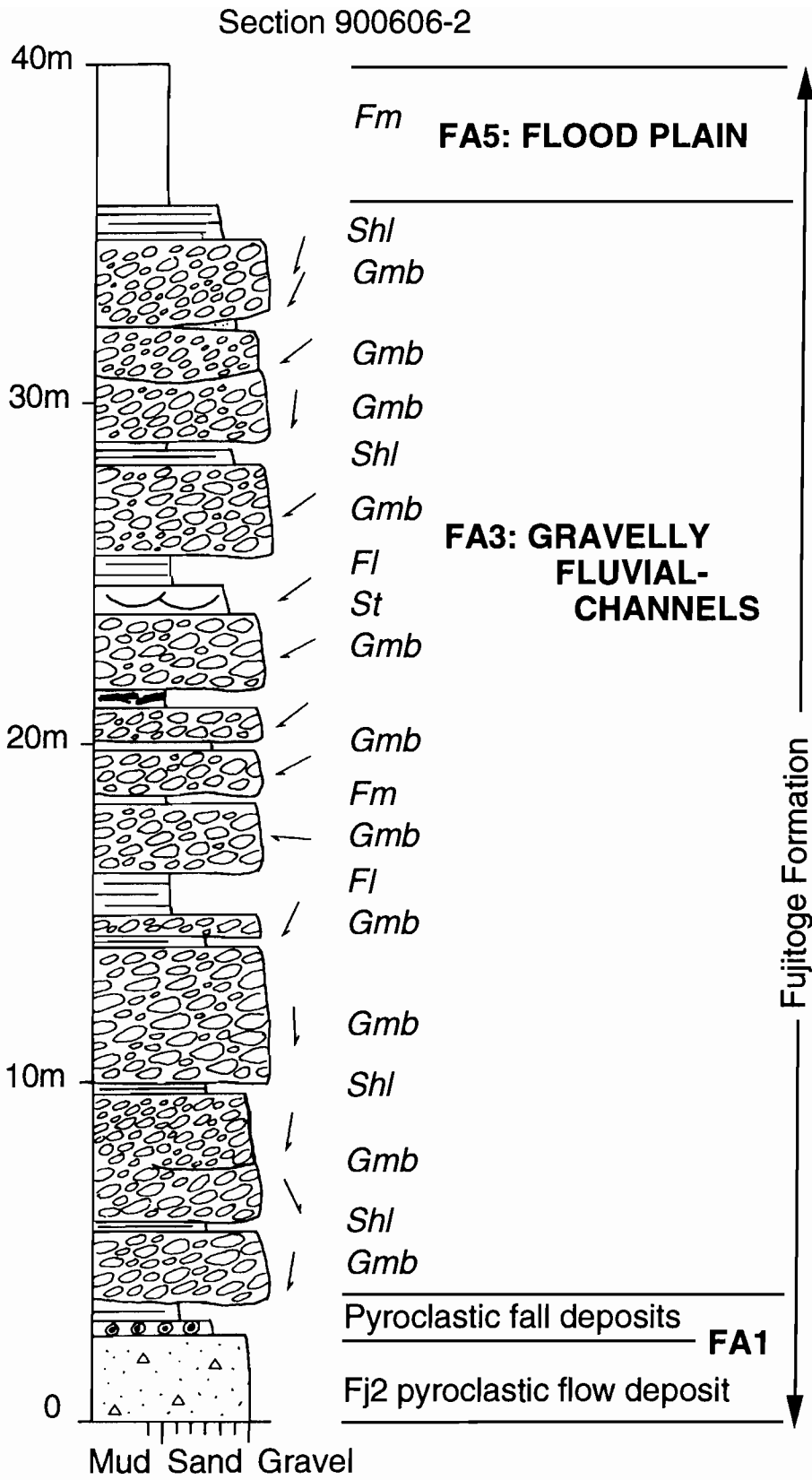
## Section 900606-2



Fig. 16. Typical section of gravelly fluvial-channel deposits in the Fujitoge Formation, 2 km east of R2 (Fig. 11).

rounded and typically imbricated pebbles and cobbles. This association is occasionally interbedded with fine-grained deposits (*Fl* and *Fm*) which contain plant debris and rootlets.

*Interpretation*

Facies *Gmb* is interpreted to represent traction transport and deposition in a fluvial channel, primarily as longitudinal bars. The dominance of *b* parallel to flow fabric supports tractional processes (Rust 1972). Associated thin beds of sandstone represent waning-flow deposition on bar tops or margins (Miall, 1977). Facies *Gmb*-dominant features indicate proximal braided rivers or lower alluvial fans (Miall, 1978; Rust, 1978; Kraus, 1984).

## Facies association 4: Sandy fluvial-channel deposits

*Description*

This facies association (Table 4; Fig. 17) is dominated (>50 %) by trough-crossbeds developed in very coarse- to medium-grained sandstone (*St*; Fig. 18), which consists mainly of rounded quartz crystals. Lesser amounts of trough crossbedded pebbly conglomerate (*Gt*), current ripple-laminated medium- to very fine-grained sandstone (*Sr*), and fine-grained sediments (*Fl* and *Fm*) are also present. They form a fining-upward sequence, 80 cm to 5 m thick; facies *Gt* occurs at the base and facies *Sr* characteristically overlies normal-graded facies *St*. Within thick *Gt-St* sheets, trough-set size decreases upwards from 50 to 10 cm. The sequence has a sharp but irregular scoured basal contact and contains rip-up clasts of siltstone. Paleocurrent azimuths from trough-crossbeds and ripple are unimodal.

*Interpretation*

Sedimentary structures within the sandstone are indicative of traction deposition in a fluvial channel (Miall, 1977; Cant and Walker, 1978). Their erosive bases, internal scour, and low paleocurrent variance would reflect the avulsive behavior of a braided river system, and the most deposits lack lateral accretion elements favoring a meandering river system. Furthermore, facies *Sp*, related to migrating transverse bars or sand flat (Cant and Walker, 1978), is almost

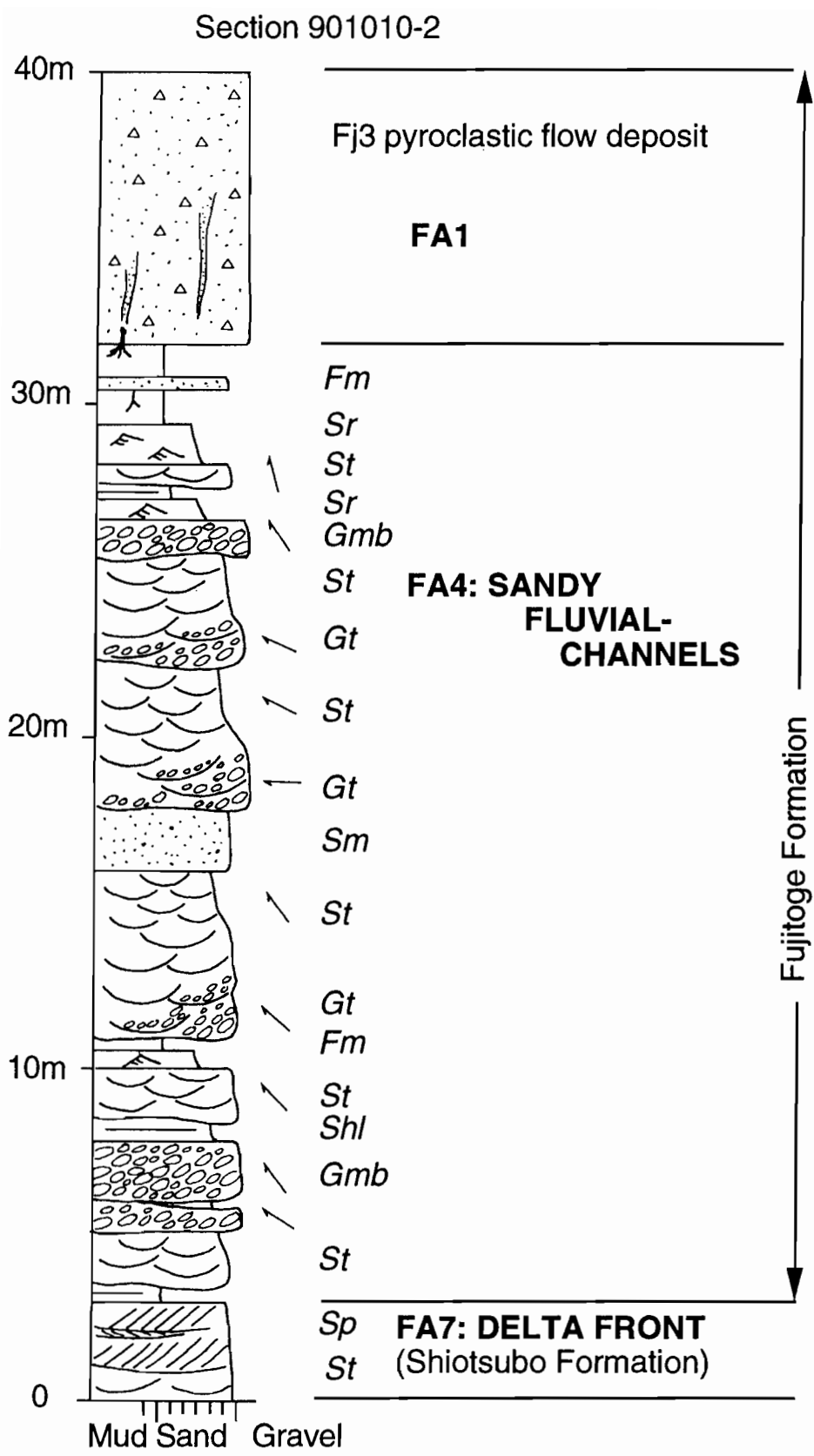Fig. 17. Typical section of sandy fluvial-channel deposits in the Fujitoge Formation, the middle part of R1 (Fig. 11).
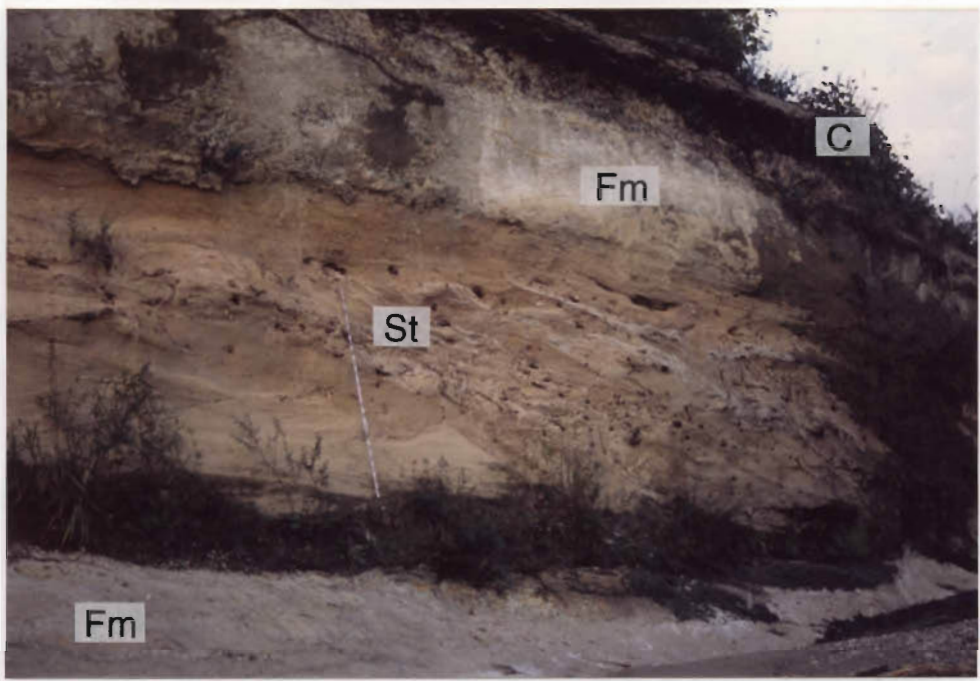
Fig. 18. Outcrop photograph of alternating trough-crossbedded sandstone (*St*), massive silt (*Fm*), and lignite (*C*) in the Izumi Formation (Maki, Kitakata City, 3 km east of R5; Fig. 11). Sandstone represents a fluvial-channel fill and contains abundant wood fragments. The scale is 2 m.

absent within the deposits. Although the predominance of trough-crossbeds indicates lower flow regime, these sandy channels might represent products from single flood events in a distal position, similar to the case of the Miocene volcaniclastic aprons (Smith, 1988).

## Facies association 5: floodplain deposits

*Description*

Interbedded massive siltstone (*Fm*), current ripple- or parallel-laminated siltstone to very fine- to medium-grained sandstone (*Fl*, *Sr*, and *Shl*), and massive or trough-crossbedded medium- to coarse-grained sandstone (*Smg* and *St*) form a fine-grained facies association (Table 4; Fig. 19). This sequence may be 4 or more meters thick. Massive siltstone beds (Fig. 18) contain abundant leaf fossils and minor freshwater mollusc fossils, and are occasionally interbedded with lignite beds (*C*) and light-brown-colored oxidized, organic rich beds (*Fr*). Facies *Shl*, *Sr*, and *Smg* comprise thinner (5 - 100 cm) tabular or lenticular beds, and facies *St* consists of thinner (< 50 cm) beds having erosive base and flat top. Some sandstone beds are normally graded and occasionally form fining-upward sequences.

*Interpretation*

The occurrence of fine-grained lithologies and abundant fossil remains suggest deposition in overbank environments. The absence of desiccation cracks in siltstone beds suggests the floodplains were always water-saturated with the local occurrence of facies *C* and *Fr* indicating swamp and pedogenical settings, respectively. Thin sandstone beds are interpreted as products of discrete overbank flooding events. Some sandstone beds adjacent to the fluvial-channel deposits may be natural levee or crevasse-spray deposits, however, there is no evidence of a coarsening-upward sequence produced by lateral progradation of a meandering channel-belt (Elliott, 1974); avulsion appears to be a relatively abrupt process in this association.

## Facies association 6: tidal flat deposits
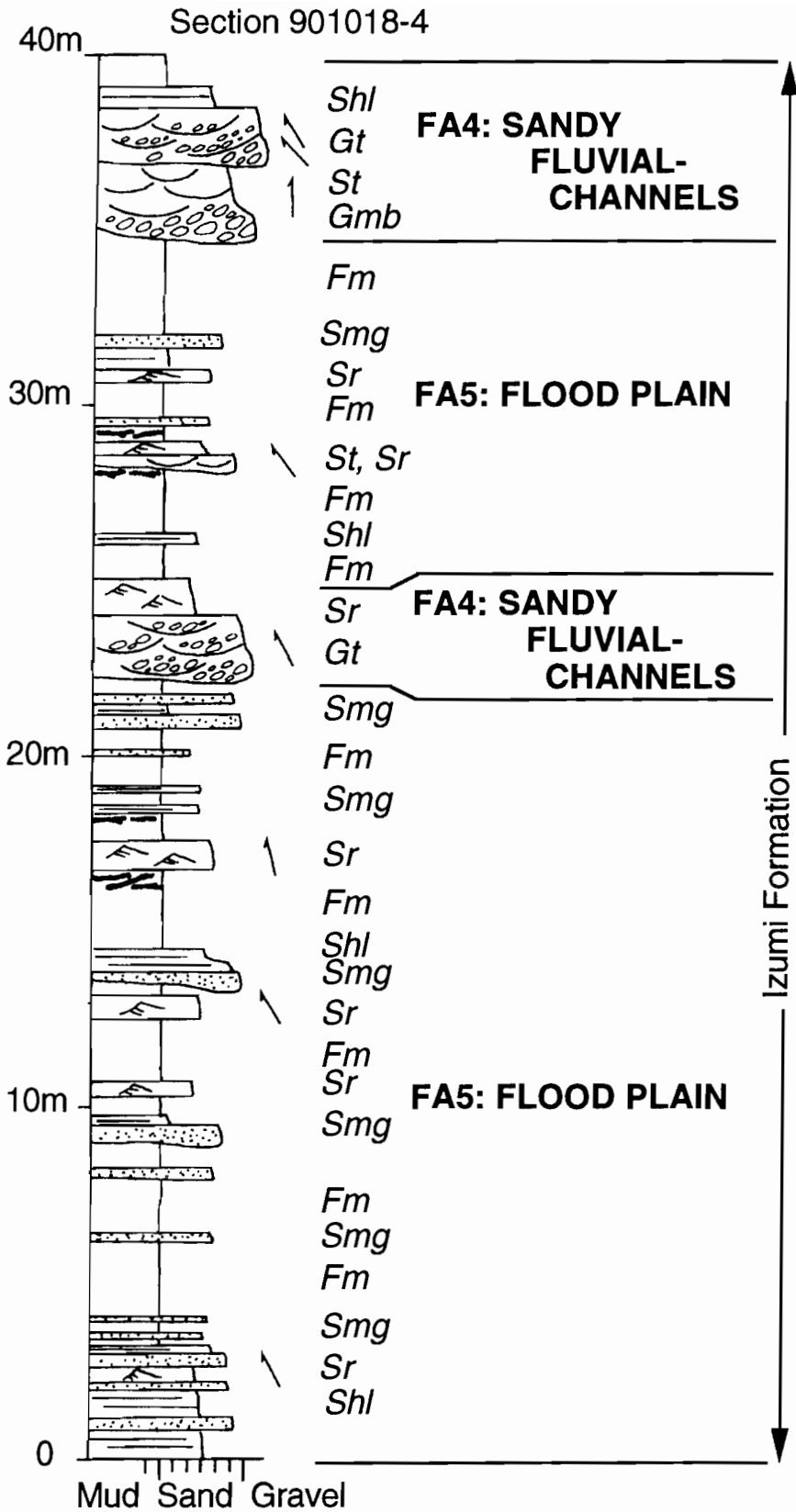
Section 901018-4

Fig. 19. Typical section of floodplain deposits accompanied by minor sandy fluvial-channel deposits in the Izumi Formation, the lower part of R7 (Fig. 11).

*Description*

Alternating beds of 3- to 10-cm-thick wave ripple-laminated, fine- to medium-grained sandstone (*Sr*) and 1- to 10-cm-thick parallel-laminated, very fine grained sandstone to siltstone (*Fl*), or herringbone crossbedded thick sheets of coarse-grained sandstone (*St* and *Sp*) form a minor facies association, that is less than 3 m thick (Table 4; Fig. 15). Wave ripples of Facies *Sr* are accompanied with flasers or drapes of siltstone, or convolute bedding; the wavelength of individual ripples are 5 to 15 cm. Some beds are bioturbated. This association is only interposed within fluvial sediments in the lowermost part of the Fujitoge Formation.

*Interpretation*

This facies association is interpreted to be tidal plain sediments based on the sedimentary structure of facies *Sr* (Reineck and Singh, 1980, p.112-118). Facies *St* and *Sp* may be tidal channel fills.

## Facies association 7: delta front deposits

*Description*

Trough- and planar-crossbedded, well-sorted very coarse- to medium-grained sandstone and granule- to pebble-conglomerate (*St, Sp, Gt*, and *Gp*) form a prominent facies association in the uppermost part of the Shiotsubo Formation (Table 4; Figs. 20 and 21). This association is 15 to 20 m thick that may be laterally continuous for ten kilometer or more and occasionally interbedded with poorly sorted massive sandstone to conglomerate containing abundant rounded pumiceous pebbles (*Sm* and *Gms*). The thickness of crossbedded units ranges from 20 to 200 cm. The sandstone consists mainly of rounded quartz crystals. The conglomerate is typically concentrated in the axial portion of the trough sets, and where concentrated in thicker sets, the pebble may be imbricated. Pebbly foresets in the trough units may be either normally or inversely graded; in the tabular sets, where pebbles are generally less abundant, the pebble-bearing foresets grade upward into coarse-grained sandstone.
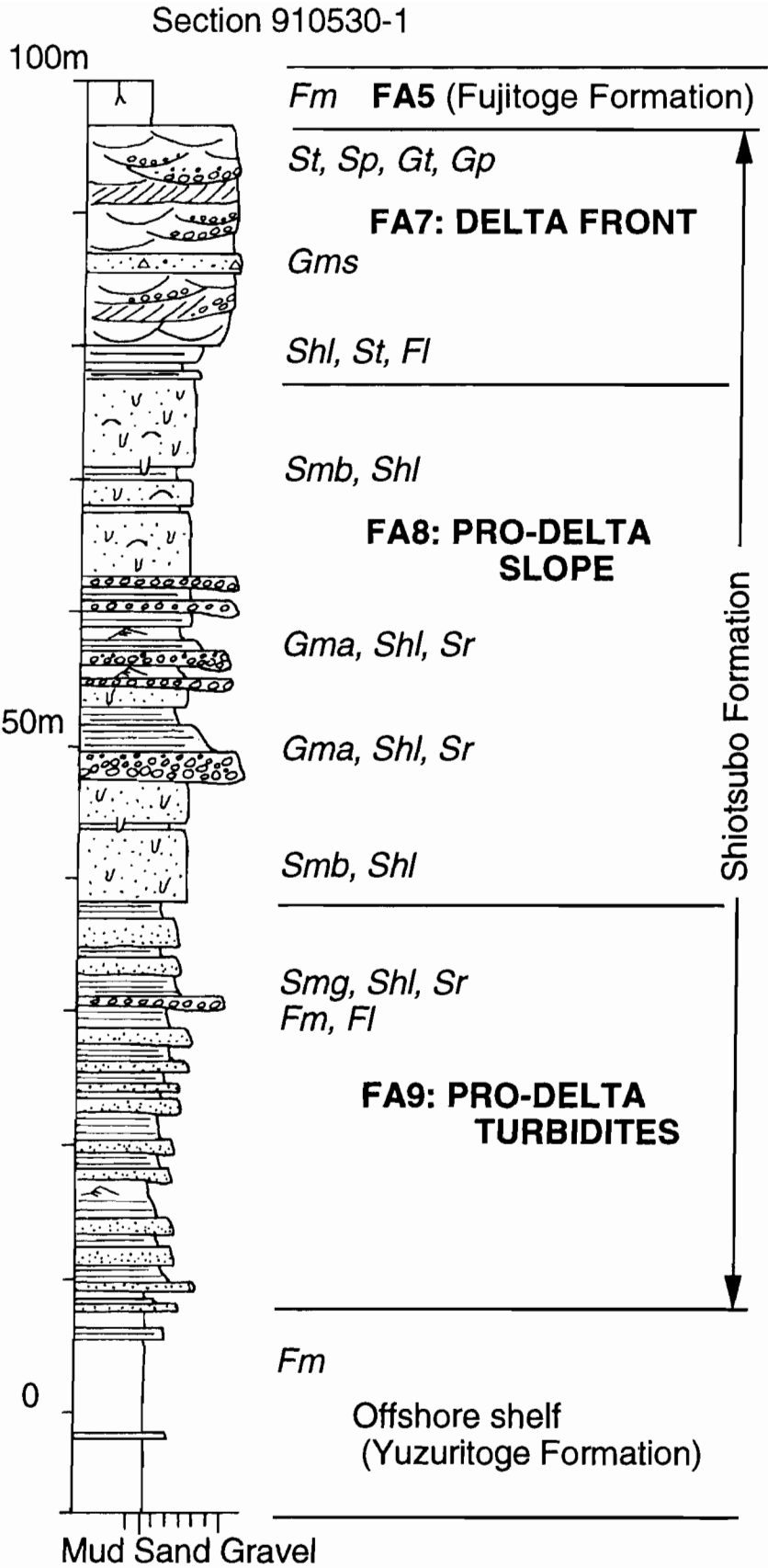
Fig. 20. Measured section of the Shiotsubo Formation, showing a coarsening-upward deltaic succession, the lower part of R1 (Fig. 11).

Fig. 21. Typical outcrop of delta front deposits (facies association 7), made up of trough- and planar-crossbedded sandstone and conglomerate in the Shiotsubo Formation, Mikawa, Nishi-aizu Town (R1; Fig. 11). The paleocurrents of sandstone are opposite to ones of conglomerate. The scale is 2 m.
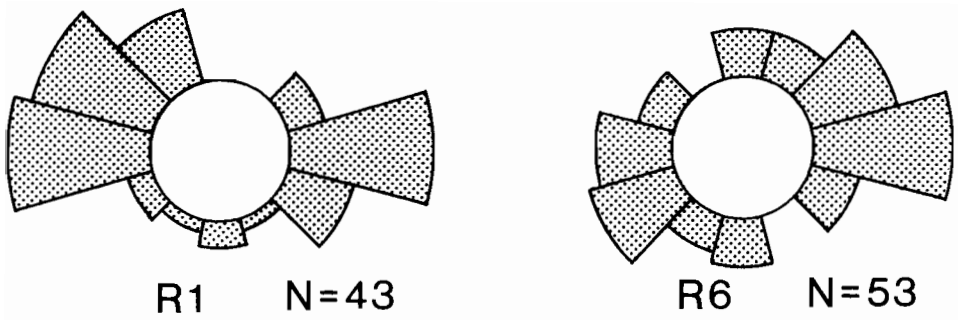
Fig. 22. Bimodal paleocurrent trends of crossbedding within delta front deposits (facies association 7) in the Shiotsubo Formation. R1 and R6 are the route numbers of sections (Fig. 11).

Paleocurrent directions of the trough crossbedding show a bimodal pattern (Fig. 22); herringbone crossbeds are common. Erosional structures in the crossbeds include channel-form scours and reactivation surfaces. Some reactivation surfaces are accompanied with very thin beds of subordinate current ripples. The basal part of this sub-association, that is 0 to 2 m thick and finer grained than the main part, consists of parallel- or cross-laminated siltstone to fine- to medium-grained sandstone (*Shl, St,* and *Fl*).

*Interpretation*

This association is interpreted as a delta front environment because of its stratigraphic position between marine and fluvial deposits. Sedimentary structures within the coarse-grained crossbeds are indicative of tractional deposition by tidal currents (Phillips, 1984; Okazaki and Masuda, 1992). These crossbeds represent deposition as braided channel-fills and distributary mouth bars, and finer basal parts may be distal bars. Facies *Sm* and *Gms* are interpreted to be debris flow deposits (Middleton and Hampton, 1976) filling distributary channels, and probably associated
with alluvial lahar events.

**Facies association 8: pro-delta slope deposits**

*Description*

This facies association (Table 4; Fig. 20) consists mainly of massive sandstone (*Smb*), but contains some intercalated well-sorted graded conglomerate containing rounded pumiceous granule or small pebble (*Gma*) and parallel- or ripple-laminated sandstone (*Shl* and *Sr*), lying beyond delta front deposits. The thickness of the association is 30 to 40 m. Facies *Smb* is moderately to poorly sorted, heavily bioturbated, fine- to coarse-grained sandstone, that contains small pumiceous and lithic pebbles and marine mollusc shells arranged in clusters or scattered randomly. The mollusc fossils indicate inner sublittoral zone (Suzuki et al., 1986). Facies *Gma, Shl,* and *Sr* form a 0.5 to 5-m-thick fining-upward sequence having a erosional base. The conglomerates are normally graded or inversely-to-normally graded with rip-up

clasts; its fabric shows a tight packing of clasts and a weak imbrication of pebbles. The overlying laminated sandstones are very fine- to medium-grained, often with thin beds of pumiceous granule.

*Interpretation*

Heavy bioturbation in the massive sandstone beds indicates quiet-water, biological-processes-dominated pro-delta deposition below the effective depth of water erosion. Facies *Gma* may resemble traction carpets at the base of a high-density turbidite, as described by Lowe (1982). The interposed fining-upward pebbly sequence is interpreted to be a deltaic distributary channel fill.

**Facies association 9: pro-delta turbidite lobes**

*Description*

Multiple fining-upward sets of a 20- to 150-cm-thick sandstone bed (*Smg*) and overlying parallel- or ripple-laminated, very fine- to medium-grained sandstone (*Shl* and *Sr*) form the lower part of the Shiotsubo Formation (Table 4; Fig. 20). Lesser amounts of thin siltstone beds (*Fm* and *Fl*) and pyroclastic fall deposits, containing abundant accretionary lapilli, are also interposed. The association is 20 to 30 m thick, and overlies massive siltstone of the Yuzuritoge Formation. Fine- to medium-grained *Smg* bed is massive to normally graded with a sharp base, but medium- to very coarse-grained pumice-pebbly one is normally or reverse-to-normally graded and scour underlying beds. Very fine- to fine-grained sandstone consists of abundant bubble-wall glass shards and pumice shards. Mollusc fossils indicate middle sublittoral zone (Suzuki, et al., 1986).

*Interpretation*

Facies *Smg* indicates transport by turbidites, and repeated fining- and thinning-upward sandy sequences indicate this facies association is suprafan lobes (Walker, 1978) at the base of pro-delta slops.

57

# 6. DEPOSITIONAL SEQUENCES AND PALEOGEOGRAPHIC MODELS

Although the caldera-forming volcanism had been primary active since late Miocene, the distribution of facies associations and paleocurrent data of the extracaldera formations show two major depositional systems in different stages: 1) westward prograding volcaniclastic aprons, made up of fan delta, braidplain, pyroclastic flow sheet, and incised braided river deposits, in the late Miocene- early Pliocene Shiotsubo and Fujitoge Formations (Fig. 23); and 2) reverse fault-generated intra-arc basins, filled by alluvial fan, anastomosed river, and pyroclastic flow sheet deposits, in the late Pliocene to early Pleistocene Izumi and Nanaorezaka Formations (Figs. 24 and 25). The boundary of two sedimentary systems is recognized as an abrupt shift of faces associations and sediment dispersal patterns (Fig. 26), and represents a significant change of tectonic setting.

## The Shiotsubo and Fujitoge Formations

### Fan deltas

The Shiotsubo Formation is a 70- to 100-m-thick coarsening-upward deltaic succession, formed by pro-delta turbidite (facies association= FA 9), pro-delta slope (FA 8), and delta front deposits (FA 7), in ascending order (Fig. 20). This succession displays a westward progradational geometry, downlaps onto offshore shelf deposits of the Yuzuritoge Formation, and is overlain by fluvial sediments of the Fujitoge Formation (Fig. 23). These stratigraphic relationships and paleocurrent data suggest that this delta was located at the backarc-side margin of the emergent volcanic arc (Fig. 26A).

A gravity-flow-dominated feature of the succession is similar to subaqueous deposits in some non-volcanic fan deltas (Postma, 1984; Massari, 1984; Nemec et al., 1984), although this deltaic succession lacks a subaerial alluvial-fan component. The occurrence of volcaniclastic coarse-grained lithologies suggests sediment supply waxed as a result of subaerial lahar events related to felsic pyroclastic eruptions, similar to modern deltas adjacent to active volcanoes (Kuenzi et al., 1979) and ancient sub-lacustrine deltas in the early Miocene
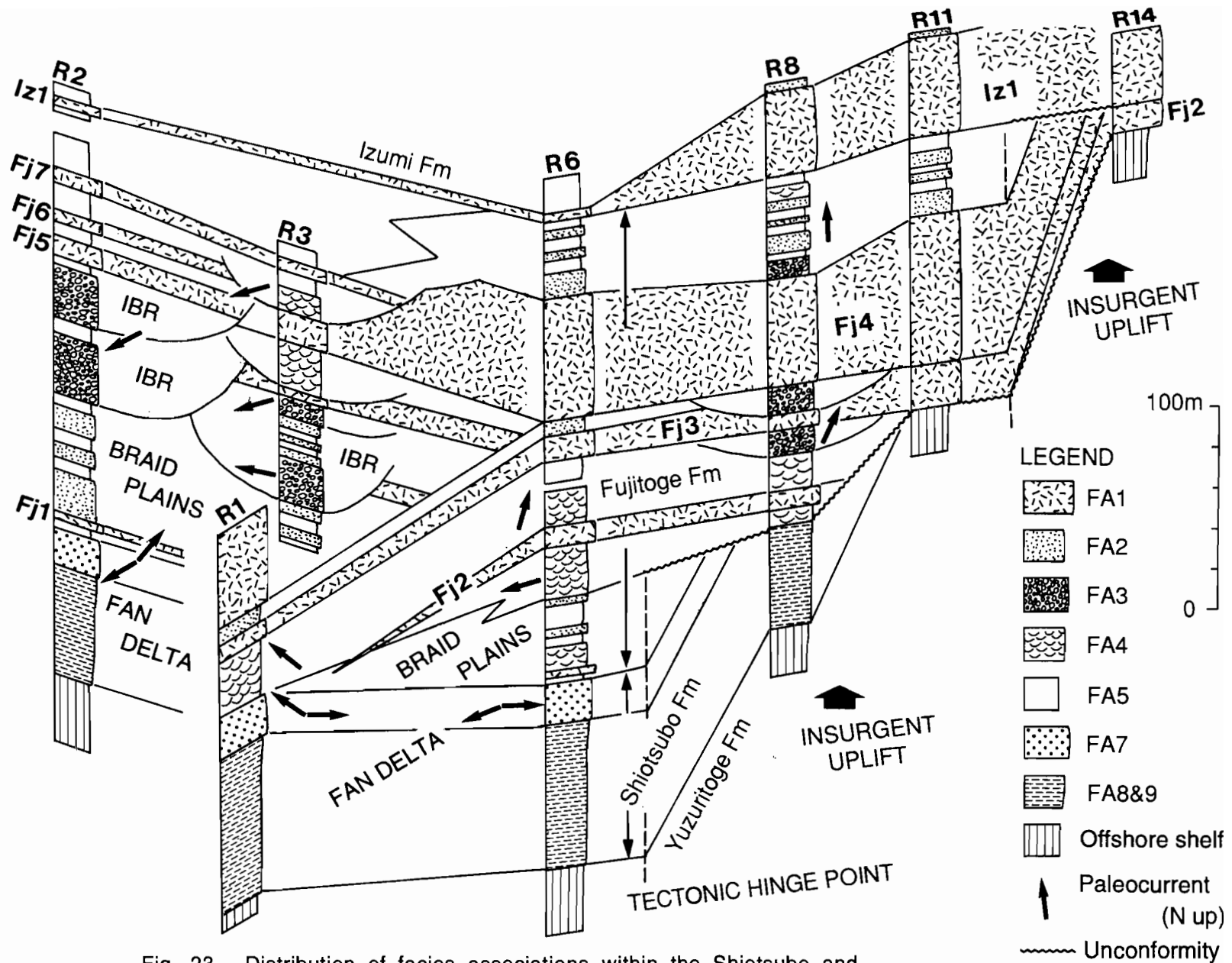
Fig. 23. Distribution of facies associations within the Shiotsubo and Fujitoge Formations, showing westward progradation of volcaniclastic aprons and local uplift around caldera volcanoes. Location of sections is shown in Fig. 11. IBR= incised braided rivers.
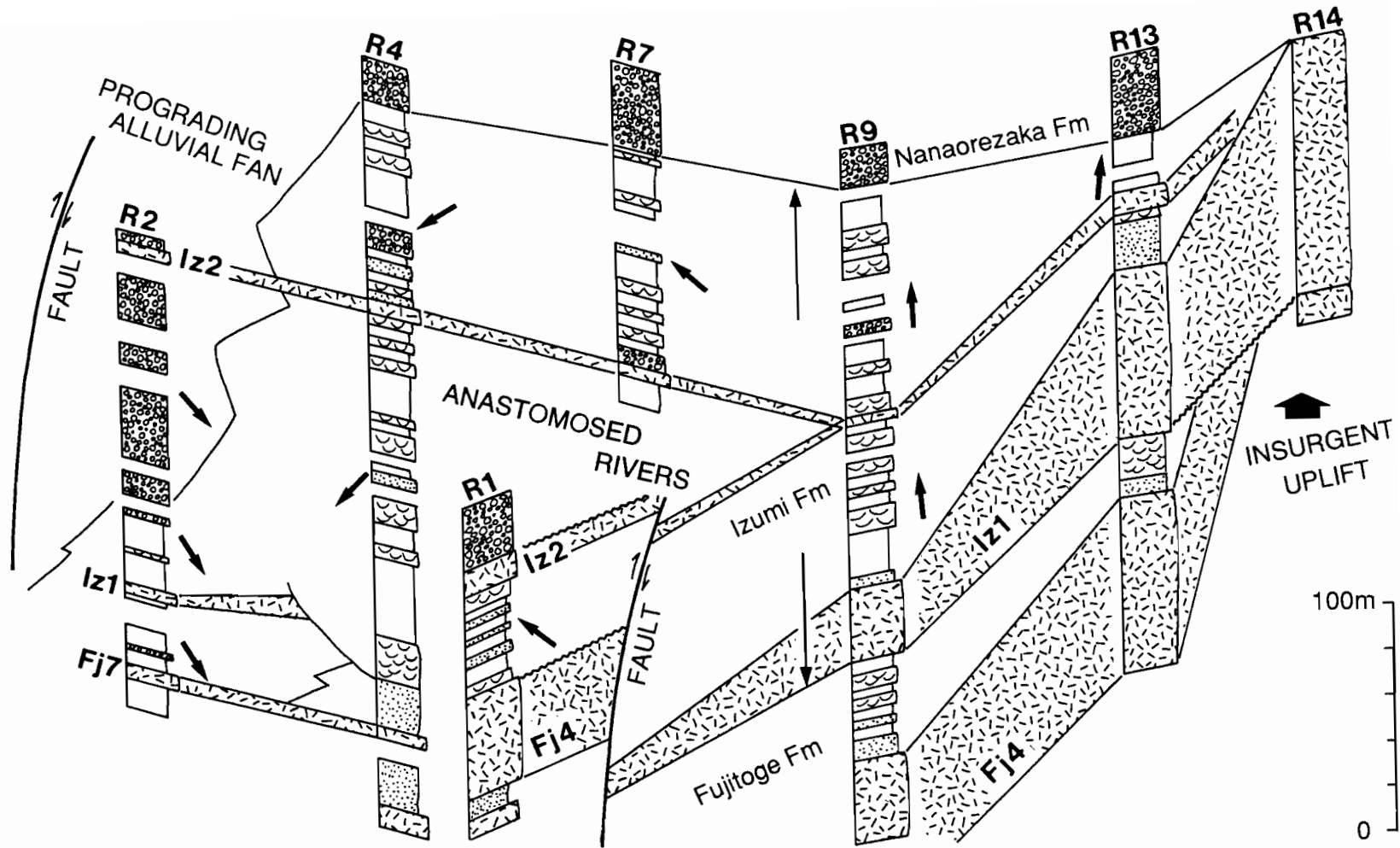
Fig. 24. Distribution of facies associations within the Izumi Formation, showing flexural subsidence resulted by reverse-faulting and southeastward progradation of alluvial fan deposits. Location of sections is shown in Fig. 11.
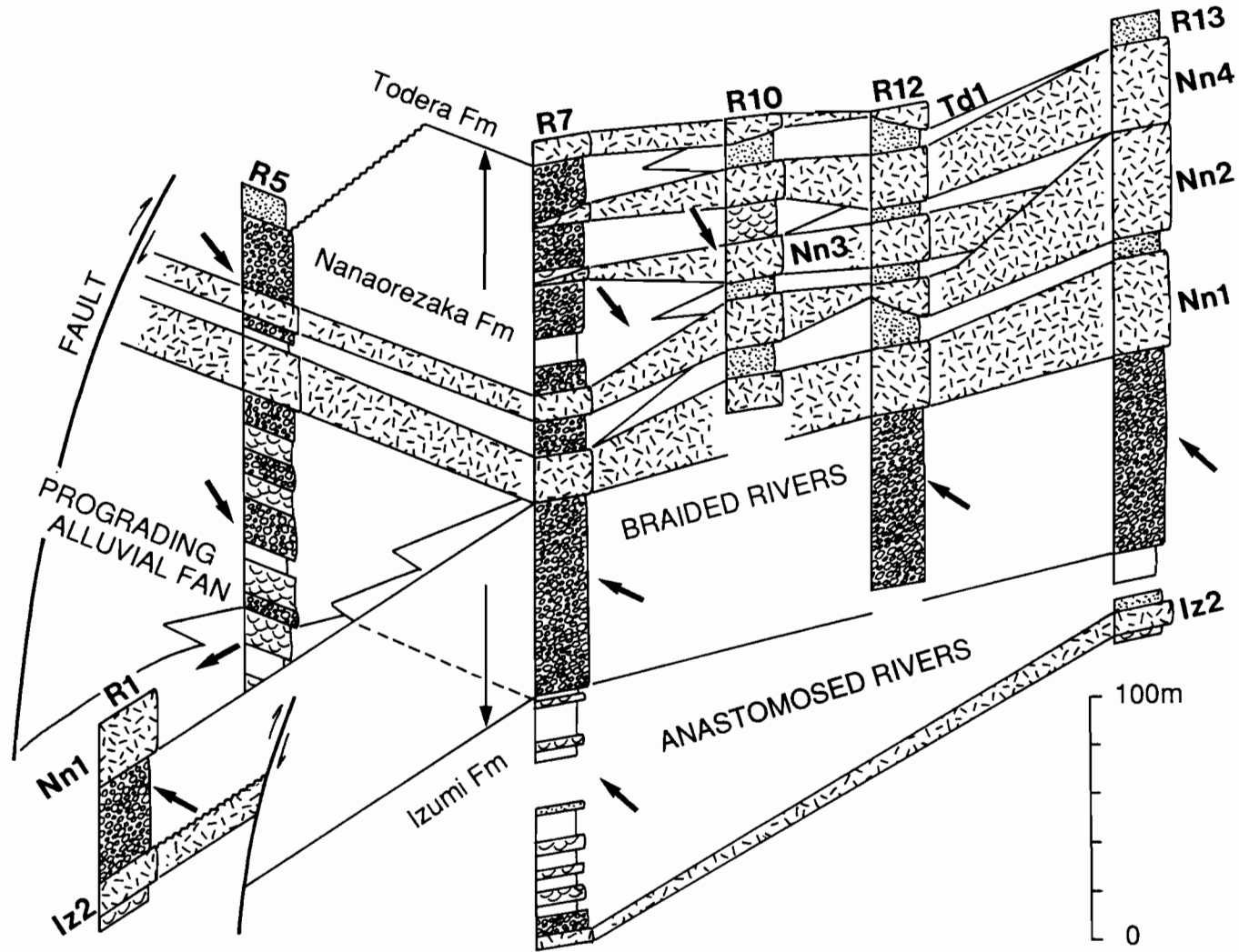
Fig. 25. Distribution of facies associations within the Nanaorezaka Formation, showing southeastward progradation of alluvial fan deposits and vertical stacking of pyroclastic flow sheets shed from the southeast of the basin. Location of sections is shown in Fig. 11.
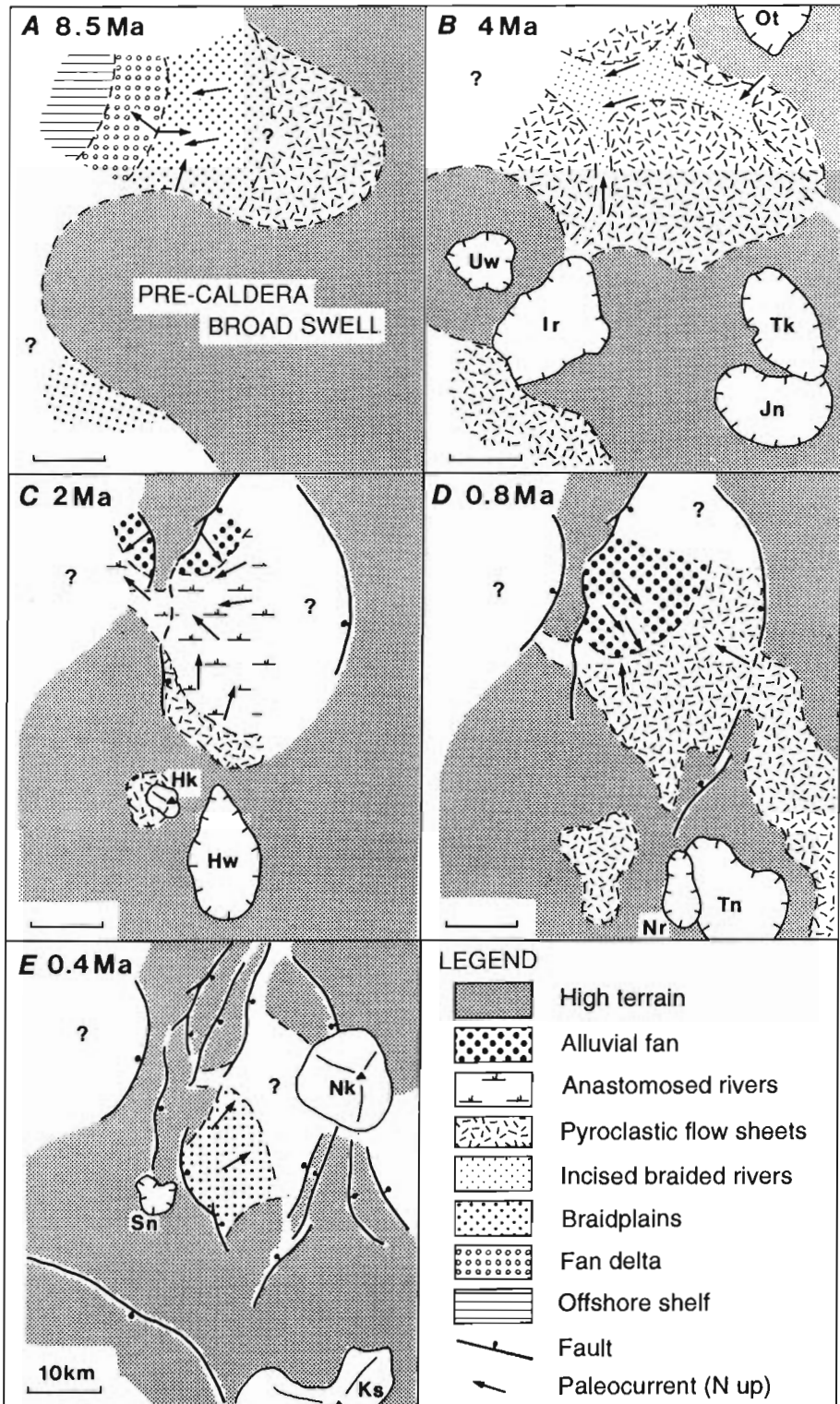
Fig. 26. Schematic representation of paleogeography and paleocurrents in the Aizu district from Late Miocene to Middle Pleistocene. A. Westward progradation of volcaniclastic aprons and pre-caldera insurgent uplift in the volcanic field at about 8.5 Ma (the Shiotsubo and lower Fujitoge Formation). B. Formations of large caldera volcanoes and extensive ignimbrite sheets at about 4 Ma (the upper Fujitoge Formation). C. Reverse faulting and anastomosed rivers filing the resulted flexural basin at about 2 Ma (the Izumi Formation). D. Southeastward prograding alluvial fans and ignimbrite eruptions at about 0.8 Ma (the upper Nanaorezaka Formation). E. Basin migration and a medium-caldera eruption at about 0.4 Ma (the Todera Formation). Map E is modified from Yamamoto (1992b).

62

backarc basin (Kano, 1991).

*Braidplains*

The lower part of the Fujitoge Formation is a sandy lahar-dominated fluvial succession (Fig. 15), that consist mainly of unchannelized sandstone sheets (facies *Ss* and *Shb*) with floodplain (FA 5), sandy fluvial-channel (FA 4), tidal flat (FA 6), and the Fj1 pyroclastic flow deposits (FA 1). This succession aggradationally overlies the delta front deposits (FA 7) and displays a westward oblique progradational geometry with the underlying deltaic succession (Fig. 23). The occurrence of tidal flat deposits (FA 6) and these stratigraphic relationships indicate that this succession forms the subaerial part of a fan delta complex.

Unchannelized sand-bedload regime represents aggrading sheet-flow braidplains, similar to ancient arc-adjacent alluvial plains induced by explosive volcanism (Smith, 1987; 1988). Here, runoff and sediment accumulation are controlled by frequent hyperconcentrated floods over a broad river plain with very shallow channels, and short-term aggradation of lahars reflects disequilibrium between sediment supply and capability of a river to transport sediments. Observations in Guatemala indicate that eruptions producing sediment loads in excess of geomorphic thresholds permitting aggradation may control sedimentation for several decades following eruptions (Kuenzi et al., 1979; Vessell and Davies, 1981). Obviously, these distal lahars in this succession were also formed in response to felsic pyroclastic eruptions on the volcanic highland, because of their lithological features and existence of accompanied pyroclastic fall deposits.

Long-term aggradation of the braidplain deposits without incised deep channels implies that high-sediment-load deposition occurred during a eustatic highstand at about 9 Ma, according to the age data of the Fj1 pyroclastic flow deposit (Table 1). Thus, those fan delta-braidplain deposits represent a highstand system tract (Posamentier and Vail, 1988) at the edge of the late Miocene island arc (Fig. 26A). Progradation of the aprons clearly resulted from intense volcanic eruptions in the Aizu volcanic field.

*Pyroclastic flow sheets*

63

The southern upper part of the Fujitoge Formation consists mainly of the extensive Fj2, Fj3, and Fj4 pyroclastic flow deposits (FA 1) and overlying lahar deposits (FA 2); they form an northward sloping and thinning sheets (Fig. 23). As mentioned above, these pyroclastic flows were shed from the caldera volcanoes on the south of the basin (Fig. 26B); the pyroclastic flow sheets unconformably overlie basinward-tilted formations around the caldera volcanoes (Fig. 23). Minor fluvial-channel deposits (FA 3 and 4), representing braided rivers, are filling isolated shallow valleys above the pyroclastic sheets.

The thick pyroclastic flow sheets represent sudden aggradation during caldera-forming eruptions. However, inter-ignimbrite-eruption sediments were less preserved above the syn-eruption sheets since the Fj2 eruption, although subsequent post-caldera eruptive events were recorded within the source caldera volcanoes. And, the age data of the pyroclastic flow deposits shows hiatuses between the pyroclastic sheet during 1 to 2 million years; long-term degradation processes were prominent above the sheets. In fact, an extracaldera product of the Iriyamazawa caldera-forming eruption at 7.1 Ma was perfectly removed in this region. The observed long-term degradation may have been caused by changes in base level for deposition.

*Incised braided river*

The northern upper part of the Fujitoge Formation is composed of incised valley-fills representing axial westward drainage systems (Fig. 23- R2, R3). These narrow valleys were especially deepened at levels lower than the base of syn-eruption sheets, and were aggradationally refilled by gravel-bedload channel (FA3), floodplain (FA5), and lahar deposits (FA 2) representing inter-ignimbrite-eruption facies (Fig. 16). Their facies *Gmb*-dominant features and channel geometries indicate proximal braided rivers (Miall, 1978; Rust, 1978; Krause, 1984).

These river systems seem to be controlled by sea-level changes, because some of the valleys incised into deltaic braidplain deposits (Fig. 23). The incision occurred corresponding to rapid fall of a sea-level, and rise of one caused the channel-fill deposition. No marine transgression is, however, found within the channels; it is indicated that high-sediment-load deposition had continued during this period independently of the sea-level changes. Based on

64

the age information, the major incisions immediately after the Fj2, Fj3, and Fj4 eruptions are presumably corresponding to the sequence boundaries at 8.2, 6.3, and 4.2 Ma, respectively (Haq et al., 1988).

## The Izumi and Nanaorezaka Formation

*Anastomosed rivers*

The main part of the Izumi Formation (Fig. 19) is composed of alternating 1- to 5-m-thick sandy-fluvial channel deposits (FA4) and 2- to 20-m-thick floodplain deposits (FA5). These deposits aggradationally overlie the Iz1 pyroclastic flow deposit, that was shed from Hiwada caldera (Fig. 26C), and form a northwestward-thickening wedge, that displays asymmetric flexural subsidence, except for the R1 section west of the syn-depositional reverse faults (Fig. 24). Paleocurrents of the channel deposits indicate a westward drainage system across the faults (Fig. 26C). Thin overflowing deposition shown in the R1 section (Fig. 24) suggests that their sedimentation rate was high enough to compensate for the subsidence. Hornblende-quartz dacitic lithology of the sandstones and paleocurrent data indicate that most detritus was primarily derived from the Iz1 pyroclastic flow deposit surrounding the basin.

These fines-dominated fluvial deposits represent rarely-known anastomosed rivers (Smith, 1983; Miall, 1985), because of isolated stacking feature of narrow sandy-channels and scarcity of lateral accretion within the channels; these channels appear to have formed inter-connected networks, instead of meandering belts. Although interchannel areas accumulated overbank fines, shallow lacustrine mud, and peat, crevasse sprays are common in floodplains. These low-gradient fluvial features were obviously caused by the syn-depositional faulting on the western margin of the basin. Frequent flooding and avulsion of sand-bedload channels suggest vertical accretion at high rates. Also, paucity of pedogenic features in floodplain deposits implies rapid aggradation of fine-grained detritus.

*Alluvial fans*

The northern parts of the Izumi and Nanaorezaka Formations (Figs. 24 and 25) is a

southeastward-prograding wedge, that consists mainly of gravelly-channel deposits (FA 3) with minor sandy-channel deposits (FA 4). This wedge was located in the eastern foot of a faulted highland, and interbedded with anastomosed rivers in the main part of the Izumi Formation, braided rivers in the lower part of the Nanaorezaka Formation, and pyroclastic flow sheets in the upper part of the Nanaorezaka Formation, in ascending order. Southward migration of westward axial drainage systems within the basin occurred simultaneously during this progradation (Fig. 26C-D). Most gravels were derived from pre-Neogene basement formations, and channel deposits occasionally contains abundant wood debris.

Their prograding morphology and abrupt facies change at the margin suggest that the gravel-bedload streams represent medium to distal parts of humid alluvial fans, although the upper reach of the fan adjacent to syn-depositional faults was perfectly removed. This clastic wedge lacks debris flow deposits (facies *Gms*) representing an arid alluvial fan setting (Gloppen and Steel, 1981), because humid climates and abundant vegetation generally reduce mechanical erosion and reworking of debris. Initiation of the progradation was recorded as an abrupt change of paleocurrents from westward to southeastward at the level above the Fj7 pyroclastic flow deposit in the R2 section (Fig. 24). So, the reverse faulting started at least 3 Ma; this timing is contemporaneous with other parts of the Northeast Honshu arc (Amano and Sato, 1989). However, the progradation of alluvial fans suddenly vanished due to eastward migration of fault systems before the Todera period (Fig. 26-E; Yamamoto, 1992b).

*Braided rivers*

The southern lower part of the Nanaorezaka Formation consists of gravel-bedload streams (FA 3) forming a northwestward axial drainage system across syn-depositional faults, and conformably overlies the anastomosed rivers with sharp contact within the basin (Fig. 25). No change of the direction of transport and the facies occurred along the drainage axis, but the thickness of these deposits increases toward the center of the basin. Lateral grain-size changes in these streams are weak and do not show a rapid downstream diminishment like fan deposition. Also, there is no vertical grain-size change, such as a coarsening-upward or fining-upward sequence. Paleocurrent data indicates these streams received sediments from several

local sources around the basin, not from a point source as fans.

These gravel-dominated fluvial deposits represent proximal braided rivers (Miall, 1978; Rust, 1978; Kraus, 1984) based on the geometry, although their facies association is same as one of alluvial fans. The abrupt facies change from anastomosed to braided rivers, between the Izumi and Nanaorezaka Formations, is presumably caused by the increase of a stream gradient due to uplift of a highland southeast of the basin, because no significant climatic change was recorded in abundant plant fossils (Suzuki et al., 1977). This coarse-grained sediment discharge started at the base of the Olduvai event according to the previous paleomagnetic study (Manabe, 1980), but ceased quickly corresponding to caldera-forming eruptions within the rising terrain (Fig. 26D).

*Pyroclastic flow sheets*

The southern upper part of the Nanaorezaka Formation (Fig. 12) consists mainly of the extensive Nn1, Nn2, Nn3, and Nn4 pyroclastic flow deposits (FA 1) and overlying lahar deposits (FA 2). They form northward sloping and thinning sheets, interbedded with the alluvial fan deposits shed from the highland northwest of the basin (Fig. 25). As mentioned above, these pyroclastic flows were shed from the caldera volcanoes on the southeast of the basin (Fig. 26D)). Minor gravelly fluvial-channel deposits (FA 3) are rarely filling isolated, incised valleys above the pyroclastic sheets.

**Todera Formation**

As mentioned above, basinward migration of the fault systems occurred suddenly at the end of the Nanaorezaka Formation, producing abrupt changes of sediment-dispersal patterns. Especially, uplift of a high terrain southwest of the basin became more prominent, and the Sunagohara caldera was formed within the uplifted block (Fig. 26E). The caldera-forming Td1 pyroclastic flow deposit is filling northeastward valleys incised into the Nanaorezaka Formation (Fig. 25) and covered by 80-m-thick braidplain deposits, including the Td2 pyroclastic flow deposit (Yamamoto, 1992b).

# 7. DISCUSSION

## Eruptive style of the caldera volcanoes

The Aizu volcanic field is characterized by various types of caldera volcanoes, which form the single volcanic cluster under a same stress field. The large caldera volcanoes, Iriyamazawa, Takagawa, Uwaigusa, Hiwada, and Tonohetsuri calderas, which are >10 km in diameter and filled by >100 km³-volume caldera-forming pyroclastic flow deposits, have similar internal features to well-known "Valles type" calderas, such as Long Valley (Bailey et al., 1976) and Yellowstone (Christiansen, 1983), although it is uncertain whether the caldera floor is a coherent plate or incoherent breccia. On the contrary, the medium to small calderas, less than 10 km in diameter, lack typical features for depression along a ring fault zone. Based on the bore hole data (NEDO, 1985), Sunagohara caldera, 6 by 4 km across, has been interpreted as a diatremelike subsurface structure (Fig. 8B), which is common in Japanese Quaternary calderas (Aramaki, 1984). Narioka caldera, 8 by 4 km across, erupted about 40 km³ of dacite magma at 0.9- 0.7 Ma; this caldera may represent an intermediate-size between a large collapsed caldera and a small diatremelike one. Such medium to small calderas were formed after the last large-caldera formation of Tonohetsuri at 1.4- 1.2 Ma (Fig. 5), but the strong compressional stress field has been already dominant since 3 Ma based on the significant facies change from the Fujitoge to Izumi Formations. Thus, the type of calderas is independent of a regional stress field, such as compression or extension.

The formations of large caldera volcanoes have occurred at six times in this field since about 8 Ma at every 1 to 2x10⁶ years intervals (Fig. 4); an average eruption rate of large-caldera-forming magma is roughly estimated as >100 km³/ 10⁶ years. And medium- to small-caldera-forming eruptions tend to have occurred at shorter recurrence intervals (<10⁵ years) since about 1.5 Ma (Fig. 5). During Pliocene and late Miocene periods, medium- to small-volume volcanic products among the large-caldera-forming eruptions are less preserved in this district, because the repeated large-caldera depressions covered and caved away much of

preceding smaller volcanoes. And, the major degradation above the Fj2- 4 pyroclastic flow sheets presumably removed abundant tephra deposits around the volcanoes. For example, the Iz2 pyroclastic flow deposit, less than 10 km$^3$ in magma volume, appeared to be shed from a vanished small caldera in the post-Iz1 eruption period. The change of eruptive behavior from early to middle Pleistocene (Fig. 5) is attributed to a long-term (>10$^6$ years) magma cycle rather than a change of magma plumbing systems corresponding other tectonic events. Also, occurrence of basaltic to andesitic stratovolcanoes, which characterize the recent volcanism in this field, traces back to late Pliocene Hakaseyama volcano, the early Pliocene post-caldera products within the Uwaigusa Formation, and the late Miocene uppermost post-caldera products within the Takagawa Formation (Fig. 4); the eruption style representing the Quaternary volcanism has presumably continued at least since 6 Ma.

Similar long-term cycles (10$^6$ years) of large-caldera formations have been also observed from other volcanic fields in this arc, such as the Hakkoda (Muraoka et al., 1991) and Kurikoma fields (Sakaguchi and Yamada, 1988). However, these eruption rates are about ten times as small as the rate of well-known other Cenozoic caldera volcanoes accompanied with extensional graben. For example, seventeen large-volume ignimbrite eruptions (>100 km$^3$) occurred during 3 x10$^6$ years in the San Juan field (Lipman, 1984), and Yellowstone caldera has erupted 6500 km$^3$ of rhyolite magma in the last 2x10$^6$ years (Christiansen, 1983) in the western United State. Furthermore, four large-volume ignimbrite eruptions (>100 km$^3$) occurred during last 1.5x 10$^5$ years in the Kagoshima graben, north end of the Ryukyu arc, Japan (Nagaoka, 1988), and caldera volcanoes in the Taupo volcanic zone, New Zealand, have erupted >10$^4$ km$^3$ of dominantly rhyolitic magma during the last 1x 10$^6$ years at more frequent intervals (Wilson et al., 1984).

**Emergence of the arc and initiation of the caldera-forming volcanism**

Eustasy and subsidence combine to make the space available for sediment to fill, and the results of this changing accommodation are the onlapping and offlapping depositional strata
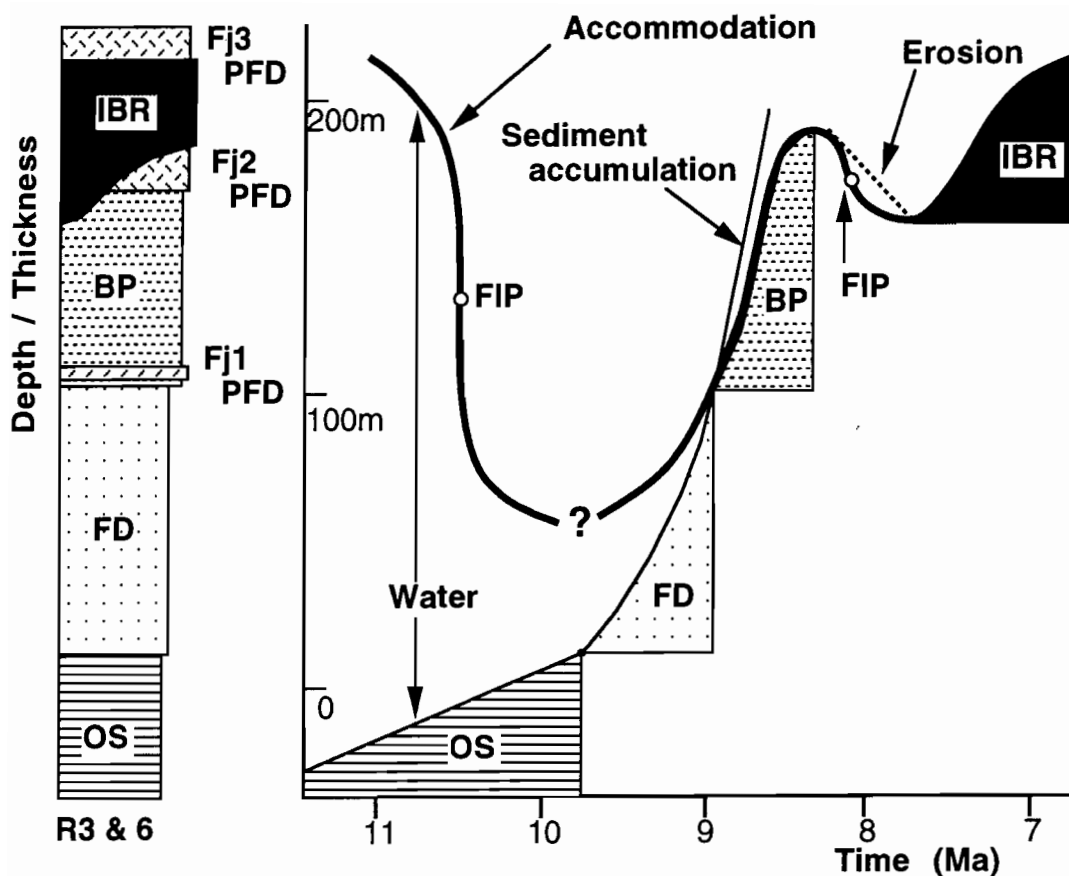
69

Fig. 27. Relationship of accommodation and sediment accumulation during deposition of the Shiotsubo and Fujitoge Formations in the sections R3 and 6. Paleodepth of the marine facies is indicated by the mollusca fauna (Suzuki et al., 1986), and time of the curve is determined from the calcareous nannoplankton zone within the marine facies (Suzuki et al., 1986) and the fission track ages of the pyroclastic flows (Yamamoto, 1992a). See text for details.

patterns observed on basin margins (Jervey, 1988; Posamentier and Vail, 1988). Relationship of sediment accumulation to accommodation (Fig. 27), determined from the depositional environments of the Shiotsubo and Fujitoge Formations, suggest that an abrupt increase of the sediment supply rate occurred at 9.5- 10 Ma. The low-rate deposition of offshore shelf sediments of the Yuzuritoge Formation may have been reflected progradation of a coastline and represented bottomset units of pro-delta aprons, corresponding to the decline in accommodation at the 10.5 Ma sequence boundary. However, the subsequent increase of the influx rate of pro-delta sediments, which exceeded the rate of contemporaneous sea-level rise, caused the sediment surface to the sea level, and a thick sequence of deltaic-plain sediments was deposited as accommodation continued to increase (Fig. 27). Excess sediments, which could not be accommodated, was bypassed basinward. After the Fj2 eruption, the decrease in accommodation at the 8.2 Ma sequence boundary resulted in subaerial incision of profound valleys.

This eustasy-controlled depositional system within the Shiotsubo and Fujitoge Formations indicates basin-subsidence at a very slow rate, because the amplitude of relative sea level changes represented by the observed accommodation (Fig. 27), is almost same as one of the absolute sea level changes (Haq et al., 1988). No vertical stacking of highstand system tracts had occurred above the Fj2, Fj3, and Fj4 pyroclastic flow sheets (Fig. 23), although the incised valleys were refilled by fluvial sediments at a high accumulation rate in the next cycles. In this period, volcano-induced debris had been transported through the coastal alluvial channels to far-backarc offshore basins, prograding the extracaldera volcaniclastic aprons.

The high rate of sediment supply, started at about 10 Ma (Fig. 27), reflected an increase in volcanic activity, preceding the large-caldera formation in this field. The aggrading sediments were mainly derived from dacitic or rhyolitic pyroclastics and transported as lahars into the basin, but no basaltic or andesitic debris, which suggests preexisting volcanic edifices, is found within the Shiotsubo and lower Fujitoge Formations. Felsic resedimented volcaniclastics are also interbedded with siltstones within the Yuzuritoge Formation (Yamamoto and Yoshioka, 1992), but their accumulation rate is very low. This flare-up of the felsic volcanism has been synchronously identified in the whole Northeast Honshu arc at the

Late Miocene (Amano and Sato, 1989; Ito et al., 1989). Small caldera volcanoes may have been formed in the volcanic field corresponding to the begininng of high sediment supply, although the subsequent large caldera-forming events caved away much of the near-source records of initial volcanoes.

**Broad magmatic uplift**

The Aizu volcanic field was topographically high during the caldera-forming volcanism (Fig. 26) and its volcanoes unconformably overlie early to middle Miocene marine formations, although the extracaldera basin had subsided at a very slow rate (Fig. 27). Furthermore, flexural deformations and local unconformities within the extracaldera formations around the caldera volcanoes show regional buoyant uplift of the field. Especially on the north side of the Iriyamazawa and Hiwada calderas (Figs. 23 and 24), the pre-caldera strata dip 15- 30 outward and are horizontally buried by caldera-forming pyroclastic flows and younger fluvial deposits. The lower unconformity was already described by Komuro (1978), but he misunderstood that this swell had preceded the formation of Sunagohara caldera. The edges of the both swells are marked by hinge lines having the radiuses of 20- 25 km from individual caldera-centers. Furthermore, the doming seems to have started at least 1- 1.5 million years prior to the caldera-forming eruptions based on the age data.

This broad doming is inferred to have been caused by growth of felsic magma chambers preceding the individual caldera-forming eruptions, as described by Smith and Bailey (1968) and Gudmundsson (1988). However, similar outcrop evidence of insurgent uplift has been rarely reported from Tertiary caldera volcanoes (Cristiansen et al., 1977); pre-historical such deformation is elusive. In contrast, active inflation has been well observed at both Long Valley caldera, USA (Hill et al., 1985) and Rabaul caldera, Papua New Guinea (McKee et al., 1985), but uplift is confined to the interior of the caldera. At these sites, such deformation may reflect either continued postcaldera resurgence or the beginning of a new magmatic cycle that lead to pyroclastic eruptions.

In general, high topographic elevations characterize young large caldera volcanoes such

as Yellowstone, the Jemez Mountains, USA (Christiansen, 1983), and the Cenozoic ignimbrite fields such as the San Juan field, USA (Lipman, 1984). Furthermore, these caldera clusters are accompanied by negative Bouguer anomalies enclosing whole of the clusters and grabens breaking the calderas; they are interpreted as reflecting distension and buoyant uplift over an extensive low-density batholith beneath the clustered areas (Lipman, 1984). On the contrary, the Aizu volcanic field is associated with a regional positive gravity anomaly (GSJ, 1993) and lacks extensional deformation; they are inconsistent with emplacement of batholithic magma bodies at a high level. Although plutonic rocks are exposed within the two eroded resurgent calderas in the Aizu field, such plutonic masses are probably more discontinuous and more dense than those thought to underlie the San Juan field. These features suggest that the observed long-term cycle of large-caldera formations in the Aizu field has been directly caused by a slow rate of magma accumulation in the crust beneath the volcanoes.

# 8. CONCLUSION

Four conclusions are evident from current data.

First, within the Aizu volcanic field, late Miocene to Recent six large calderas, >10 km in diameter, form a prominent cluster, about 60 by 30 km across, with several medium to small calderas and stratovolcanoes. These volcanoes are built on a WNW-ESE trending topographic high terrain, resulted by broad magmatic uplift. This volcanic field is, however, coincident with regional positive Bouguer gravity anomalies enclosing the calderas; this feature suggests the lack of low-density batholithic magma bodies at a high-level beneath the volcanoes.

Second, the large calderas are characterized by voluminous intracaldera pyroclastic flow deposits (>100 $km^3$), ring-like patterns of postcaldera igneous activity, and resurgent uplift within the calderas; these features are similar to well-known "Valles type" calderas. On the other hand, the medium to small calderas have been interpreted as diatremelike subsurface structures, based on the borehole data. Both of them were formed under a same compressional stress field, that caused progradation of alluvial fans and flexural subsidence of the intra-arc basin due to reverse-faulting, since 3 Ma.

Third, the caldera-forming felsic volcanism started at about 10 Ma. This volcanism caused a high rate of sediment supply in the basin and insurgent updoming at individual caldera-sites. Its eruptive products were transported mainly as gravity flows into the basin; resulted volcaniclastic aprons had prograded toward the back-arc side controlled by sea-level changes until about 3 Ma.

Fourth, the large-caldera formation have occurred at six times at every 1 to $2\times10^6$ years intervals. This cycle is more than ten times as long as those of well-known other Cenozoic caldera volcanoes accompanied with extensional grabens, such as Yellowstone caldera, the San Juan volcanic field, the Taupo volcanic zone, and the Kagoshima Graben. The observed long-tern cycle seems to be directly caused by a slow rate of magma accumulation in the crust beneath the Aizu volcanic field.

# References

Amano, K. and Sato, H. (1989) Neogene tectonics of the central part of Northeast Honshu Arc. *Memor. Geol. Soc. Japan*, no.32, p.81-96. (in Japanese with English abstract)

Ando, S. (1983) Structure of the Nigorikawa caldera interpreted from the bore hole data. *Earth Mon.*, vol.5, p.116-121. (in Japanese)

Aramaki, S. (1984) Formation of the Aira caldera, southern Kyushu, 22,000 years ago. *J. Geophys. Res.*, vol.89(B10), p.8485-8501.

Bailey, R.A., Dalrymple, G.B., and Lanphere, M.A. (1976) Volcanism, structure, and geochronology of Long Valley caldera, Mono County, California. *J. Geophys. Res.*, vol.81, p.725-744.

Ban, M. and Fujimaki, H. (1992) Petrology of Nasu volcanic group, Northeast Japan arc. *Prog. Abst. Volcanol. Soc. Japan, 1992, No.2*, p.95. (in Japanese)

Best, J.L. (1992) Sedimentology and event timing of a catastrophic volcaniclastic mass flow, Volcan Hudson, Southern Chile. *Bull. Volcanol.*, vol.54, p.299-318.

Cant, D.J. and Walker, R.G. (1978) Fluvial processes and facies sequences in the sandy south Saskatchewan river, Canada. *Sedimentology*, vol.25, p.625-648.

Crandell, D.R. (1971) Post-glacial lahars from Mt. Rainier Volcano, Washington. *U.S. Geol. Surv. Prof. Pap.*, 677, 75p.

Christiansen, R.L. (1983) Yellowstone magmatic evolution: Its bearing on understanding large-volume explosive volcanism. In *Explosive Volcanism: Inception, Evolution, and Hazard*. National Academy Press, Washington, D.C., p.84-95.

Christiansen, R.L., Lipman, P.W., Carr, W.J., Byers, F.M.Jr., Orkid, P.P. and Sargent, K.A. (1977) Timber Mountain- Oasis Valley caldera complex of southern Nevada. *Geol. Soc. Am. Bull.*, vol.88, p.943-959.

Chuman, N. and Yoshida, T. (1982) On the geology of the southern foot of Mt. Bandai. In *The Nature of Lake Inawashiro in Fukushima Prefecture, Japan*. Annual Rept., Fukushima Univ., no.3, p.21-32. (in Japanese with English abstract)

Danhara, T., Kasuya, M., Iwano, H. and Yamashita, T. (1991) Fission-track age calibration using internal and external surfaces of zircon. *J. Geol. Soc. Japan*, vol.97, p.977-985.

de Silva, S.L. (1989) Geochronology and stratigraphy of the ignimbrites from the 21 30'S to 23 30'S portion of the Central Andes of northern Chile. *J. Volcanol. Geotherm. Res.,* vol.37, p.93-131.

Elliott, T. (1974) Interdistributary bay sequences and their genesis. *Sedimentology,* vol.21, p.611-622.

Fisher, R.V. and Schmincke, H.-U. (1984) *Pyroclastic Rocks.* Springer-Verlag, 472p.

Fridrich, C.J., Smith, R.P., DeWitt, ED, and Mckee, E.H. (1991) Structural, eruptive, and intrusive evolution of the Grizzly Peak caldera, Sawatch Range, Colorad. *Geol. Soc. Am. Bull.,* vol.103, p.1160-1177.

Geological Survey of Japan (1993) *Gravity Map series 4 Gravity Map of Niigata District (Bouguer Anomalies).*

Gloppen, T.G. and Steel, R.J. (1981) The deposition, internal structure and geometry in six alluvial fan- fan delta bodies (Devonian- Norway)- a study in the significance of bedding sequence in conglomerates. In Ethridge, F.G. and Flores, R.M. (eds.): *Recent and Ancient Nonmarine Depositional Environments: Models for Exploration.* Soc. Econ. Paleont. Miner. Spec. Pub., no.31, p.49-69.

Gudmundsson, A. (1988) Formation of collapse calderas. *Geology,* vol.16, p.808-810.

Hakaseyama Collaborative Research Group (1990) Pliocene Hakaseyama volcanic formation in the southwestern part of the Aizu-Basin, Fukushima Prefecture, Northeast Japan. *Earth Science (Chikyu Kagaku),* vol.44, p.113-126. (in Japanese with English abstract)

Haq, B.U., Hardenbol, J. and Vail, P.R. (1987) Mesozoic and Cenozoic chronostratigraphy and cycles of sea-levels change. In Wilgus, C.K. and others (eds): *Sea-Level Changes: An Integrated Approach.* Soc. Econ. Paleont. Miner. Spec. Pub., no.42, p.71-108.

Hill, D.P., Bailey, R.A. and Ryall, A.S. (1985) Active tectonic and magmatic processes beneath Long Valley caldera, eastern California: an overview. *J. Geophys. Res.,* vol.90(B13), p.11111-11120.

Ito, T., Utada, M. and Okuyama, T. (1989) Mio-Pliocene calderas in the Backborn Region in northeast Japan. *Memor. Geol. Soc. Japan,* no.32, p.409-429. (in Japanese with English abstract)

Jervey, M.T. (1988) Quantitative geological modeling of siliciclastic rock sequences and their seismic expression. In Wilgus, C.K. and others (eds): *Sea-Level Changes: An Integrated Approach.* Soc. Econ. Paleont. Miner. Spec. Pub., no.42, p.47-69.

Kano, K. (1991) Volcaniclastic sedimentation in a shallow-water marginal basin: the Early Miocene Koura Formation, SW Japan. In Cas, R. and Busby-Spera, C. (eds.): Volcaniclastic Sedimentation. *Sediment. Geol.*, vol.74, p.309-321.

Kitamura, N., Sugawara, Y., Suzuki, Y., Fujii, K., Ito, O. and Takahashi, S. (1968) *Geology of the Miyashita district.* With geological sheet map at 50, 000. Fukushima Prefectural Government Office, 21p. (in Japanese)

Kobayashi, S. and Inomata, K. (1986) K-Ar ages of the Hakaseyama volcanic rocks, Aizu district. *Earth Science (Chikyu Kagaku)*, vol.40, p.453-454. (in Japanese)

Komuro, H. (1978) The formation of the late Miocene collapse basin at the Yanaizu district, Fukushima Prefecture, Japan. *Earth Science (Chikyu Kagaku)*, vol.32, p.68-83. (in Japanese with English abstract)

Komuro, H. (1984) Uplift and volcanic collapse depression during middle to late Miocene age in the Miyashita district, Aizu, Fukushima Prefecture, Northeast Japan. *J. Geol. Soc. Japan,* vol.90, p.441-454. (in Japanese with English abstract)

Kraus, M.J. (1984) Sedimentology and tectonic setting of early Tertiary quartzite conglomerates, northwest Wyoming. *Sedimentology of Gravels and Conglomerates.* Can. Soc. Petrol. Geol. Mem., vol.10, p.203-216.

Kuenzi, W.D., Horst, O.H. and McGehee, R.V. (1979) Effect of volcanic activity on fluvial-deltaic sedimentation in a modern arc-trench gap, southwestern Guatemala. *Geol. Soc. Am. Bull.*, vol.90, p.827-838.

Lambert, M.B. (1974) The Bennet Lake Cauldron subsidence complex, British Columbia and Yukon Territory. *Geol. Surv. Can. Bull.*, no.227, 213p.

Lipman, P.W. (1976) Caldera-collapse breccias in the western San Juan Mountains, Colorado. *Geol. Soc. Am. Bull.*, vol.87, p.1397-1410.

Lipman, P.W. (1984) The roots of ash flow calderas in western North America: windows into the tops of granitic batholiths. *J. Geophys. Res.*, vol.89(B10), p.8801-8841.

Lowe, D.R. (1982) Sediment gravity flows:II. Depositional models with special reference to the deposits of high-density turbidity currents. *J. Sed. Petrol.*, vol.52, p.279-297.

Lowe, D.R., Williams, S.N., Leigh, H., Connor, C.B., Gemmell, J.B. and Stoiber, R.E. (1986) Lahars initiated by the 13 November 1985 eruption of Nevado del Ruiz, Colombia. *Nature*, vol.324, p.51-53.

Machida, H. and Arai, F. (1992) *Atlas of Tephra in and around Japan.* Univ. Tokyo Press, 276p.

McKee, C.O., Johnson, R.W., Lowenstein, P.L., Blong, R.J., de Saint Ours, P. and Talai, B. (1985) Rabaul caldera, Papua New Guinea: volcanic hazards, surveillance, and eruption contingency planning. *J. Volcanol. Geotherm. Res.,* vol.23, p.195-237.

Manabe, K. (1980) Magnetostratigraphy of the Yamato Group and the Sendai Group, Northeast Honshu, Japan (II). *Sci. Rept., Fukushima Univ.*, no.30, p.49-71.

Massari, F. (1984) Resedimented conglomerates of a Miocene fan-delta complex, southern Alps, Italy. In Koster, E.H. and Steel, R.J. (eds.): *Sedimentology of Gravels and Conglomerates.* Can. Soc. Petrol. Geol. Mem., vol.10, p.259-278.

Masuda, K., Shibata, T., Akutsu, J. and Nakagawa, Y. (1974) *Geology of the Tajima district.* With geological sheet map at 50, 000. Fukushima Prefectural Government Office, 33p. (in Japanese)

Mathisen, M.E. and Vondra, C.F. (1983) The fluvial and pyroclastic deposits of the Cagayan Basin, Northern Luzon, Philippines -- an example of non-marine volcaniclastic sedimentation in an interarc basin. *Sedimentology*, vol.30, p.369-392.

Miall, A.D. (1977) A review of the braided river depositional environment. *Earth Sci. Rev.*, vol.13, p.1-62.

Miall, A.D. (1978) Lithofacies types and vertical profile models in braided river deposits: A summary. In Miall, A.D. (ed.): *Fluvial Sedimentology.* Can. Soc. Petrol. Geol. Mem., vol.5, p.597-604.

Miall, A.D. (1985) Architectural-element analysis: a new method of facies analysis applied to fluvial deposits. *Earth Sci. Rev.*, vol.22, 261-308.

Middleton, G.V. and Hampton, M.A. (1976) Subaqueous sediment transport and deposition

by sediment gravity flows. In Stanley, D.J. and Swift, D.J.P. (eds.): *Marine Sediment Transport and Environmental Management*. New York, Wiely, p.197-218.

Ministry of International Trade and Industry (1970) *Report of investigation of a Large Region, S.44, Nishi-aizu district.* 31p. (in Japanese)

Ministry of International Trade and Industry (1978) *Fundamental Investigation Report for Geothermal Development, no.5, Nishiyama district (I).* (in Japanese)

Mizugaki, K. (1992) A small caldera in Sunagohara, Yanaizu Town, Fukushima Prefecture, Japan. *Abst. 99th Annual Meeting Geol. Soc. Japan*, p.424. (in Japanese)

Muraoka, H., Yamaguchi, Y. and Hase, H. (1991) Clustered calderas founded in the Hakkoda geothermal field, Northeast Japan. *Rept. Geol. Surv. Japan*, no.275, p.97-111. (in Japanese with English abstract)

Nagaoka, S. (1988) The Late Quaternary tephra layers from the caldera volcanoes in and around Kagoshima bay, southern Kyushu, Japan. *Geograph. Rep. Tokyo Metropolitan Univ.*, no.23, p.49-122.

Nemec, W., Steel, R.J., Porebski, S.J. and Spinnangr, A. (1984) Domba conglomerate, Devonian, Norway: process and lateral variability in a mass flow-dominated, lacustrine fan-delta. In Koster, E.H. and Steel, R.J. (eds.): *Sedimentology of Gravels and Conglomerates*. Can. Soc. Petrol. Geol. Mem., vol.10, p.295-320.

New Energy Development Organization (1985) *Geothermal development research report, no.8, Oku-aizu region.* 811p. (in Japanese)

New Energy Development Organization (1990) *Explanatory text of the volcano-geological map and compiled geological map of Nasu geothermal area.* 98p. (in Japanese)

Okazaki, H. and Masuda, F. (1992) Depositional systems of the Late Pleistocene sediments in Paleo-Tokyo Bay area. *J. Geol. Soc. Jpn.*, vol.98, p.235-258. (in Japanese and English abstract)

Orton, G.J. (1991) Emergence of subaqueous depositional environments in advance of a major ignimbrite eruption, Capel Curing Volcanic Formation, Ordovician, North Wales -- an example of regional volcanotectonic uplift? In Cas, R. and Busby-Spera, C. (eds.): Volcaniclastic Sedimentation. *Sediment. Geol.*, vol.74, p.251-286.

Palmer, B.A. and Neall, V.E. (1991) Contrasting lithofacies architecture in ring-plain deposits related to edifice construction and destruction, the Quaternary Stratford and Opunake Formations, Egmont Volcano, New Zealand. In Cas, R. and Busby-Spera, C. (eds.): Volcaniclastic Sedimentation. *Sediment. Geol.*, vol.74, p.71-88.

Phillips, R.L. (1984) Depositional features of Late Miocene, marine cross-bedded conglomerates, California. In Koster, E.H. and Steel, R.J. (eds.): *Sedimentology of Gravels and Conglomerates*. Can. Soc. Petrol. Geol. Mem., vol.10, p.345-358.

Pierson, T.C. and Scott, K.M. (1985) Downstream dilution of a lahar: Transition from debris flow to hyperconcentrated streamflow. *Water Resources Res.*, vol.21, p.1511-1524.

Posamentier, H.W. and Vail, P.R. (1988) Eustatic controls on clastic deposition II - Sequence and systems tract models. In Wilgus, C.K. and others (eds): *Sea-Level Changes: An Integrated Approach.* Soc. Econ. Paleont. Miner. Spec. Pub., no.42, p.125-154.

Postma, G. (1984) Mass-flow conglomerates in a submarine canyon: Abrioja fan-delta, Pliocene, southern Spain. In Koster, E.H. and Steel, R.J. (eds.): *Sedimentology of Gravels and Conglomerates*. Can. Soc. Petrol. Geol. Mem., vol.10, p.237-258.

Reineck, H.-E. and Singh, I.B. (1980) *Depositional Sedimentary Environments*. Springer-Verlag, 549p.

Rust, B.R. (1972) Structure and process in a braided river. *Sedimentology*, vol.18, p.221-245.

Rust, B.R. (1978) Depositional models for braided alluvium. In Miall, A.D. (ed.): *Fluvial Sedimentology*. Can. Soc. Petrol. Geol. Mem., vol.5, p.605-625.

Sakaguchi, K. and Yamada, E. (1988) "The Kitagawa Dacite", pyroclastic flow deposits around the Onikobe caldera, northeast Japan. *Rept. Geol. Surv. Japan*, no.268, p.37-59. (in Japanese with English abstract)

Sangawa, A. (1987) Damage by the 1611 Aizu Earthquake in relation to surface faulting. *J. Seism. Soc. Japan*, vol.40, p.235-245. (in Japanese with English abstract)

Smith, D.G. (1983) Anastomosed fluvial deposits; modern examples from Western Canada. In J.D. Collinson and J. Lewin (eds.): *Modern and Ancient Fluvial Systems*. Int. Assoc. Sediment. Spec. Publ., no.6, p.155-168.

Smith, G.A. (1986) Coarse-grained nonmarine volcaniclastic sediment: terminology and depositional process. *Geol. Soc. Am. Bull.*, vol.97, p.1-10.

Smith, G.A. (1987) The influence of explosive volcanism on fluvial sedimentation: The Deschutes Formation (Neogene), central Oregon. *J. Sed. Petrology*, vol.42, p.384-388.

Smith, G.A. (1988) Sedimentology of proximal to distal volcaniclastic dispersed across an active foldbelt: Ellensburg Formation (Late Miocene), central Washington. *Sedimentology*, vol.35, p.953-977.

Smith, R.L. and Bailey, R.A. (1968) Resurgent cauldrons. In Coats, R.R. and others (eds.): Studies in volcanology (Williams volume). *Geol. Soc. Am. Mem.*, no.116, p.613-662.

Sugawara, H. (1991) K-Ar age of the Numazawa volcano, Fukushima Prefecture. *Bull. Volcanol. Soc. Japan*, vol.36, p.443-445. (in Japanese with English abstract)

Suto, S. (1987) Large scale felsic pyroclastic flow deposits in the Sengan geothermal area, northeast Japan: Tamagawa and Old-Tamagawa Welded Tuffs. *Rept. Geol. Surv. Japan*, no.266, p.77-142. (in Japanese with English abstract)

Suzuki, K. (1951) The Geology of the west region of the Aizu Basin, Fukushima Prefecture. Part I Central Area. *J. Geol. Soc. Japan*, vol.57, p.379-386, 449-456. (in Japanese with English abstract)

Suziki, K., Ueda, Y. and Manabe, K. (1976) K-Ar dating on some tuffs of the late Cenozoic strata in the southern part of the Tohoku district, Japan. *Sci. Rept., Fukushima Univ.*, no.26, p.57-63. (in Japanese with English abstract)

Suzuki, K., Yoshida, T. and Manabe, K. (1977) The Geologic development of inland basins in southern part of the Tohoku district, Japan. *Memor. Geol. Soc. Japan*, no.14, p.45-64. (in Japanese with English abstract)

Suzuki, K., Yoshimura, T., Shimazu, M. and Okada, H. (1986) Transect Route No. 27 (Sado, Yahiko- Tsugawa- Kitakata- Azumayama- Fukushima). In Kitamura, N. (ed.): *Geological data of Cenozoic Northeast Honshu arc*, vol.3, Hobundo, Sendai. (in Japanese)

Suzuki, K., Fujita, Y., Yashima, R., Yoshida, T., Manabe, K., Hakozaki, T., Hagiwara, S., Shuto, K. and Tsunoda, F. (1972) *Geology of the Wakamatsu district.* With geological sheet map at 50, 000. Fukushima Prefectural Government Office, 61p. (in Japanese)

Takahashi, M. and Sugawara, H. (1985) Volcanic history of the Numazawa volcano (abstract). *Bull. Volcanol. Soc. Japan*, vol.30, p.125-126. (in Japanese)

Turbeville, B.N., Waresback, D.B. and Self, S. (1989) Lava-dome growth and explosive volcanism in the Jemez Mountains, New Mwxico: Evidence from the Plio-Pleistocene Puye alluvial fan. *J. Volcanol. Geothermal. Res.,* vol.36, p.267-291.

Vessel, R.K. and Davis, D.K. (1981) Nonmarine sedimentation in an active fore arc basin. In Ethridge, F.G. and Flores, R.M. (eds.): *Recent and Ancient Nonmarine Depositional Environments: Models for Exploration.* Soc. Econ. Paleont. Miner. Spec. Pub., no.31, p.31-45.

Walker, R.G. (1978) Deep-water sandstone facies and ancient submarine fans: models for exploration for stratigraphic traps. *Am. Ass. Petrol. Geol. Bull.*, vol.62, p.932-966.

Wilson, C.J.N., Rogan, A.M., Smith, I.E.M., Northey, D.J., Nairn, I.A., Houghton, B.F. (1984) Caldera volcanoes of the Taupo volcanic zone, New Zealand. *J. Geophys. Res.*, vol.89(B10), p.8463-8484.

Yamamoto, T. (1991) Large scale slope failure during caldera collapse: structural development of the Late Miocene Takagawa caldera, Northeast Japan. *Bull. Volcanol. Soc. Japan*, vol.36, p.1-10. (in Japanese with English abstract)

Yamamoto, T. (1992a) Chronology of the Late Miocene- Pleistocene caldera volcanoes in the Aizu district, Northeast Japan. *J. Geol. Soc. Japan.*, vol.98, p.21-38. (in Japanese with English abstract)

Yamamoto, T. (1992b) The Middle Pleistocene explosive volcanism in Sunagohara caldera volcano, Aizu, Japan: evidence from non-marine volcaniclastic facies of the Todera Formation. *J. Geol. Soc. Japan*, vol.98, p.855-866. (in Japanese with English abstract)

Yamamoto, T. and Yoshioka, T. (1992) *Geology of the Wakamatsu district.* With Geological

Sheet Map at 1:50, 000, Geol. Surv. Japan, 73p. (in Japanese with English abstract)

Yamaguchi, Y. (1986) K-Ar dating of pyroclastic flow deposits in Tajima area, Fukushima Prefecture, Northeast Japan. *Essays in Geology, Professor N. Kitamura Commemorative Volume*, p.629-636. (in Japanese with English abstract)

Yamaguchi, Y. (1991) Geothermal resources assessment of Minami-Aizu Area, Southern Tohoku District, Northeast Japan. *Rept. Geol. Surv. Japan*, no.275, p.199-227. (in Japanese with English abstract)

Yoshida, H. and Takahashi, M. (1991) Geology of the eastern part of the Shirakawa pyroclastic flow field. *J. Geol. Soc. Japan*, vol.97, p.231-249. (in Japanese with English abstract)

## Appendix: sample descriptions and results of dating

**GSJ R60143.** Kachikata, Aizubange Town, Fukushima Prefecture. 139 47'33"E, 37 31'50"N, 255 m height (Site 36; Fig. 3).

Dacite lapilli tuff (the Td1 pyroclastic flow deposit within the Todera Formation). Vitroclastic unwelded matrix of pumice and glass shards. Crystals of plagioclase, quartz, clinopyroxene, orthopyroxene, hornblende, and zircon.

**GSJ R60144.** Tamanashi, Kanayama Town, Fukushima Prefecture. 139 32'31"E, 37 24'34"N, 545 m height (Site 32; Fig. 3).

Rhyolite lapilli tuff (the Uw1 pyroclastic flow deposit within the Uwaigusa Formation). Vitroclastic unwelded matrix of pumice and glass shards. Crystals of quartz, plagioclase, biotite, opaques, hornblende, clinopyroxene, orthopyroxene and zircon. Lithic fragments of rhyolite and meta-tuff.

**GSJ R60145.** Hayasaka-toge, Kanayama Town, Fukushima Prefecture. 139 33'19"E, 37 25'56"N, 750 m height (Site 30; Fig. 3).

Andesite lava flow (the post-caldera unit of the Uwaigusa Formation). Phenocrysts of plagioclase, clinopyroxene, orthopyroxene, and quartz. Intersertal groundmass of plagioclase, clinopyroxene, orthopyroxene, opaques and zircon.

**GSJ R60146.** Ashinohara, Shimogo Town, Fukushima Prefecture. 139 55'48"E, 37 18'15"N, 405 m height (Site 25; Fig. 3).

Dacite lapilli tuff (The Tn1 pyroclastic flow deposit within the Tonohetsuri Formation). Vitroclastic unwelded matrix of pumice and glass shards. Crystals of plagioclase, quartz, clinopyroxene, orthopyroxene, opaques, hornblende, and zircon. Lithic fragments of tonalite and hornfels. Small irregular cavities with calcite.

**GSJ R60147.** Yogai-san, Kitashiobara Village, Fukushima Prefecture. 139 56'45"E, 37 39'09"N, 310 m height (Site 2; Fig. 3).

Dacite welded tuff (the Nn2 pyroclastic flow deposit within the Nanaorezaka Formation). Densely welded glassy matrix of pumice shards. Crystals of plagioclase, clinopyroxene, opaques, quartz, orthopyroxene, hornblende, and zircon. Lithic

fragments of dacite and meta-tuff.

85

Fission-track ages of zircon (Table A1) were determined by Kyoto Fission-Track Co., Ltd. using ED2 method (Danhara et al., 1991). A sample for K-Ar dating was crushed and divided into 32-60 mesh size fraction. This fraction was examined under binoculars and large phenocrysts were removed by hand picking. A K-Ar age (Table A2) was determined by Teledyne Isotopes Co., Ltd.

Table A1.    Result of fission track ages.

| Unit/ [Site] Sample | Mineral/ Number of grains | Spontaneous $\rho s$ [Ns] $(10^5/cm^2)$ | Induced $\rho i$ [Ni] $(10^6/cm^2)$ | $P(\chi^2)$ (%) | Dosimeter $\rho d$ [Nd] $(10^4/cm^2)$ | r | U (ppm) | Age±1σ (Ma) |
|---|---|---|---|---|---|---|---|---|
| **Todera Formation** [36] Td1 PFD (Opx-Hb-Cpx dacite lapilli tuff) | | | | | | | | |
| GSJ R60143 | zircon 30 | 5.75 [30] | 1.66 [867] | 59 | 7.49 [2307] | 0.437 | 180 | 0.96±0.18 |
| **Nanaorezaka Formation** [2] Nn2 PFD (Hb-Opx-Cpx dacite welded tuff) | | | | | | | | |
| GSJ R60147 | zircon 27 | 1.24 [73] | 3.25 [1914] | 94 | 8.63 [1330] | 0.486 | 300 | 1.2±0.1 |
| **Tonohetsuri Formation** [25] Tn1 PFD (Hb-Opx-Cpx dacite lapilli tuff) | | | | | | | | |
| GSJ R60146 | zircon 30 | 6.84 [38] | 1.60 [887] | 31 | 8.63 [1330] | 0.493 | 150 | 1.4±0.2 |
| **Uwaigusa Formation** [32] Uw1 PFD (Opx-Cpx-Hb-Bt rhyolite lapilli tuff) | | | | | | | | |
| GSJ R60144 | zircon 30 | 4.99 [442] | 3.78 [3348] | 65 | 8.63 [1330] | 0.753 | 350 | 4.2±0.2 |

(1) $\rho$ and N are density and total number of fission tracks counted respectively.

(2) All analyses by external detector method using 0.5 for $2\pi/4\pi$ and 1 for $2\pi/4\pi$ geometry correlation factor.

(3) Age calculated using dosimeter glass SRM612 and $\zeta$ ED1 = 370±4, $\zeta$ ED2 = 372±5.

(4) $P(\chi^2)$ is probability of obtaining $\chi^2$-value for $\gamma$ degree of freedom (where $\gamma$= number of grains).

(5) r is correlation coefficient between $\rho s$ and $\rho i$.    (6) U is uranium content.

Table A2.  Result of K-Ar age

| Unit/ [Site] Sample | Rock | Material | Age (Ma) | $^{40}Ar^*$ ($10^{-5}$scc/gm) | $^{40}Ar^*$ (%) | K (%) |
|---|---|---|---|---|---|---|
| **Uwaigusa Formation** [31] | | | | | | |
| Postcaldera lava: | | | Av. 3.22±0.16 | | | |
| GSJ R60145 | Hb-Opx-Cpx andesite | gm | 3.14±0.16 | 0.018 | 59.9 | 1.48 |
| | | | 3.31±0.17 | 0.019 | 66.1 | 1.47 |

$\lambda\beta=4.962\times10^{-10}$/y,  $\lambda\epsilon=0.581\times10^{-10}$/y,  $^{40}K/K=1.167\times10^{-2}$atm%